AIRFLOW DYNAMICS IN TRANSVERSE DUNE INTERDUNES

A thesis submitted to the University of Leicester in partial fulfilment of the requirements for the degree of Doctor of Philosophy

Matthew C. Baddock

Division of Environmental Science
School of Applied Sciences
University College Northampton

2005

ProQuest LLC
789 East Eisenhower Parkway
P.O. Box 1346
Ann Arbor, MI 48106-1346

Abstract

Aeolian dune interdunes have been relatively ignored when compared with the research attention on the morphodynamics of the dune bodies themselves. This neglect is in spite of the possible significance of interdune dynamics for the geomorphology of the sand dune system as a whole, especially with regard to dune spacing.

This project involved the collection of geomorphologically relevant airflow data for four relatively simple transverse dune interdunes. The study locations were chosen in order to sample interdunes with different size and surface type characteristics, the dynamics of which were investigated for when incident flow was normal to the upwind crest. The findings confirm existing models of aeolian dune lee-side flow in terms of flow re-attachment length and recovery attributes. A consistent pattern of increasing near-surface velocity downwind of re-attachment provides a mechanism for interdunes as sand-free features. Where studies for comparison from other aeolian examples are limited, the field-measured turbulence shows the importance of the shear layer as a source of turbulence, and agrees with studies from sub-aqueous bedforms. The importance of shear stress variability and the possible contribution of turbulence structures to the maintenance of sediment transport at re-attachment where velocity and mean stress is low or negative is also emphasised. At the downwind edge of interdunes, the mean and turbulent velocity properties, and therefore morphodynamics, vary according to the interdune size. In this case, interdune length leads to greater recovery, and a balance exists in this region between the recovering flow at the surface, dissipating wake from above and the obstacle effect of the dune.

The flow dynamics are characterised for the different types of interdune observed. Dynamics accordant with the flow response model are seen to characterise the interdune setting with the closest spacing. The occurrence of other "extended" aeolian interdunes with a length well over that for flow separation demanded the development of a new descriptive model to characterise the dynamics therein. In this model, the variation in near-surface flow allowed process zones to be identified through the interdune. The geomorphological significance of the processes dominating each zone are discussed and comparisons are made between the flow response case and the new interdune model from this study.

Acknowledgements

Many people contributed this project in a variety of ways, and I should like to extend thanks to them all, and mention some in particular.

Firstly, throughout the course of the project, my supervisors in Ian Livingstone and Giles Wiggs have provided many valued suggestions, discussions and angles on the work. Their experience of aeolian fieldwork, associated stories and field cooking skills were also vital. A parallel study accompanying this research has been an investigation into their patience reserves. Despite my concerted attempts to discover the bottom of it, this tolerance has been found to be limitless, for which I am deeply grateful to them both for.

Permission for the fieldwork in the Skeleton Coast and Namib-Naukluft National Park was granted by Ministry of Environment and Tourism permit number 463/2001, through Holger Kolberg's assistance. In the Skeleton Coast, National Park Ranger Brian Patterson was very helpful. Harmen de Hoop and "Elvis" proved to be sterling field assistants, and Jeremy, Graham, Steve and Ingo *et al.* the most interesting subjects of study.

Thanks to the Department of Geography at the University of Sheffield for the use of cup and the sonic anemometers, as well as to Dr. Jo Bullard for the cup anemometers owned by the Department of Geography, Loughborough University. Namibia Polytechnic and Gobabeb Research Station were kind enough to loan surveying equipment.

Through the various meetings I have attended, I have had the benefit of useful and stimulating talks with many dune and aeolian researchers who have helped inspire and inform me. In particular Dr. Ian Walker, Prof. Gary Kocurek and Prof. Nicholas Lancaster all gave of their knowledge, with Nick also contributing his extensive knowledge of Skeleton Coast field locations at the start of the project. Brian Garvey's honest grappling with the sonic anemometer before me, and his advice on its use and output data were altruism itself.

The fieldwork would not have been possible without the financial help of the Leslie Church Research Award and the project was a UCN studentship. Grants from the British Geomorphological Research Group helped me to attend the international conferences which improved the project.

At UCN, the cartographer Paul Stroud produced the diagrams and maps, Tina Fairless helped assemble the fieldwork kit, members of the School chivvied me along and the NCR staff looked after me in a good many ways

For providing a distraction I must mention Pitsford and County Hall cricket clubs as well as Abington Rangers, Llamas and UCN football clubs and the people involved. Finally, the fortunes of Norwich City helped keep things in perspective.

My office colleagues have put up with a lot, but still gave much in return, particularly AS, SN and FT right at the end. I am lucky to have many good friends who have offered support, encouragement and a supply of good humour, especially that coming from Sackville Road *et al.*, which has all helped me greatly along the way.

Finally, I should mention my parents. Their constant backing and patience (a recurring theme?) has been immeasurable to me through this project. And for some time before that.

Contents

List of Figures

Chapter 1

Chapter 2

Chapter 3

List of Tables

Chapter 1
Introduction

1.1 Background

Aeolian sand deposits cover approximately 5% of the global land surface area, with 99% of these deposits being found in vast sand seas (Wilson, 1973). Within the areas of wind-lain sand, aeolian dunes are identifiable as common bedforms. Dunes are created by the deposition of sand-sized sediment into accumulations and the subsequent shaping of these accumulations as controlled by the wind-driven transport of particles. The particular form exhibited by dunes makes them compelling expressions of aeolian geomorphology, a fact which has acted to inspire considerable investigation into these landforms. Attempts to understand the distribution, pattern and formative processes of sand dunes have occupied researchers for around a century, with the early studies of dune form being largely descriptive and speculative (e.g. Cornish, 1897). A landmark was Bagnold's (1941) work which established a framework for all the research into aeolian dunes that has since followed. This subsequent body of work has included detailed studies on elements of flow dynamics and sand movement over dunes, and the large scale analysis of dune form and pattern afforded by the advent of remote sensing (see reviews in Thomas, 1997; Goudie, 1999).

Despite considerable research into the morphodynamics of sand dunes, a key area where challenges remain for our understanding concerns the controls on the spacing of dunes (Cooke *et al.*, 1993; Lancaster, 1996). Interdunes are those areas between dunes in sand seas and dunefields and they have received relatively little research attention in their own right (e.g. Sweet and Kocurek, 1990). This lack of a consideration regarding interdune dynamics is in spite of their potential significance for the sand dune system as a whole, especially with respect to the factors that govern dune spacing. The aim of this study is to increase our understanding of aeolian dunes through an investigation dedicated to the dynamics of the interdune component of the system.

1.2 The nature of interdunes

Ahlbrandt and Fryberger (1981: p. 293) produced a definition for the term aeolian interdune, stipulating "...a geomorphic surface commonly enclosed or at least partially bounded by dunes or other aeolian deposits such as sand sheets". Similarly, El-Sayed (2000: p. 306) put forward

the idea that interdunes "...are generally flat to gently sloping areas between dunes, and are commonly topographically enclosed by them". The variety of terms that have been used to describe interdune areas has been considerable, a fact which reflects the nature of their study. Often, the names used for interdunes have been suggestive of their general form, or the processes occurring within them. According to the extensive review of terminology by Breed and Grow (1979: pp. 295-296), it was Bagnold (1941) who first used the interdune term when discussing 'interdune hollows' in North Africa. Examples of some subsequently employed alternatives have included 'dune valleys' (e.g. Stone, 1967) and 'intradunes' (e.g. Sharp, 1979). The term interdune is used in the remainder of this thesis as it is now the most common term.

Interdunes have only recently become regarded as integral parts of dune systems (Kocurek, 1981) and the limited state of knowledge concerning interdune morphology has been lamented by several workers (e.g. McKee, 1983; Lancaster and Teller, 1988; Lancaster, 1995). All of these have pointed out a requirement for even basic information on the characteristics and occurrence of interdunes in the context of modern dune areas. The absence of knowledge on the nature and morphology of interdunes has resulted from a scarcity of research aimed specifically at the feature. As such, we have a definite gap in our appreciation of the aeolian dune system, to the extent that Lancaster and Teller (1988) stressed the significance of interdunes for the system simply in terms of their spatial extent. Furthermore, studies of the interdune sediments within both the ancient rock record and modern deposits can yield information on the chronology of bedform dynamics in the ancient or modern setting (Ahlbrandt and Fryberger, 1981). In these sediments, interdunes are represented by thin, planar strata sometimes of mud and silt, and also by bounding surfaces, where they separate sets of cross-strata. Such interdune deposits may even be preferentially preserved in comparison to dune sediments (Kocurek, 1981; McKee, 1983).

1.2.1 Interdunes and dune type

Information on the dimensions, shape and relative spatial extent of interdune within regions of dunes has largely been derived as a by-product from studies dedicated to the dune bedforms themselves (e.g. Breed and Grow, 1979). As a consequence of this, it has become apparent that an important control on many of the spatial characteristics of an interdune is related to the type of dune by which it is bounded. In this thesis, dune types are discussed in terms according to the accepted classification of dune forms developed by McKee (1979).

As a basic consideration, the overall shape of the interdune is necessarily related to the type of dune with which it is associated (Lancaster and Teller, 1988). The most straightforward example might be for the case of linear dunes. The interdune segments of the landscape that lie between linear dunes in effect mirror the alignment of these dunes, and in turn are relatively straight and elongated corridors. Some individual interdunes can be identifiable for lengths of tens of kilometres in the Namib Sand Sea (Lancaster, 1982b, 1989a; Livingstone, 1988) and Erg Bilma of the Sahara (Mainguet, 1984). In other sand seas, linear dunes often demonstrate a joining of the ridges to form 'Y' shaped junctions, with the open segment facing upwind. In these cases, the shape of the interdune can change with distance as it effectively narrows nearer to the junctions, as has been reported in the Simpson Desert, Australia (Mabbutt and Wooding, 1983) and for the Kalahari, southern Africa (Bullard *et al.*, 1995).

Transverse dune ridges formed in unidirectional winds have relatively straight brinklines, and differ from the more highly curved slip faces displayed by crescentic or barchanoid ridges (McKee, 1979). The resulting shape of the interdune between these two transverse dune types is therefore also different. Interdunes exhibited between the compound crescentic ridge dunes of the Algodones chain are roughly triangular (Sharp, 1979), shaped by the sinuosity of the windward slope margin. In southern and northern coastal extremities of the Namib Sand Sea, sinuous crestlines lead to sub-circular interdune patches at the base of the concave slip faces (Lancaster and Teller, 1988; Lancaster, 1989a). For dunes displaying particularly crescentic plan form, linguoid horn elements have been found to extend across the entire interdune as far as the next dune downwind. This interdune arrangement is seen on a large scale for the mega-barchanoids in the Liwa district of the United Arab Emirates. Here the horns of the large dunes extend to join the subsequent dune body and create cellular interdunes comprised of closed 'basins' (El-Sayed, 2000). Such an assemblage effectively divides the area between the ridges into separate enclosures.

Although of different dynamic origin, a further interdune pattern of similar appearance to that described above is found in the rectilinear pattern (or *aklé*) of dune networks (Cooke *et al.*, 1993). Here, the closely-spaced interdunes are all formed in continuous sand cover, and the pattern is a result of smaller ridges that dissect the interdune by developing from the primary transverse ridges. This is a result of the 'dune memory' property of the transverse ridge as a response to the main wind, and the influence of secondary elements of the wind regime that

lead to the dissecting forms (Warren and Kay, 1987). Such dissecting forms have been found to lie transverse to less frequent wind signatures within the overall wind regimes of the Wahiba Sands, Oman (Warren, 1988) and the southwest Tengger, China (Ha *et al.*, 1999) (Figure 1.1).

Figure 1.1 Closely spaced network dunes with dissected interdunes in Algeria (from Livingstone and Warren, 1996).

For smaller barchan dunes, where an interdune area is not so easily identifiable in terms of it being enclosed by two bedforms, the effective interdune is the space between the trailing horns and next downwind dune. This is particularly evident when barchans are arranged in corridors of offset 'trains', such as in the Skeleton Coast dune field (Lancaster, 1982a), Imperial Valley, California (Long and Sharp, 1964) and southern Morocco (Hersen *et al.*, 2004).

For star dunes, the shape of the intervening interdune is simply a reflection of the positioning of individual dunes. In this case, the interdunes are expansive, and occupy contiguous regions

that lie around the bedform without being divided by the dune into discrete interdune areas. This is particularly evident in plan view from the Dumont Dunes, California (Nielson and Kocurek, 1987) and the Gran Desierto, Mexico (Lancaster, 1989b). Referring back to the definition of interdunes by Ahlbrandt and Fryberger (1981), star dunes act as only 'partial boundaries' at best.

Hummel and Kocurek (1984) state that interdune areas are an integral part of aeolian sand seas, and part of this importance must be a result of their spatial extent. Linked to the fact that interdune shape is associated with the type of dune, the extent of the overall area that can be described as interdune also varies according to the variety of dune types surrounding it. In the Namib Sand Sea, the portions of linear dune areas which were estimated to represent the space between dunes ranged from between 38% and 73% of the total dune area. This depended on the complexity of the form, with a mean of 60%. For star dune regions, interdunes cover a mean of 48% of the total area. Elsewhere, for the areas dominated by crescentic dune forms, interdunes made up only around 10% (Lancaster and Teller, 1988). There are certain difficulties in delimiting the exact bounds of interdunes however, and the basis of the Namib percentage figures for spatial extent is simply what could be "...considered as lying in between the dunes themselves" (p. 93).

The arrangement of transverse dune forms in close proximity can mean that recognisable, flat interdunes are nearly eliminated, rendered virtually non-existent with the slip face of one bedform abutting the windward slope of the next feature downwind. This has been recorded for both small features, such as 2 m high reversing dunes in the Silver Peak dunefield, Nevada (Walker, 1999) as well as for much larger compound crescentic forms (up to 40 m high) in the Namib Sand Sea (Lancaster, 1989a). McKee (1983) stated that interdunes may be effectively absent altogether where one dune begins to climb up the windward slope of the preceding form. He illustrated one case in the Great Sand Dunes in Colorado, USA. Here the Sangre de Cristo Range blocks easterly passage of the dunes, and the crests of migrating transverse ridge dunes are unusually close, with no near-horizontal interdune sections. The dunes here overlap like roof tiles (a "shingle structure"), similar in appearance to the rectilinear pattern described earlier for network dunes.

1.2.2 Classification of interdunes

A simple classification for interdunes was proposed by Ahlbrandt and Fryberger (1981). Their approach sees the diverse range of interdune types split into two groups, which are divided by the surface nature of the interdune. They took the exhibited surface type as reflecting the dominance of processes operating within the interdune, and this led to the identification of *deflational* and *depositional* interdunes. Lancaster and Teller (1988) also subscribed to this type of classification for their investigation of interdunes in the Namib.

In addition to the division proposed by Ahlbrandt and Fryberger (1981) however, a third type of interdune may also be recognised on the basis of the dominant process operating within it. It has been suggested that particular interdunes may be *transportational* in their nature, where there is no net increase or decrease of sediment within the interdune over time. This has been proposed as a central consideration to a model for linear dune dynamics offered by Livingstone (1986).

DEFLATIONAL INTERDUNES

A deflational interdune is characterised by an absence of deposited sand, and these interdune types can display a diverse range of surface types. These typically include interdunes of exposed bedrock, non-aeolian deposited substrates and lag deposits (e.g. desert pavement) (see Table 1.1). These deflational surfaces are uncovered and kept bare by the dominantly erosive potential of the wind continuously removing sand.

Ahlbrandt and Fryberger (1981) suggested that bare interdunes are most likely to be associated with transverse dunes formed in unimodal wind regimes. This is supported by the data presented in Table 1.1, and also in findings from the Namib Sand Sea (Lancaster and Teller, 1988), White Sands (McKee, 1966) and Skeleton Coast (Lancaster, 1982a). Barchan and transverse dunes are commonly found at the margins of sand seas and in areas of high sand transport (Lancaster, 1995). For both these cases, there are reasons why the interdunes may be of an erosional nature. First, at the edges of sand seas and dune fields, sediment supply is limited, providing the opportunity for the formation of crescentic or transverse dunes (Wasson and Hyde, 1983). Second, the unimodal wind regimes of transverse dunes commonly generate high transport rates (especially with regard to barchans), such as the high energy corridors of sand movement that couple source and deposition areas. A consequence of this is that a typical wind in these regions will ensure that interdunes are consistently

subject to considerable erosive potential, resulting in the removal of sand cover. The interdunes that result therefore often exist as expressions of the underlying substrate. Sand in these corridors of increased transport is concentrated into dunes, and is subsequently conveyed in this form, passing along surfaces left bare of sand, such as gravels beneath barchan dunes at the south of the Namib Sand Sea (Corbett, 1993).

Table 1.1 A sample of deflationary interdune surface types.

Interdune Surface	Dune Type	Location	Source
Deflated bedrock	Barchan	Meob-Conception Bay coastal area of Namib Sand Sea	Lancaster (1989a)
Fluvial substrate	Barchan	Tsondab Flats, Namib Sand Sea	Lancaster (1980)
Sebkha	Barchan	Jafurah Sand Sea, Saudi Arabia	Glennie (1970), Fryberger *et al.* (1983)
Desert pavement	Barchan, simple transverse ridge	Skeleton Coast dunefield, Namibia	Lancaster (1982a)
Old aeolian substrate	Barchan, crescentic ridge	White Sands, New Mexico	Simpson and Loope (1985)
Alluvial substrate	Compound transverse	Algodones, California	Sharp (1979)

DEPOSITIONAL INTERDUNES

The most obvious type of surface for an interdune area where depositional processes are dominant is a covering of aeolian sand. These sandy interdune surfaces merge with the dune bodies, and act as a transitional facies between interdune and dune. Sedimentological differences exist between the sand in the interdunes and on the ridges, with the former generally coarser and less well sorted than for the dune bodies, as exemplified by the variation measured on Kalahari linear dunes (Livingstone *et al.*, 1999) and Taklimakan transverse dunes (Wang *et al.*, 2002). However, these distributions are not consistent. Whilst transverse dunes generally show finer sediments at the crest, linear dunes might reveal no distinct sediment texture pattern (e.g. the Ténéré Desert, Warren, 1972) or even a reversal of the

transverse dune norm with a coarser fraction at the crest (e.g. Kalahari, Thomas, 1988). Such differences have been attributed to the source material (Livingstone and Warren, 1996). In the interdune, there can be an obvious bi-modality in grain size distribution which reflects the presence of a fine fraction from the saltation load and a coarse group which is slow-moving and trapped in the interdune trough (Lancaster and Teller, 1988). The dune-interdune sedimentological differences are more pronounced when there is an input into the interdune of extraneous sediments, such as those delivered fluvially (Stanistreet and Stollhofen, 2002).

A relatively common presence within depositional interdunes where sand cover is total, and particularly those that separate linear dunes, are *zibars*. These features are low rolling 'dunes' which do not have slip faces, and typically display gentle height changes of 1–2 m over hundreds of metres (Holm, 1960; Lancaster, 1995). Composed of relatively coarse firm sand and devoid of vegetation, zibars are features that can be found in those interdunes which are characterised as being of a depositional nature, even irrespective of dune type as shown within the Rub' al Khali, Saudi Arabia (Holm, 1960). Zibars are frequently found in interdune environments, because their formation is encouraged in the relatively low-lying areas that interdunes represent between dunes.

TRANSPORTATIONAL INTERDUNES

The notion of a transporting interdune relates to a region between dunes that shows no net change in the sediment contained therein. In transporting interdunes, moving sediment effectively passes from one dune form to another.

Interdunes dominated by this process were described by Livingstone (1986) as part of an explanation for the dynamics of large complex linear dunes. For such dunes in the Namib Sand Sea, Livingstone found that wind speeds and therefore the sediment carrying competence of the wind were more or less constant through the interdune corridors. This was a consequence of the secondary flow patterns caused by the dunes being restricted to the upper parts of the large dune forms. Lee-side airflow therefore recovered on the dune body and was of a steady strength by the time it entered the interdune, remaining so for the distance across the whole interdune. Sand was therefore not prevented from leaving the dune but, if entrained on the lower downwind slopes of the upwind dune, was carried across the interdune

and onto the next dune. The steady flow within the interdune ensured that sediment was neither deposited nor eroded within this region.

Given the suggested mechanism that would create such transport dominated interdunes, this type of interdune may be intrinsically related to large dunes given the effect of the dune size on the secondary flow, and large linear dunes in particular when the effect of the formative bimodal winds is considered. The bi-directional winds may help to maintain the dune (and therefore interdune) sediment balance over time (Livingstone, 1986).

1.2.3 Summary of the nature of interdunes

The spatial distribution of interdune types shows considerable diversity resulting from the dominant processes operating within them. For instance, a fluvial influence will only be exerted on interdune surfaces that are in the vicinity of ephemeral watercourses, and for deflational interdunes, bedrock exposures will be commonly located in areas of high sand transport rates, such as the corridors linking aeolian sediment sources and sinks (e.g. Lancaster, 1982a). Ahlbrandt and Fryberger (1981) stress that one consequence of the migration of mobile dunes would be a change in the interdune shapes and sediments therein, which demonstrates a dynamic relationship. It follows that another feature of this relationship would be that changes in sediment transport rates over time will also lead to changes in the type of interdune.

Mabbutt and Wooding (1983) have suggested that whilst predominantly determined by the control exerted by airflow, for the case of linear dunes in the northwestern Simpson Desert, another significant control on the bedforms is "...in part the nature of the exposed intervening surface" (p. 68). This has been demonstrated through changes in these intervening surfaces being identified as the cause of relatively rapid spatial shifts in the equilibrium pattern of the dunes, where a key for dune equilibrium is the spacing.

1.3 The context of interdune dynamics for dune systems

There is considerable uncertainty surrounding the extent of the geomorphological significance of interdunes and the operation of processes within them. This situation is in spite of the considerable importance that the study of interdune dynamics may have for our understanding of sand dune systems as a whole.

In particular, through studying the dynamics of interdunes, our understanding of their potential role in controlling dune spacing may be improved. A characteristic of aeolian dunes is that they frequently exist in patterns where their form and mode of arrangement is conspicuously repeated. Satellite imagery and aerial photographs have been especially effective at showing evidence of these often impressive layouts at the regional scale (e.g. Breed and Grow, 1979). Cooke *et al.* (1993) used the term "replication" for the succession of like dunes. Within such patterns, it is the factors which control the spacing of bedforms which are one of the least well understood areas of dune morphology (Lancaster, 1988).

A range of theories exists to explain the spacing exhibited between dunes, with each theory crucially incorporating a different view concerning the dynamic role of interdunes, and in turn, the significance of flow within the interdunes. Livingstone and Warren (1996) pointed out that the models are not mutually exclusive, and that the hypotheses are better developed for dunes forming underwater. Four models can be broadly distinguished.

1.3.1 Delayed response model

The effect of kinematic instability within the airflow is the basis of one idea for dune spacing, which was largely derived from Kennedy's (1969) work on sub-aqueous flows. The model incorporates a delay factor that magnifies the initial disturbance to the airflow (caused by the first initiated dune) until the instability reaches an equilibrium size and shape. Once this equilibrium is achieved the pattern subsequently becomes propagated downstream. The first delay caused by disturbance is to the airflow, which then manifests itself as a perturbation in the longitudinal distribution of sediment transport capacity which establishes the amplitude of bedforms. Problematically, this model includes a role for suspended sediment which is unrealistic for the aeolian setting (Cooke *et al.*, 1993).

1.3.2 Organised turbulence model

The organised turbulence suggestion incorporates a pre-existing pattern in the flow which becomes anchored by the original bedform. The regularity of flow turbulence establishes the position of the dunes, and therefore their spacing. Yalin (1977) maintained that the wavelengths of dunes are already fixed before their growth actually begins.

In particular, linear dunes have often been held up as evidence of organised turbulence as a control on dune formation. The roll-vortex hypothesis was advanced by Bagnold (1953) who

suggested double helical roll-vortices were established by convection from the heated desert surface, coupled with the influence of a geostrophic wind. These vortices operating in tandem would act to sweep sand toward one another, forming a central linear dune. In this case, the corridor-type interdunes apparent in linear dune fields might be produced, and their pattern and form controlled by, the roll-vortices themselves (Figure 1.2).

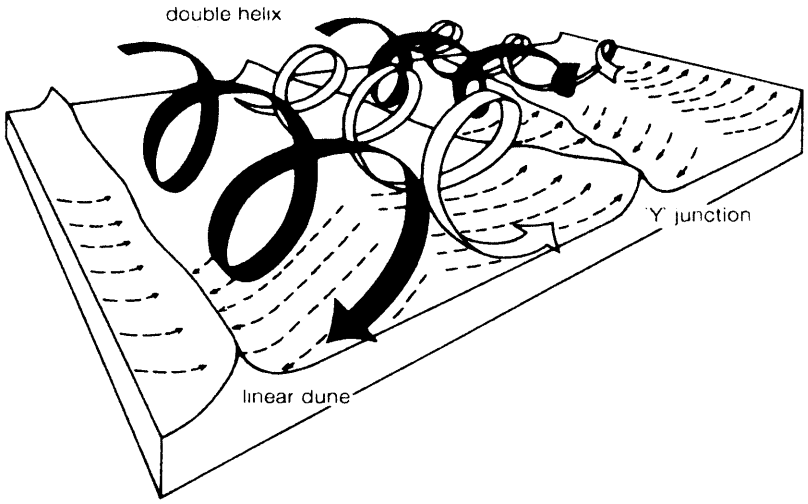

Figure 1.2 Roll-vortices as elements of organised turbulence in a model for controlling linear dune spacing (from Warren, 1979).

Despite several supporters for this mechanism of dune spacing (e.g. Hanna, 1969; Glennie, 1970; Folk 1971; Tseo 1993), empirical data from studies on linear dunes have discredited this as a control for this dune type.

1.3.3 Flow response model

Within the flow response model, interdune spacing is governed by the length downwind of a dune required for flow to recover to its upwind characteristics given the perturbation to primary flow generated by a dune. The relevant characteristics of flow include the flow velocity profile and its turbulent structure (McLean and Smith, 1986; Nelson and Smith, 1989).

Flow response is grounded in the existence of lee-side secondary flow patterns which form due to the perturbation caused by the dune. Flow separation at the brink results in a separated flow that re-attaches at some distance downwind. At the point where flow re-couples with the surface, the growth of an internal boundary layer (IBL) starts close to the surface and under the wake and develops in height with downwind distance (Figure 1.3).

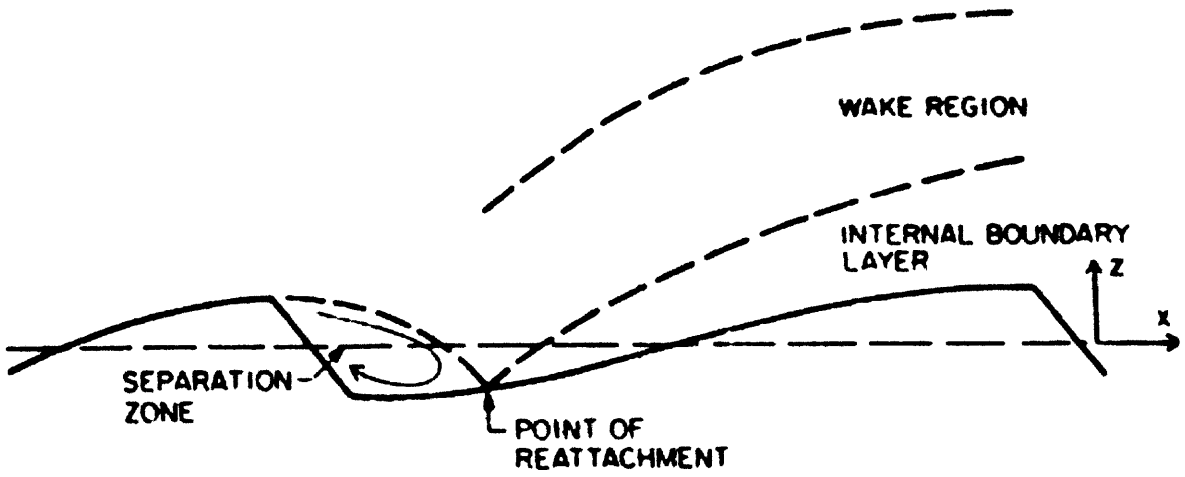

Figure 1.3 Schematic diagram showing the key structures of the flow response model for dune spacing (after McLean and Smith, 1986).

Flow acceleration within the IBL is initially driven at the expense of the wake, and near bed velocity and bed shear stress increase. An equilibrium in shear stress is achieved when momentum input from the wake is balanced by deceleration within the IBL, caused by its vertical growth, or thickening. When there is no downwind bedform interfering with this development, the distance where shear stress reaches equilibrium sees a change from erosion and transport to deposition. This establishes the downwind bedform. The flow response model therefore holds that dune spacing is controlled by the downwind distance before deposition can occur, which is a factor of the IBL development after the disturbance to primary flow by the upwind dune. The same erosion and deposition pattern exists when a subsequent downwind dune *is* present. As a result, the model accounts for not just replication but it also controls dune shape and spacing once they have been established.

1.3.4 Dynamically neutral model

The three previous groups of theories concerning dune spacing all have the nature of interdune flow as intrinsic to the distance between dunes. A fourth idea holds that interdune dynamics have no significance for dune geomorphology, and interdunes can therefore be classed as 'dynamically neutral' in terms of dune development. In this model, the airflow pattern and the processes operating within the interdune are not responsible for the spacing exhibited by dunes. Interdune dynamics have no role in this respect. Instead, the interdune spaces are merely a consequence of the position of the dune bodies themselves.

If interdunes are considered dynamically neutral in terms of spacing, then the types of controls that do govern spacing may be macro-controls, such as the effects of upwind sand supply and regional wind regime. Dune spacing will be a reflection of the interaction of these variables, and the spacing represents the statistical expression of this interaction.

The influence of these types of factors has been considered by Lancaster (1988). Lancaster suggests that the relation between dune height and spacing is a consequence of the amount of sand available for the construction of dunes, and the wind regime (the directionality and strength). A healthy sand supply and a wind regime that encourages the deposition of sediment on dunes are dune-building conditions, which in turn tend to result in dune height increasing more rapidly than dune spacing. Lancaster's data suggested this may be the case for complex linear dunes in the Namib, and star dunes in the Gran Desierto. This model therefore also accounts for the different evolution of the McKee (1979) dune groups (e.g. simple linear dunes extending, star dunes accreting). The Lancaster investigation is also interesting in that it goes some way to revealing the degree of similarity in the height and spacing relationship for dunes of the same type but in different dunefields. In discrete locations, similar dune types will exist in conditions of different wind regimes and sediment supply volumes, both of which could affect the spacing, and consequently the strength of the height/spacing relationship.

1.4 Approaches to the study of dune geomorphology

Given the uncertainty that exists concerning the controls on dune spacing, it is worthwhile to review the approaches that have been employed to investigate this and other aspects of dune morphology. As befits the wide study of aeolian dune morphodynamics and behaviour, a variety of approaches has been utilised in the research.

First, there is the approach based on the empirical observation of variables that quantify the key processes operating on and around dunes. This includes direct measurement of flow velocity, turbulence elements and sediment transport (see Lancaster, 1996). Such measurements can be conducted either in the field or through the reproduction of field conditions within wind tunnels (e.g. Tsoar *et al.*, 1985; Castro and Wiggs, 1994). As an approach, this technique has produced a vast wealth of process information for studies on all kinds of aeolian dunes (Table 1.2).

Table 1.2 A sample of empirical studies on different types of aeolian dunes.

Transverse and Reversing Dunes
Burkinshaw and Rust, 1993; Frank and Kocurek, 1996a, 1996b; Lancaster, 1985a; Lancaster *et al.*, 1996; McKenna Neuman *et al.*, 1997, 2000; Mulligan, 1988; Sweet and Kocurek, 1990; Walker, 1999; Wang *et al*, 2002; Wiggs, 1993; Wiggs *et al.*, 1996.
Linear Dunes
Lancaster, 1989a; Livingstone, 1986; Tseo, 1993; Tsoar, 1983a.
Star Dunes
Lancaster, 1989b.
Other Desert Dunes
Havholm and Kocurek, 1988 (draa); Tsoar, 1983b (echo and climbing dunes); Ha *et al.*, 1999 (reticulate).
Coastal Dunes
Arens *et al*, 1995; Hesp and Hyde, 1996; Hesp *et al.*, 2005.

Second, there is an approach that can be identified by the varied use of mathematical models to study dunes in order to replicate natural dune behaviour. This is a very broad group as many different aspects of dune study have been investigated through the development and application of models (see Wiggs, 2001).

Early attempts strove to model aspects such as the windspeed controlled sand transport and resultant dune dynamics of isolated bedforms (Howard *et al.*, 1978; Wipperman and Gross, 1986). Improved field data have certainly helped models to become more sophisticated. Now, dune simulation also includes attempts to reproduce the turbulence field around dunes (van Boxel *et al.*, 1999) as well as the sand transport that is dynamically coupled to turbulence (van Dijk *et al.*, 1999). Computational Fluid Dynamics techniques have also been taken from their fluvial origins to be applied to dune flow fields (Parsons *et al.*, 2004a, 2004b). Furthermore, recent advances in modelling have allowed the interactions between dunes to be investigated at the scale of multiple bedforms in dune field situations (e.g. Momiji *et al.*, 2000; Bishop *et al.*, 2002; Lima *et al.*, 2002; Hersen *et al.*, 2004). A key morphometric attribute of the dune field is the spacing between dunes and Schwämmle and Herrmann (2003) have recently attempted to model collisions of barchans. When dune spacing is considered along with the relative part played by interdune dynamics, bedform collisions represent a product of the change in spacing between forms over time. Momiji *et al.* (2000) investigated the passage of

transverse dunes and the equilibrium of spacing between the bedforms which linked interdune form explicitly with transport shadow zones in the lee of the dunes. The use of a modelling approach has been demonstrated to be highly applicable to the study of many different aspects of dune behaviour, with notable advances regarding simulating the spacing between dunes.

A third approach to studying dunes has been the application of *complex systems theory* in a bid to understand better sand dune behaviour. Referring back to the role of interdunes within the four models of dune spacing presented in Section 1.3, complex systems approaches essentially treat the interdune area as being dynamically neutral (Section 1.3.4). Complex systems aim to deal with the complexity inherent in certain earth surface systems (Phillips, 1999). For sand dunes in particular, it has been suggested that particular attributes of the dune system allow it to be described with relation to the theory of non-linear dynamical systems (NDS) (Werner, 1995). Such attributes include the fact that the aeolian sand transport which drives dunefield evolution is non-linear (i.e. grain flux does not depend linearly on wind velocity), and that it is a dissipative process (losing energy as it operates). These non-linear characteristics of fluid flow and sand transport imply that dunes can be modelled in a way that sees understanding of the fundamental mechanisms being bypassed (Werner and Kocurek, 1999).

Dune fields typically tend to show an evolution to a finite quantity of steady states, termed 'attractors', and reach these states from broad initial conditions, where the attractors are the dunes themselves (Anderson, 1996). Dunes could therefore be said to show emergent behaviour. As such, it has been argued that sand dune systems can be classified as a type of NDS called complex systems. Emergent behaviour is the type of self-organising behaviour over large time and space scales that, whilst based on microscopic physics, is decoupled from the small scale (Werner, 1995). It was through characterising a dunefield as a complex system that the position, behaviour and evolution of dunes were accurately simulated in a qualitative fashion by way of a computer algorithm (Werner, 1995; cf. Nishimori *et al.*, 1998 and Momiji *et al.*, 2000). In another study, the complicated process of variation in bedform spacing was simulated, using similar complex system principles (Werner and Kocurek, 1997).

Complex systems are considered as an alternative to reductionist attempts to produce models of dunefield evolution, the latter of which have proven largely unsuccessful. Werner (1999) argues that this is because the reductionist approach may be too simplistic, and does not

provide a suitable methodology to simulate the non-linear, open systems that characterise natural landform patterns, including dunes. For dune systems, Werner (1995) states that the complicated nature of air flow and the related sand erosion, transport and deposition over a dune means that a satisfactory reductionist path of understanding from the physics of sand transport to dune evolution is not currently attainable. He considers the attempts made to characterise dune systems based on reductionist methods, and notes the limited application of many of these dune formation models, since the models have been of an empirical nature (Werner, 1995).

Furthermore, the imperfection of the relationship between dune height as a control for spacing demonstrate the difficulties for the reductionist approach to the study of these variables. Certain attributes of non-linear, complex systems suggest that new ways of modelling may characterise natural landform patterns, including dunes, in a more satisfactory manner (Werner, 1995; 1999).

1.4.1. Investigating the role of interdunes for dune spacing

The kinematic instability, organised turbulence and flow response models presented in Section 1.3 have all been suggested as a mechanism for the replication of sub-aqueous and sub-aerial dunes, and each of them sees the flow in the interdune as a having a role in this. The notion of dynamic neutrality, however, does not imply a significant geomorphological role for the flow patterns within interdunes. In a conceptual consideration of the potential geomorphological significance that interdune flow has for controls dune spacing, the 'flow response' and the 'dynamic neutrality' models best represent end points in a continuum.

The four models presented above account for the replication of similar dune forms, and also the spacing between each successive bedform. Associated with each of these mechanisms governing spacing however are different roles for the flow and operation of geomorphological processes within the interdunes. It is apparent, therefore, that it remains necessary to investigate interdune dynamics in order to explore their nature and the possible extent of their role. Furthermore, it is argued here that the empirical investigation of these fundamental processes represents a well-founded way to lead the research.

Such an assumption regarding the methodology for the present study is grounded in the successful prior application of such an approach. For geomorphology in general, significant

benefits have been made from a reductionist approach to the study of landforms. Dedicated empirical studies see carefully designed and executed experiments applied to smaller scale constituent parts (e.g. landforms) in order to drive investigations of larger geomorphic systems (Harrison, 1999). This has undoubtedly been the case specifically for aeolian geomorphology, beginning with Bagnold (1941). Detailed studies into the processes operating on single dunes have done much to increase our understanding of the prevalent controls for dune morphodynamics (Table 1.2). Despite the benefits of, and the widespread application to dunes themselves, the empirical approach remains largely unapplied to the interdune portions of dune areas. The majority of field enquiries that have included mention of the interdune, and have conducted measurements of geomorphologically relevant variables within them, have done so whilst remaining focused on the dune body itself. Whilst these studies have yielded flow and sand transport data from interdune areas, the interdunes themselves have essentially been dealt with only as an extension of the dune lee-side (e.g. Ha *et al.*, 1999; Walker, 1999).

The derivation of data from empirical investigations that are focused on single dunes is recognisable as a fruitful approach, and one which has formed the foundations for much of our understanding of dune dynamics. Therefore, a legitimate first stage for an investigation into the potential significance of interdunes is the measurement of the fundamental processes operating within them. This can be successfully led by a reductionist-based detailed study of flow within interdune situations.

Given the three broad approaches to studying dune geomorphology presented earlier, the case for the empirical study of interdune airflow is further strengthened when the relationship between the possible approaches is considered. For both the modelling and complex systems methods, empirically derived data are vital to test the accuracy of any developed model, and to assess the degree to which complex systems successfully reflect natural patterns (Phillips, 1999). It is worth noting that the output of Werner's (1995) purely complex systems-based consideration of dune field modelling was greatly improved when even simple findings from flow dynamics measured in the field were incorporated (Momiji *et al.*, 2000). The relative lack of field data for flow velocity, direction, sand transport and especially field-derived turbulence estimates in interdunes gives a small scale observation of these key geomorphological variables even more utility.

1.4.2 Primary aim of the research

The main aim of this research is to characterise the flow patterns within several different types of interdune in order better to understand the operation of geomorphological processes therein. The use of an empirical approach to achieve this is justified in light of the benefits found for similar research over the dune itself. The implications of the process data are used to further investigate the significance of interdune dynamics for the sand dune system as a whole.

1.5 Flow over dunes and across interdunes

It has been argued here that the empirical study of flow within interdunes is essential to develop our understanding of the role that interdune processes play within the dune system, and especially in governing bedform spacing. It is therefore necessary to review briefly our existing understanding concerning the way in which dunes are known to influence airflow. With an appreciation of what is already understood, the findings of the current study will be better grounded and discussed.

The body of knowledge concerning the influence of dunes on airflow was increased through a recognition by aeolian geomorphologists that similarities in morphologies meant much physical theory could be obtained from meteorological and engineering-based studies of boundary layer flow over hills (e.g. Jackson and Hunt, 1975; Taylor *et al.*, 1987; Hunt *et al.*, 1988). This original research has subsequently been fortified by different types of work specific to studying flow over dunes. There is now a well-developed body of knowledge concerning different elements of flow over sand dunes themselves, and the morphodynamics that are coupled with flow interaction with an erodible form (Wiggs, 2001).

1.5.1. Dune windward slope flow

Our understanding of flow over dunes can be divided into different parts of the dune, and for the windward slopes of dunes, studies have been conducted on many different dune types.

For airflow approaching transverse to the dune crest, wind velocity will initially slow down in the upstream area, achieving a minimum immediately before the dune, at the toe of the stoss slope (Tsoar, 1985; Wiggs, 1993). The explanation for the initial decrease in wind velocity is based on the increasing pressure gradient at this point, caused by the obstacle effect of the

dune on the approaching flow. This is reflected in the Bernoulli effect, as it has been applied for low hills (Hunt and Simpson, 1982),

$$p + \frac{1}{2} eU^2 = \text{constant} \qquad \text{Equation 1.1}$$

where p = static pressure, e = is dynamic pressure. It follows that U (mean velocity) must decrease if p rises.

Windflow accelerates on the windward slope of the dune, where static pressure is reduced, and a generally continual velocity increase occurs with a maximum at or just before the crest (Lancaster, 1985a; Mulligan, 1988; Wiggs *et al.*, 1996). The acceleration is due to the effect of the dune projecting into the atmospheric boundary layer, which leads to the compression of streamlines in keeping with the laws of continuity in fluid dynamics. Differences in dune form can exert a varied control on the nature of the airflow modification caused by the dune. The fractional speed-up ratio (δs) has been found to be well approximated for hills (Jackson and Hunt, 1975), and subsequently for sand dunes, (Tsoar, 1985; Lancaster, 1985a) by the following expression

$$\delta s = 2h / L \qquad \text{Equation 1.2}$$

where h = dune height and L = length at half height parallel with wind. The variables in the expression relate to the shape of the dune, and the formula goes some way to characterise the importance of dune form for the degree of acceleration produced up the windward slope. The height value is a factor of the dune type and shape, and the length value can be effectively modified with the direction of the wind. Studies of speed-up on the stoss slope often involve winds blowing near perpendicular to the dune crest, where compression of streamlines is greatest (e.g. Burkinshaw and Rust, 1993; Frank and Kocurek, 1996a). The importance of this factor has been demonstrated, for example, on approximately north-south trending Namibian linear dunes (Lancaster, 1985a). Mean crestal speed-up ratios were 0.80 for westerly winds, 0.51 for south-westerly winds and 0.33 for south-south-westerly. This difference reflects the effective length presented by the dune to each wind direction, with the acceleration effect exerted by the dune reducing as winds became more parallel with the dune, and L increased. In this situation, the compression of streamlines is reduced (Lancaster, 1985a).

Lancaster (1985a) based a study of dune dynamics on the change in mean velocity over dunes, and its effects for the competence of the wind to transport sediment. Sand transport capacity (q) is linked to flow velocity with the following relationship

$$q \approx u_*^3 \qquad \text{Equation 1.3}$$

(where u_* is shear velocity, see also Equation 1.4) (Bagnold, 1941). The flow acceleration generates increasing shear stress and transport on the windward flanks of dunes and deceleration in the lee leads to deposition there, which in turn accounts for the downwind movement of migratory dunes. However, an interesting feature in relation to dune-influenced airflow and sediment transport is to be found at the stoss toe. Whilst a decrease in wind velocity is measured at this point, a complementary reduction in actual shear velocity is missing, evident by the fact that this part of the dune is not an area of deposition (Wiggs, 1993). Wiggs *et al.* (1996) suggested transport rates are maintained in this region (Zone A, Figure 1.4) due to a compensatory shear stress increase due to turbulence induced by concave streamline curvature (Bradshaw, 1969) at the upwind toe also noted in hill studies (e.g. Gong and Ibbetson, 1989). Thus, there is no deposition of sand at the toe in spite of the localised wind velocity retardation. The effects of flow behaviour in this upstream portion of the dune ensure that the toe is an area of erosion, and the dune moves downwind. Wiggs *et al.* (1996) produced a conceptual model of dune morphodynamics based upon the streamline curvature effects on flow stability (Figure 1.4).

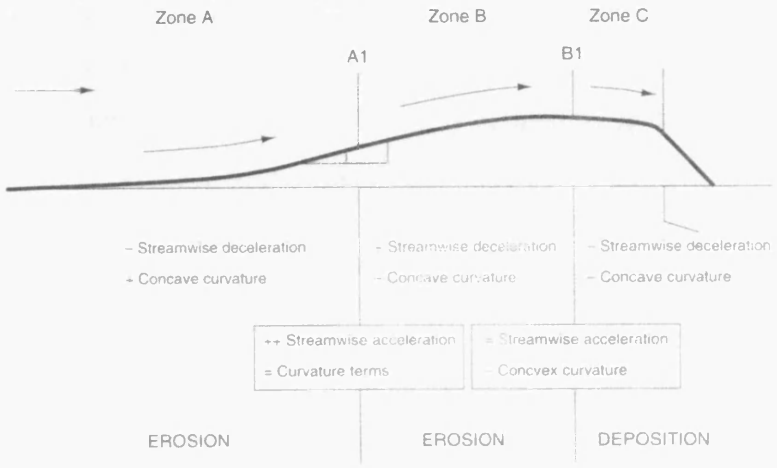

Figure 1.4 A model for dune dynamics based on an equilibrium between slope morphology and the effects of stream-wise acceleration and streamline curvature (from Wiggs *et al.*, 1996).

One important consequence of the acceleration of wind along the stoss slope, is that it prevents the accurate derivation of the expression for the vertical velocity gradient, or shear velocity (u_*) (see Walker and Nickling, 2002). Shear velocity is the conventional proxy for shear stress at the surface since shear stress is very difficult to measure directly in field settings:

$$\tau_0 = \rho_a u_*^2 \qquad \text{Equation 1.4}$$

where τ_0 is surface shear stress and ρ_a is the density of air. For a flat surface with neutral stability, shear velocity can be estimated from regression of velocity measurements against height, where a log-linear relationship is assumed to exist, since shear velocity is taken as proportional to the gradient of the velocity profile. In turn, the relationship between aerodynamic roughness (z_0), shear velocity (u_*), wind velocity (u_z) at height (z) and κ is von Karman's constant (c. 0.4) is described by the 'Law of the Wall':

$$\frac{u}{u_*} = \frac{1}{\kappa} \ln \frac{z}{z_0} \qquad \text{Equation 1.5}$$

However, since there is a breakdown in the log-linear velocity profile on the windward slope of dunes due to flow acceleration (Mulligan, 1988; Burkinshaw *et al.*, 1993; Frank and Kocurek, 1996a), this method for obtaining shear velocity is invalidated. Shear stress is only constant within a very thin 'inner surface layer' (ISL) (Jackson and Hunt, 1975) which might be approximately 1 cm for a dune around 10 m high (McKenna Neuman *et al.*, 1997). Because of this, velocity measurements over dunes are made within a 'shear stress layer' (SSL) where shear is still significant as a proxy for sampling actual surface shear stress. The height of the whole inner region (l), ISL and SSL, is defined by Jackson and Hunt (1975):

$$l = \frac{2\kappa^2 L}{\ln l / z_0} \qquad \text{Equation 1.6}$$

where κ is von Karman's constant, z_0 is surface roughness and L is dune length at half dune height. Crucially, it is within the depth l that the greatest changes to the airflow in terms of shear stress and turbulence that are caused by the dune take place, where shear changes with height within the layer (Zeman and Jensen, 1987; Kaimal and Finnigan, 1994). Velocity

profile measurements made partly outside of this inner layer have yielded an apparent decrease in shear velocity up the windward slope despite velocity increase at all heights (e.g. Frank and Kocurek, 1996a).

1.5.2 Dune lee-side flow

Despite the fact the lee-side region has received less research attention than the dynamics of windward slopes, a certain amount is understood about flow in the lee. Key controls on the occurrence of separation were found to be dune geometry (also altered by incident wind angle) and atmospheric stability (Sweet and Kocurek, 1990). When flow does become de-coupled from the dune at the brinkline, a wake region with an identifiable structure has been found to exist. Referring to previous fluvial work (McLean and Smith, 1986), Frank and Kocurek, (1996b) described the wake in detail from kinked-velocity profiles observed during field studies in the lee of transverse dunes (Figure 1.5).

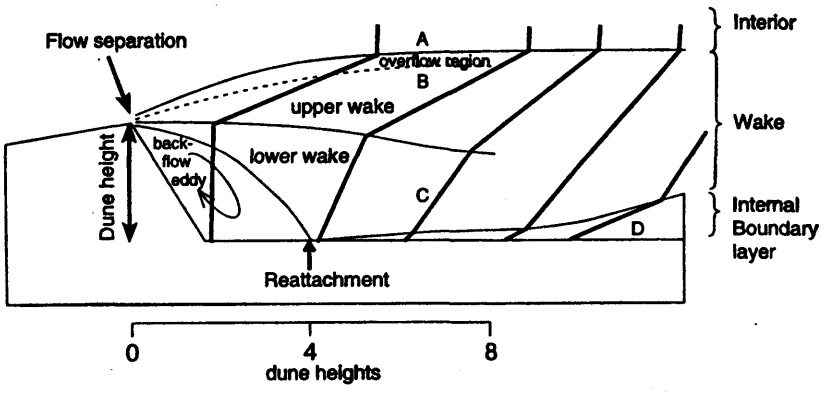

Figure 1.5 The generalised pattern of velocity in the lee of dunes with perpendicular incident flow (from Frank and Kocurek, 1996b).

On separation the accelerated flow from the brink overshoots to form the overflow region at height in Figure 1.5. This high velocity region creates lower pressure relative to the separation cell below it (through the Bernoulli Principle, Equation 1.1), and this causes a coherent eddy of flow directed back toward the dune slip face (Hoyt, 1966; Inman *et al.*, 1966; Sweet and Kocurek, 1990). Speeds are low in the lee eddy due to the expansion of streamlines seen to occur beyond the brink. Between the low velocity of the separation cell and the faster wake portions lying above it, a layer of high shear exists (Walker, 1999). The downwind limit of the separation cell is determined by the point where this free shear layer re-attaches to the surface. Frank and Kocurek (1996b) found that for small dunes (under 5 m), the mean re-attachment

distance is the equivalent of approximately 4 dune heights (h) downwind (Figure 1.5). This value was in very good agreement with fluvial equivalents (e.g. Engel, 1981; Nelson and Smith, 1989). Results of computational modelling of downwind flow fields have highlighted the effect that the simple height parameter has on re-attachment length (Parsons *et al.*, 2004b).

At re-attachment, an IBL starts to develop, a requirement that was integral to the mechanism of the flow response model in Section 1.3.3. Momentum from the still relatively faster upper wake is exchanged downwards toward the developing IBL as it grows with distance downwind. Figure 1.5 shows that Frank and Kocurek (1996b) found the velocity profiles of the upper and lower wake to be roughly equal by 8 h, indicating recovery of the wake profile, whilst the IBL still grew at the surface. Lancaster (1989a) found that it was only at 10-15 dune heights downwind of dunes that values for the wind characteristics returned to unperturbed upwind values. Significantly, for the dynamics of the dune lee-side area, the flow complexity in terms of disruption of log-linear velocity profiles, prevents the application of the 'law of the wall' approach (Equation 1.5) for deriving shear velocity. Similarly, the Jackson and Hunt (1975) model is redundant in the lee since its development for rounded hills does not equip it to deal with reversed flow, due to problems with turbulent closure models (Taylor *et al.*, 1987; Walker and Nickling, 2002).

Our understanding of the variation in turbulent flow over bedforms is largely derived from investigations of sub-aqueous features in the flume and field (e.g. Bennett and Best, 1995; Kostaschuk, 2000; Maddux *et al.*, 2003a, 2003b; Nelson *et al.*, 1993). The shear layer is a highly turbulent region and it influences airflow for long downwind distances through wake flapping and eddy shedding related to the layer (Kiya and Sasaki, 1983). Turbulence levels have been found to reflect this far downwind of dunes in the few sub-aerial dune lee-side studies with such data (Warren and Knott, 1983; Walker and Nickling, 2003). At the point of flow re-attachment, the mean surface stress will be low, but instantaneous variation is high, thus enabling entrainment and transport (Nelson *et al.*, 1995). Wiggs (2001) stressed that the apparent link between the aeolian and fluvial environments may provide an approach to increase our understanding of turbulence.

1.5.3 Flow in interdunes

The data on flow within interdunes from previous studies tend to be extensions of observations made in the immediate lee of dunes, with the interdune not being investigated

specifically. For instance, Ha *et al.* (1999) measured velocity throughout a small interdune section as part of a dune network, but failed to comment on the interdune flow patterns. Details of the flow between paired Namibian transverse dunes were presented by Lancaster (1985a; 1989a), who found that a considerably greater up-stoss acceleration was exerted on the downwind dune of pairs than for isolated dunes. Other than that the interdune flow was merely described as "highly variable in strength and direction" (Lancaster 1985a: p. 584).

There does however appear to be an improved realisation as to the potential significance for the processes occurring in interdunes. As such, interdunes as a feature in their own right are beginning to attract research attention through an identification of the significance of the secondary flow element of dune form-flow interaction (e.g. Walker, 1999; Walker and Nickling, 2003). In the wind tunnel study of Walker and Nickling, lee-side surface shear stress was measured but the interdune extended only 0.5 h downwind. This produced information on only the most limited of interdune distances, where dune influences on flow still dominated. Velocity through some relatively long, flat interdunes was sampled as an effective continuation of the lee by Frank and Kocurek (1996b). These findings had an interesting significance since they commented on the geomorphological implications of accelerating flow through the interdune, allowing for features of the deflational class. They also suggested the development of a second IBL at the downwind dune toe (cf. Frank and Kocurek, 1996a).

1.6 Aims and objectives

Flow patterns and processes occurring within interdunes are potentially of considerable relevance for increasing our understanding of the sand dune system as a whole. Despite the possible benefits for the further understanding of dune systems that interdunes hold, their significance remains under-investigated. Furthermore, in order to improve our level of understanding for interdunes toward that currently seen for dunes themselves, methods of empirical study that are dedicated to the interdune form a valid approach. To achieve a better appreciation of the role of interdune dynamics in the sand dune system, the operation of key geomorphological processes must be observed.

This project has an overall aim to increase our understanding of the geomorphological significance of a variety of interdune types in transverse sand dune areas. The aim will be achieved through two objectives:

1. To obtain data on geomorphologically relevant variables within transverse dune interdunes, in particular, the measurement of flow velocity, direction and turbulence.

2. To use the results from (1) above to characterise observed interdune dynamics and investigate the geomorphological significance of the various interdune types.

1.7 Structure of the thesis

Chapter 2 deals with the field sites and the methods employed in the fieldwork. In Chapter 3 the results of the study are presented, and explained (Objective 1, above). Chapter 4 is a discussion of the implications of the collected data. It represents an investigation into the significance of interdune dynamics for the overall geomorphology of the sand dune system (Objective 2, above). Finally, Chapter 5 draws together the conclusions of the project.

Chapter 2
Methods

2.1 Introduction to and aims of the fieldwork

This chapter relates to the strategy of the fieldwork, the selection of the study sites, the experiments undertaken for data collection and subsequent data processing.

Given the research neglect concerning the dynamics of interdunes which was highlighted in the previous chapter, fieldwork was reasoned to be an essential requirement in order to try and increase our current understanding of interdunes. In this case, the measurement of fundamental processes in natural settings would enable a variety of interdunes to be examined by using a consistent approach to their study. The twin aims of the fieldwork formed the strategy to accomplish the overall project aim:

1. To make detailed measurements of variations in the velocity, direction and turbulence of airflow over isolated crescentic dunes.

The research approach was to undertake an initial study of the simplest dune-influenced flow situation, that of an isolated crescentic dune. This was in order to collect a variety of data which would lead to the characterisation of a control airflow situation. Results from the flow conditions measured within interdunes could then be compared to the flow conditions for the case of the individual dune. It was believed that such an approach would lead to a better understanding of the processes occurring within the studied interdunes. Given the recognised importance of dune shape for flow re-attachment length (Sweet and Kocurek, 1990), and therefore for interdune flow, there was an intention to sample downwind of a crest-brink unified and a crest-brink separated dune.

2. To characterise the patterns of flow velocity, direction, turbulence in transverse dune interdune areas.

The operation of key geomorphological processes within interdunes are central to producing an understanding of the significance of interdune dynamics. Velocity and turbulent stresses are elements that are responsible for imparting shear stress to the surface, which in turn drives sand transport. The strategy behind the study was to investigate flow patterns for a variety of relatively simple interdune environments. These would be manageable examples in terms of the dominant wind regime, size and type of the bounding dunes as well as the physical extent

and topography of the interdune. In an attempt to increase the breadth of the study, it was planned that a range of different types of interdune would be examined, including those with depositional and erosional surfaces as discussed by Ahlbrandt and Fryberger (1981). These contrasting interdune types represent the dominance of different processes, a fact which may have implications for interdune dynamics.

2.2 Field sites

With the specific study site requirements governed by the aims in mind, isolated dunes and a pair of interdunes were selected for detailed investigation from two field sites in the Skeleton Coast dune field, Namibia. Another two interdunes were chosen at a location within the delta of the Kuiseb River, in the north west part of the Namib Sand Sea (Figure 2.1).

Figure 2.1 Location of the two study areas within Namibia. See Figures 2.2 and 2.3, respectively, for smaller scale maps detailing the Skeleton Coast and Kuiseb Delta study sites.

2.2.1. Skeleton Coast field site

The Skeleton Coast dune field in northwestern Namibia is a thin belt of transverse and barchanoid dunes that stretches parallel with the Atlantic coast for around 150 km. The geomorphology and climate of the region was described in a detailed study by Lancaster (1982a). A particular feature is the coastal setting and the dominance of the strongly unimodal onshore winds which are responsible for the dominantly transverse bedforms. Lancaster used five years of data from the Möwe Bay climate station (approximately 75 km north west of Terrace Bay, Figure 2.2) to determine that 98% of annual sand flow according to the Bagnold (1941) formula was from the sector south southwest to south southeast, and that sand moving winds (over 4 ms^{-1}) blew for 47.2% of the time. In then applying Fryberger's (1979) weighted equation to the data, Lancaster reported that the wind regime could be classed as an intermediate-high energy narrow unimodal variety (also Brimelow and van Heerden, 1996).

For the study of the isolated dunes, an area of suitable barchan dunes was found at the southern margin of the Skeleton Coast dune field (Field Site 1 in Figure 2.2).

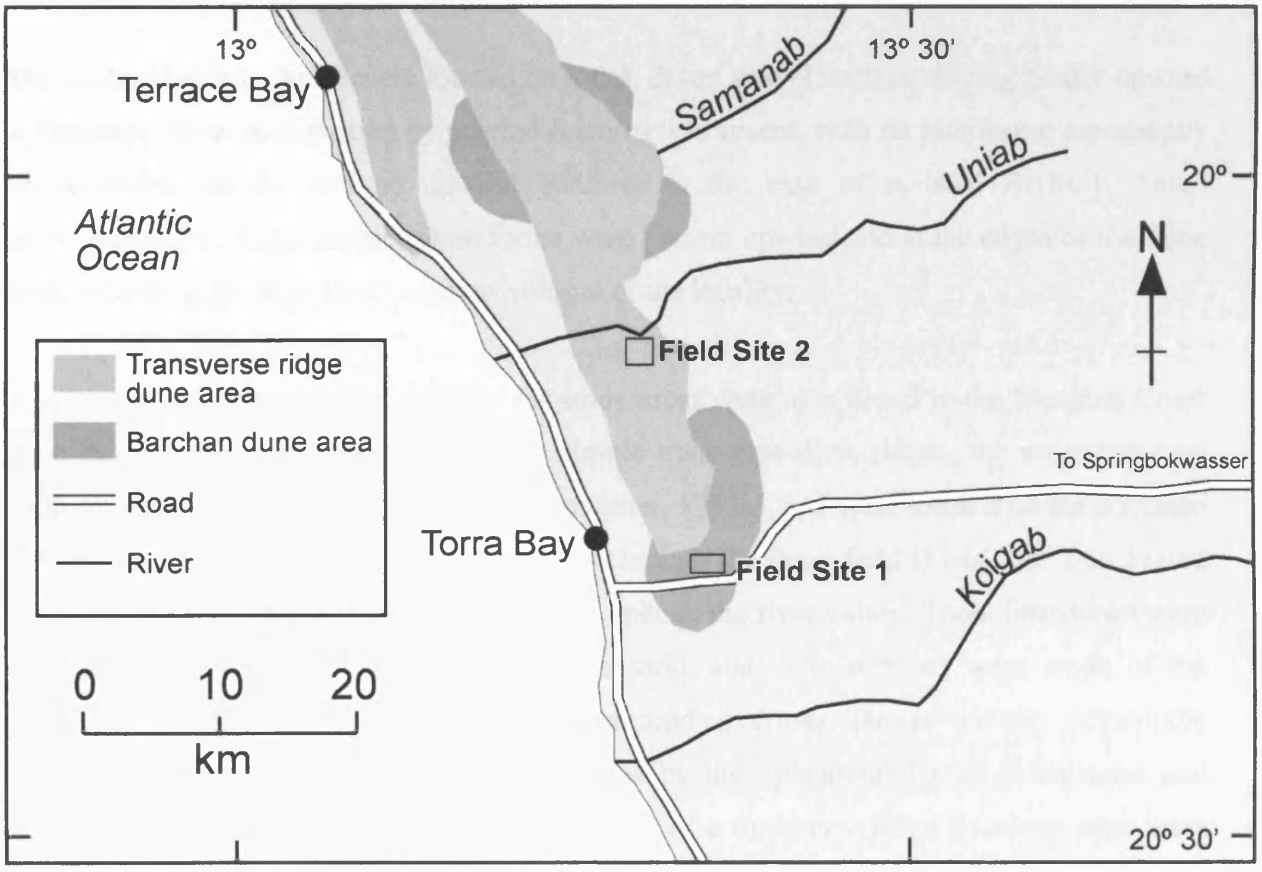

Figure 2.2 Location map of the southern half of the Skeleton Coast dune field, showing the two study sites.

The studied barchan dunes were located on the southern extremities of the dune field, with their location a result of the strongly unimodal wind regime and the limited sand supply at this upwind edge of the dunes. These barchans form part of the north to northeasterly sand transport pathway which extends from the coastal sediment source (about 10 km away) to feed the southern end of the main dune field (Lancaster, 1982a). The centrelines of the three barchan dunes here were aligned on an approximately north northeast-south southwest axis (008° and two 021°), in response to the dominant wind.

One entirely isolated barchan dune with a lee-side lacking any kind of downwind obstacle was investigated, subsequently referred to as BARC1 (20°21'03 S, 13°19'58 E)[1]. A further two barchan dunes that existed as the last pair within a 'train' of similar barchan dunes were also examined. BARC2a was the upwind and BARC2b the downwind dune comprising the pair. These dunes were also selected for the significant differences exhibited by their coarse morphology. BARC1 had separated crest and brink points, whilst BARC2a and BARC2b had these features united at a single position on the dune cross profile (see Table 2.1).

The studied barchan dunes were located on a flat, desert gravel surface sloping gently upward to the north. Flow perturbation by upwind features was absent, with no interfering topography or vegetation stands, and no upwind bedform in the case of isolated BARC1. Small (maximum 0.5 m high) coppice dune forms were present upwind and at the edges of the dune area, indicating the high sand transport volume of the locality.

Two simple interdune settings suitable for study areas were also found in the Skeleton Coast dune field. These interdunes lay between simple transverse dune ridges, the most common bedform in the interior of the dune field (Lancaster, 1982a), and were located on the southern side of the Uniab River whose course travels through the dune field (Field Site 2 in Figure 2.2). The northern end of these interdunes was open to the river valley. These interdunes were deliberately chosen for being largely bare of sand, and their surfaces were made of the prevailing desert gravel, with some dried fluvial mud coverings. This is evidence of periodic inundation of these valley bordering interdunes by the ephemeral Uniab (Stanistreet and Stollhofen, 2002; Svendsen *et al.*, 2003). The two bare transverse ridge interdune sites were identified as TRANB1 and TRANB2, where "B" refers to the bare surface (Figure 2.3).

[1] GPS system was unavailable after this reference.

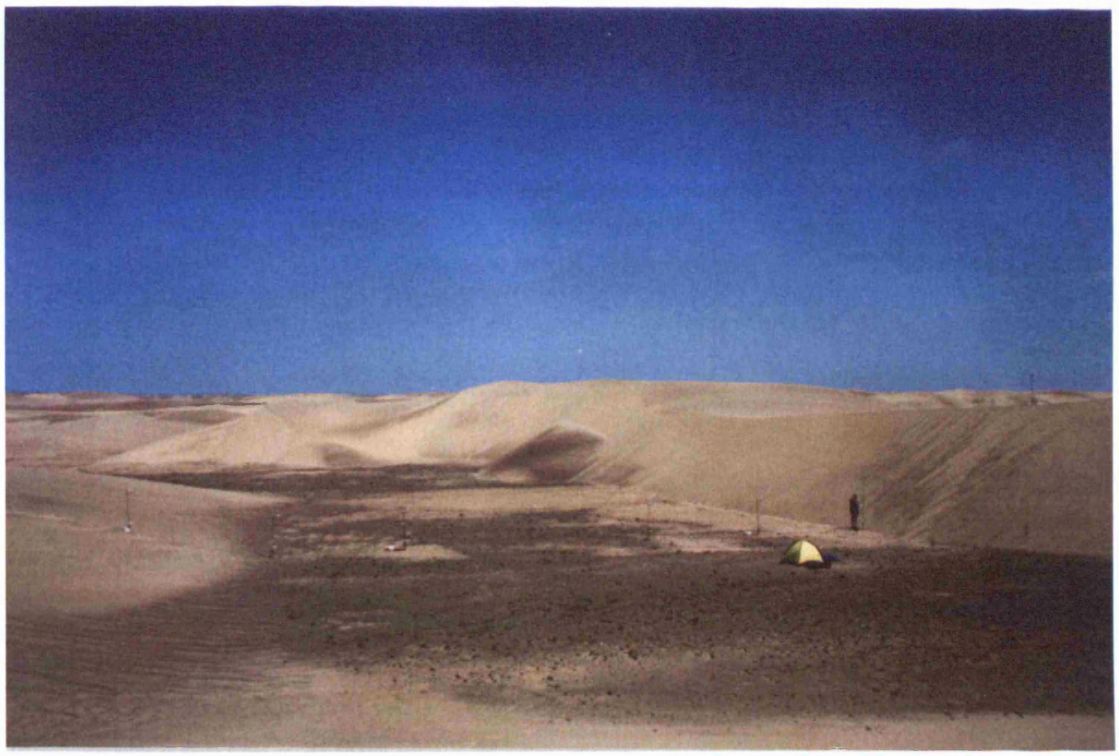

Figure 2.3 TRANB1, one of the bare transverse ridge interdunes studied in the Skeleton Coast dune field. Interdune length approximately 30 m (see Table 2.1).

Both of the upwind transverse dune ridges in the Skeleton Coast setting had relatively straight brinklines in plan view (Figure 2.3).

2.2.2 Kuiseb River delta field site

A further two transverse dune interdune settings were selected for study within the delta region of the Kuiseb River, south east of Walvis Bay. The Kuiseb is an intermittently flowing channel, but it floods with sufficient frequency to prevent dune encroachment through its channel and thus forms the northern boundary of the Namib Sand Sea (Lancaster, 1989a). Its periodic flow (around every nine years) is along an east to west course from the interior Great Escarpment to the Atlantic Ocean, with its distal portion ending as a delta. The floods result in large depositions of sediment (Nagtegaal, 1971).

The dunes in the immediate area of the Kuiseb river delta are dominated by transverse forms (Lancaster, 1989a; Slattery, 1990; Barnes, 2001). The studied interdunes were on the north side of the Kuiseb river channel, and lie between transverse ridges formed of sediment that has crossed from the sand sea to the south, and sediment that is delivered to the area fluvially by the action of the river itself (Nagtegaal, 1971). The sediment supply from these sources

and the regional wind are responsible for the dune forms in this area. Lancaster (1985b) has estimated that around 80% of the annual sand flow in this locality is from the south-southwest direction.

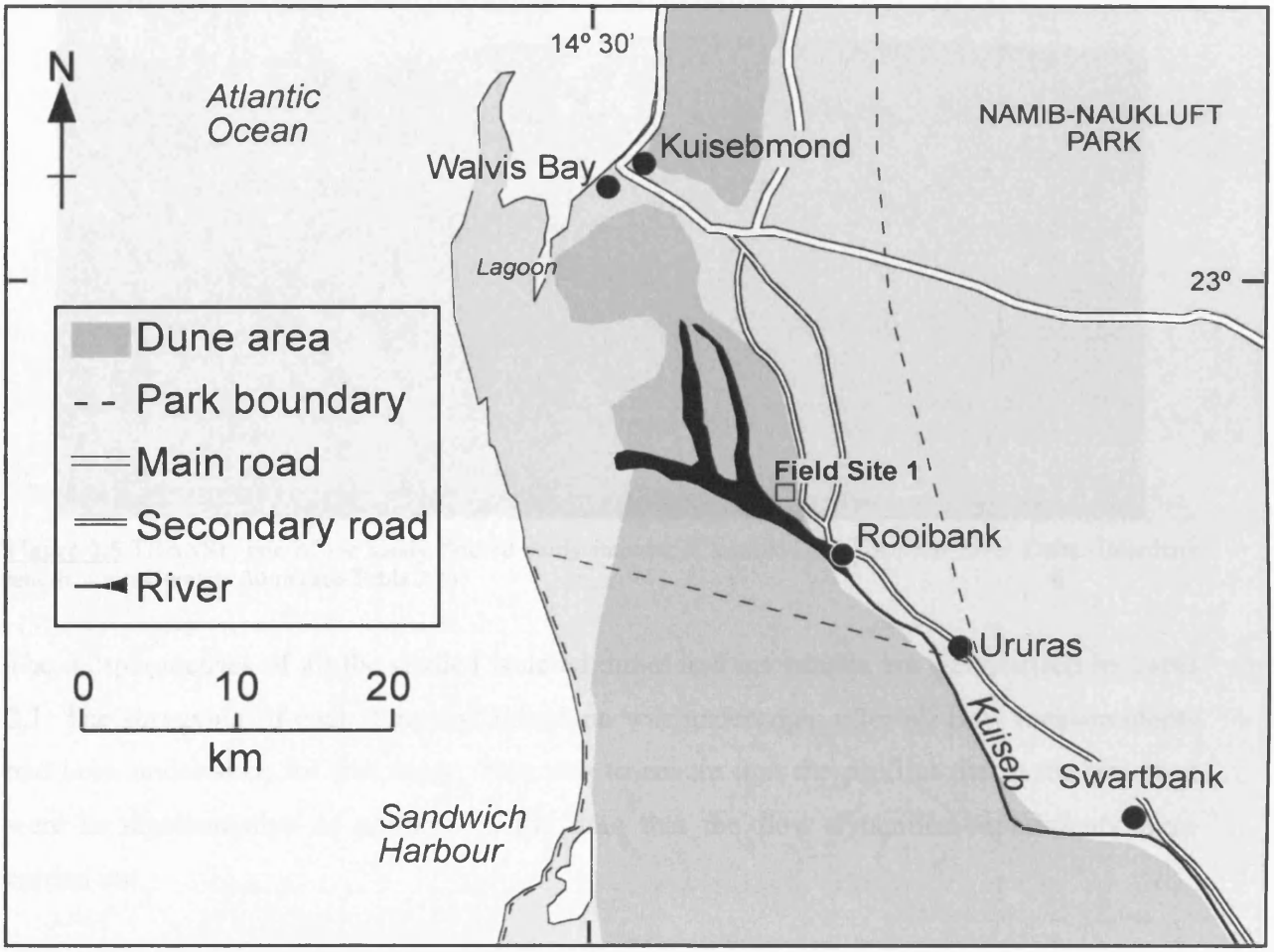

Figure 2.4 Location map of the Kuiseb River delta dune area, and the location of the area of the study interdunes.

Within the study area, two interdunes were chosen based on the suitability criteria of the simple form and relatively small size of the bounding dunes. Furthermore, these interdunes were selected for the presence of sandy, depositional surfaces, which represented the sampling by the study of variability in interdune surfaces (Section 2.1). These study interdunes were designated TRANS1 and TRANS2, reflecting the associated dune type and the "S" designating the presence of a sandy interdune surface (Figure 2.5). Both dunes were more crescentic ridge in form than the straight-crested transverse ridges of the Skeleton Coast examples (McKee, 1979).

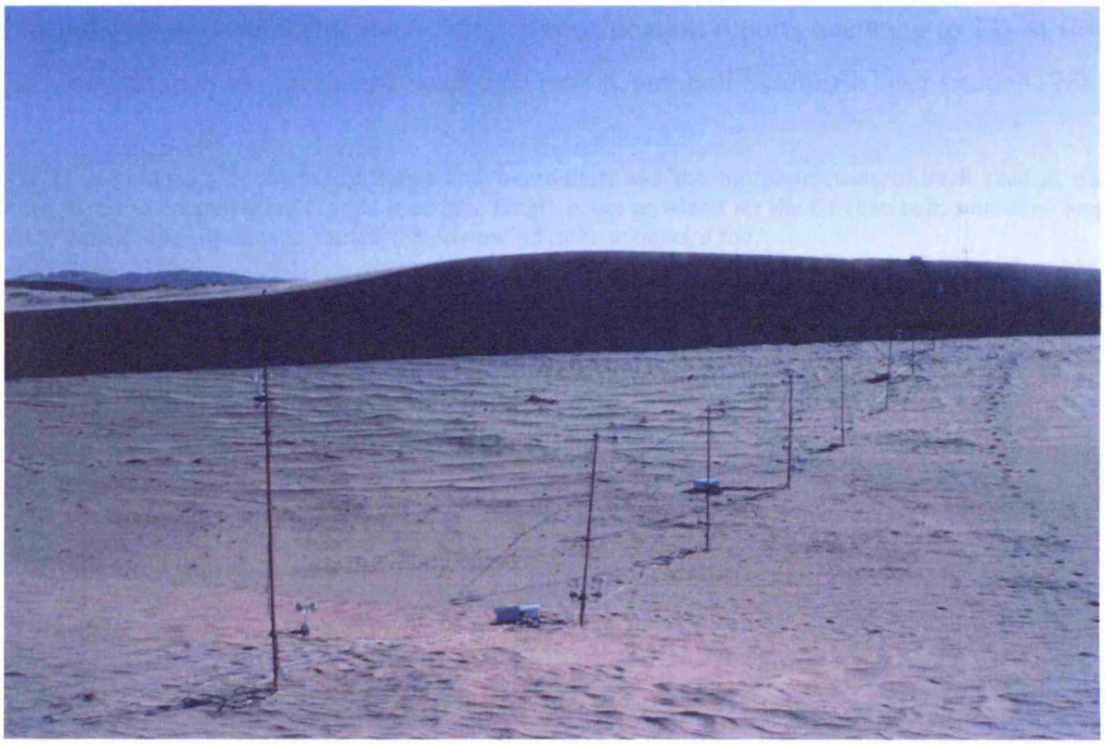

Figure 2.5 TRANS1, one of the sandy floored study interdunes located in the Kuiseb River Delta. Interdune length, approximately 30 m (see Table 2.1).

The morphometries of all the studied isolated dunes and interdunes are summarised in Table 2.1. The surveying of each dune and interdune was undertaken after all flow measurements had been undertaken for that study. This was to ensure that the profiles that were surveyed were as representative as possible of the time that the flow dynamics experiments were carried out.

2.3 Measurement of airflow velocity

2.3.1 Experimental procedure

Velocity was measured using *Vector Instruments A-100R* cup anemometers. The rotating-cup anemometer has been used extensively to characterise mean velocity patterns in aeolian dune research (e.g. Mulligan, 1988; Wiggs, 1993; McKenna Neuman *et al.* 1997; Walker, 1999). One recognised disadvantage with cup anemometers is their inability to respond entirely in accordance with fluctuating velocities. The effect of the cups is to introduce an inertia whereby the instrument will rotate even after the wind has slowed. Knott and Warren (1981) reported that inaccuracies associated with this type of device may be up to 15%. However, this error was estimated to be significantly reduced by the sensitive nature of the anemometers

used in this study. Overall, the manufacturer specification reports accuracy to 1% at flow of 0.1 ms^{-1}, and a threshold for detection of 0.25 ms^{-1} (Campbell Scientific User Guide, 1988).

Table 2.1 A summary of the study dunes and interdunes, and the morphometries of each case at time of surveying. Crest to crest spacing (λ) and interdune length is not provided for the barchan pair. Interdune length is defined as base of the slip face to start of the downwind dune windward toe.

Name	Dune crest height (m)		Dune basal length (m)	Crest to crest spacing, λ (m) [*h*]	Interdune length (m) [*h*]	Notes
BARC1	Crest 4.46	Brink 2.59	64.3	-	-	Isolated barchan, with crest-brink separated profile
BARC2a	3.32		30.6	-	-	Upwind dune in a pair of barchans. Crest-brink unified
BARC2b	4.32		31.6	-	-	Downwind dune in a pair of barchans. Crest-brink unified
	Upwind dune	D/wind dune	Upwind dune			
TRANB1	6.66	4.99	82	68.45 [10.3]	30.06 [4.5]	Bare interdune between transverse ridges
TRANB2	5.39	4.39	47.05	72.41 [13.43]	23.97 [4.4]	Bare interdune between transverse ridges
TRANS1	4.38	1.99	23.2	56 [12.78]	36.6 [8.4]	Sandy interdune between crescentic ridges
TRANS2	3.87	2.8	39.5	41 [10.6]	13.1 [3.8]	Sandy interdune between crescentic ridges

To measure the patterns of wind velocity through interdune areas, straight-line transects of anemometers were set up within the interdunes, extending from the slipface of the upwind dune body to different extents up the windward slope of the downwind dune. These transects were orientated at right angles to the local crestline of the upwind dune, and thus the sampling transects lay parallel to the dominant wind direction. Wind speed was measured along the transects by the cup anemometers clamped at two heights on iron posts where the two sampling heights (z) were 0.5 m and 1.9 m. The lower of the heights was determined by a compromise between the desire to sample velocity as close to the surface as possible, and a

concern for potential damage to the instrumentation from sand transport. z = 1.9 m was the highest sampling point that the posts afforded. The distance between posts was a function of the interdune length, and a desire to sample frequently and regularly through the whole interdune. The distance between sampling posts along each transect was nearly always regular, and intervals ranged from four to seven metres (Figure 2.6).

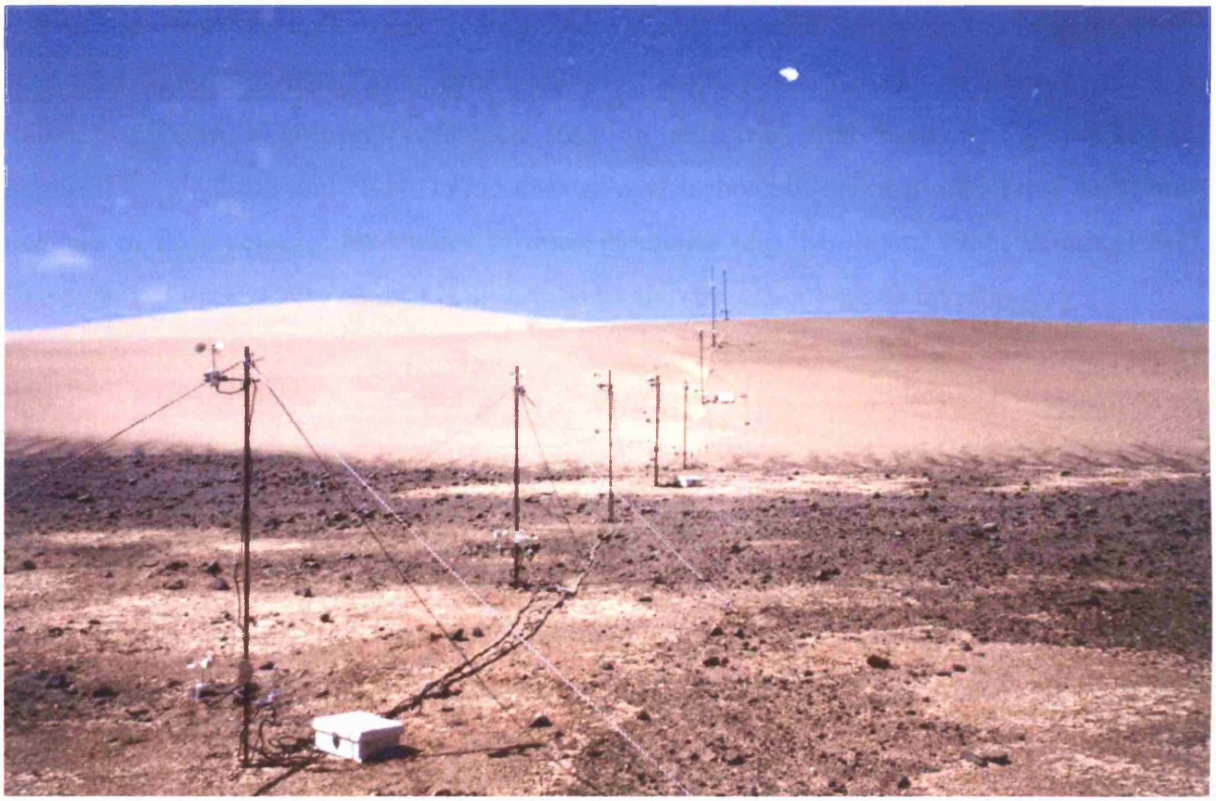

Figure 2.6 A typical experimental set up for measurement of velocity within a study interdune, looking toward a downwind stoss slope.

For the isolated dune investigations, anemometer transects of the same arrangement were established parallel with the dune centreline.

The sampling interval for mean velocity was every 10 seconds, with the number of revolutions measured for that period being totalled, and then stored in dataloggers (*Campbell Instruments CR10x*). This rate of measurement was determined by the combined requirements for obtaining frequent data on variable and turbulent general flow weighed against a consideration for datalogger memory. The total length of time for which it was possible to collect data represented a data run, and the duration of these sampling intervals, varied from one to several hours. The dataloggers were accessed at the end of each data run, and the information was downloaded to a laptop PC.

2.3.2 Processing of airflow velocity data

Actual velocity data were obtained from the raw field data by referring the field data to calibration relationships which had been established in previously conducted wind tunnel sessions.

The velocity data throughout the study, unless stated otherwise, are presented in terms of the fractional speed-up ratio. This expression for windspeed involves the normalisation of velocity data to a constant reference location and was first used for meteorological applications (Jackson and Hunt, 1975). It is now also the conventional manner of describing changes in flow velocity for studies of dune dynamics (e.g. Mulligan, 1988; Wiggs, 1993). The extent of the velocity change is described by the (fractional) speed-up ratio (δs);

$$\delta s = (u_z - U_{rz}) / U_{rz} \qquad \text{Equation 2.1}$$

where δs = fractional speed-up ratio, u_z = velocity at a height z on profile and U_{rz} = velocity at height z at a reference location (Jackson and Hunt, 1975). Where the dune has influenced flow in a way that produces a reduction in velocity compared to that at the same height at the reference, the speed-up ratio is a negative value. By definition, this ratio portrays flow acceleration or deceleration as a fraction so that, for example, δs of -0.30 represents a decrease in wind speed by 30% relative to the reference value at the corresponding height. With all time-averaged local velocity data being referred to a common reference location, direct comparisons were permitted between the mean velocity readings along a transect.

The reference station was a post recording velocity at four heights of 0.5 m, 0.8 m, 1.3 m and 1.9 m, which was an approximately log-linear arrangement. The deployment of such a reference tower for normalisation of velocity data has been successful in several other dune studies (e.g. Walker, 1999). The reference tower was fixed to sample airflow and boundary layer conditions that were as little disturbed as possible. For the isolated dune studies, the tower was positioned around 50 m upwind of the dune, in an area of homogenous surface and away from potential flow perturbations caused by the study dune or any other obstacle. With the measurements conducted within the interdunes, a similar positioning of the reference tower within an unaffected boundary layer was not possible. In these studies, the reference tower was sited in the middle, or nearer the downwind edge of the interdune area.

2.4 Measurement of turbulence

2.4.1 Reynolds stresses

Turbulence is an important parameter in the study of sedimentary bedforms, since the momentum and shear stress imparted at the ground surface is a consequence of the three dimensional flow that turbulence represents (Stull, 1988). The velocity at a point in the flow can be described by three vector components all at right angles to each other (u, v, w), where, for this study, u is the streamwise component in a horizontal direction x, v is the lateral component in a horizontal direction y, and w is the normal component in a vertical direction z, (where positive is upward) described in Figure 2.7.

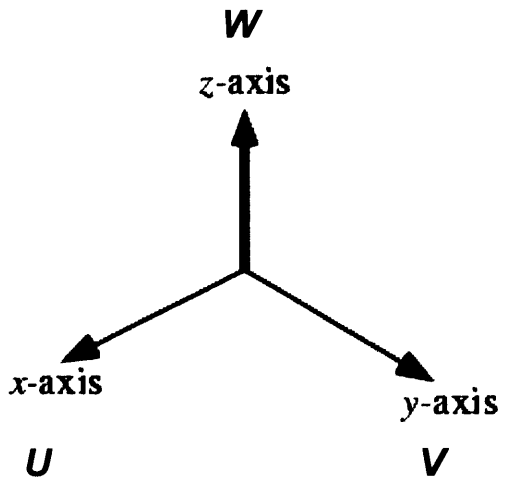

Figure 2.7 Three orthogonal axes (x, y, z) for the vectors of flow (u, v, w).

As natural wind flow is likely to be unsteady, the instantaneous velocity measurement for each of the three vectors at any one time (u, v, w), can be divided into a mean value plus a fluctuating value, thus;

$$u = \bar{u} + u'$$
$$v = \bar{v} + v' \qquad \text{Equation 2.2}$$
$$w = \bar{w} + w'$$

where the mean (overbar) value is for an interval that is 'long' in relation to the temporal scale of the turbulence being sampled and the prime (') indicates an instantaneous fluctuating value around that mean (Clifford and French, 1993). The mean of any of the vector fluctuating parts (') is zero, but the square of this turbulent part is not zero (Stull, 1988). Reynolds stress represents the momentum flux in the fluid for the measured point in the flow field, and the time-averaged turbulent Reynolds stress can be calculated for each vector as the mean of the

squares of each fluctuating part, producing $\overline{u'^2}$, $\overline{v'^2}$ and $\overline{w'^2}$. Reynolds stress has been the variable used to quantify turbulence over hills (e.g. Finnigan *et al.*, 1990) as well as in studies of sub-aqueous bedforms (e.g. McLean *et al.*, 1994). In this thesis, analysis of normal Reynolds stress is restricted to the streamwise and vertical components, with lateral stresses $\overline{v'^2}$ excluded. This is because the former two are most relevant for the surface shear stress along two dimensions. For the mixed products, the most important shear term is the product $u'w'$ which is also treated as time-averaged $-\overline{u'w'}$. Since positive u' is associated with negative w' and vice versa, the product is negative, hence the sign convention. To have units of stress (force, N m^{-2}), air density (ρ_a) needs to be included in each Reynolds stress value (e.g. $-\rho_a\overline{u'w'}$), but all values are dealt with after being normalised to reference velocity here so air density is not included and the stresses are presented as the vector product $-\overline{u'w'}$, or kinematic stress (Sterk *et al.*, 1998).

The term $-\overline{u'w'}$ is equivalent to the downward flux of streamwise momentum, and is commonly referred to as Reynolds shear stress (Kaimal and Finnigan, 1994). It is considered the most important variable for sediment transport (see Sterk *et al.*, 1998), where shear stress (τ) is

$$\tau = -\rho_a\overline{u'w'} \qquad \text{Equation 2.3}$$

and shear stress is linked to shear velocity (u_*) through Equation 2.4

$$\tau = \rho_a u_*^2 \qquad \text{Equation 2.4}$$

it therefore follows that:

$$u_* = \sqrt{-\overline{u'w'}/\rho_a} \qquad \text{Equation 2.5}$$

2.4.2 Experimental procedure

The manner in which the patterns of turbulence in the interdune flow were characterised was based on the traditional approach to studying this parameter, where the appropriate properties of a moving fluid are observed at given points within the flow (Allen, 1994). Reynolds

stresses were derived from at-a-point field measurements of wind velocity in the three mutually perpendicular directions.

Cup anemometry is not sensitive enough to measure wind velocities at the appropriate frequencies, where an interval of less than 1 Hz is necessary for turbulence studies (van Boxel *et al.*, 2004). Neither can cup anemometers differentially sample the three-dimensional components of the flow, which is a further requirement for measuring turbulence (Clifford and French, 1993). Wind velocities were therefore sampled in the field using a sonic anemometer (*Campbell Scientific Instruments CSAT-3*) which is a fast-response instrument capable of observing multi-dimensional winds, while remaining robust enough for field use. The instrument measures wind velocity in three directions (x, y, z) that are related as orthogonal axes, and the three axes of flow direction from which Reynolds stresses are derived (Figure 2.7). (See van Boxel *et al.* (2004) and Walker (2005) for recent reviews of sonic anemometer operation principles).

To derive Reynolds stresses at the field locations, the sonic anemometer was attached to a pole with its alignment carefully fixed so that the instrument was facing approximately into and parallel to the approaching wind (data were mathematically corrected in the analysis stage to ensure this). To achieve this, the sensor was aligned with transient ripple bedforms and vane directions on nearby anemometer posts. The instrument was always horizontally level (i.e. 90° to the vertical pole), and the sampling height was either z = 0.3 m or 0.5 m. This height was at the lower sampling level of the cup anemometers, which allowed comparison with spinning-cup derived streamwise velocity data (and lessened potential saltation inflicted damage) (Figure 2.8).

When moved along the sampling transects in the lee of study barchan dunes or within the interdunes, the sonic anemometer was always positioned within 2 m of a post with cup anemometers. The positioning was sympathetic to the prevailing wind direction to reduce any impact of flow perturbation from the nearby sampling post. When set up at a location and recording, the sonic anemometer measured instantaneous wind speeds in the three axes at a frequency of 10 Hz for a period of five minutes, with the data being recorded directly to a connected laptop computer. The frequency of sampling by the instrument was governed by a need to obtain sufficient readings for acceptable time averaged measurements of Reynolds

stresses, and an appreciation of recording computer memory and battery power. The measurement duration for the near-surface sampling height met the requirement suggested by van Boxel *et al.* (2004, Fig. 3) of around five minutes.

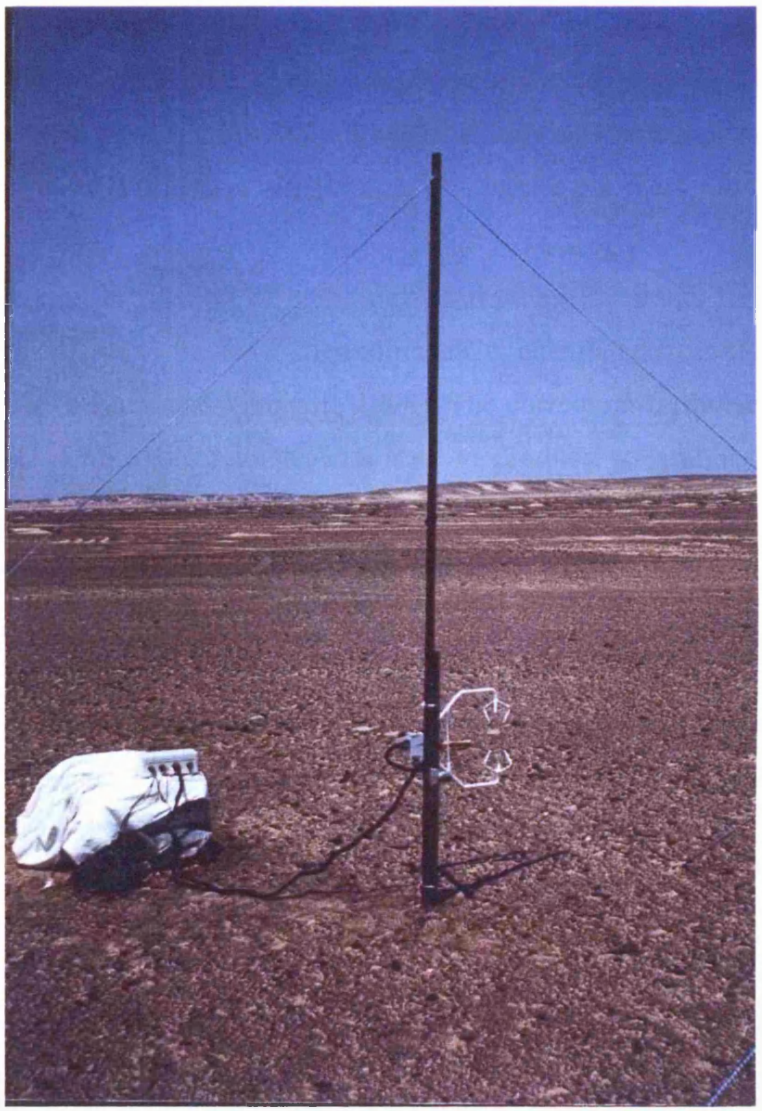

Figure 2.8 The sonic anemometer as deployed in the field at $z = 0.5$ m.

2.4.3 Processing of turbulence data

To calculate Reynolds shear stress accurately, the u component needs to be oriented horizontally with respect to wind direction, and the w component vertically. Whilst an attempt was made to reduce the crosswind component (v) at the start of each sampling interval by positioning the sonic anemometer so the sensor faced into the incoming wind, further correction of the data was performed (and for vertical misalignment too) by rotating the frame of reference of the data in subsequent analysis where necessary. Moreover, the influence of

sloping terrain needs to be accounted for, and the data corrected for the influence of slope on the stresses. Covariance in *uw* is highly sensitive to slope, and shear stress can vary 9% by a single degree of tilt (van Boxel *et al.*, 2004). Since sonic anemometry is a relatively new methodology for dune studies with their distinct topographies, the practice of rotating the data is currently a topic for discussion in aeolian geomorphology (van Boxel *et al.*, 2004; Walker, 2005). Evidence from wind tunnel studies where the effect of non-correction on Reynolds shear stress have been assessed are compelling in favour of correction being the standard (Castro and Wiggs, 1994; Wilczak *et al.*, 2001).

The standard technique in rotation of sonic data is rotating the frame of reference at each measurement point relative to the local streamline angle, calculated from the mean horizontal and vertical velocity (Kaimal and Finnigan, 1994). The correction formulae presented in van Boxel *et al.* (2004) were applied to the raw data to produce streamline aligned Reynolds stresses (correction for 'roll' was not necessary). The corrected results were verified against the alternative correction method presented by Wilczak *et al.* (2001).

From the corrected time series of each measurement run, the elements of each vector were produced (Equation 2.2). The fluctuating (or turbulent) parts of the flow component were then produced (u', v', w'). These values were subsequently squared, and then averaged over the time of measurement to yield Reynolds stress in the streamwise, spanwise and vertical directions, $\overline{u'^2}$, $\overline{v'^2}$ and $\overline{w'^2}$ respectively. Reynolds shear stress was produced from the covariance of the streamwise and vertical turbulent components ($-\overline{u'w'}$). All the values for Reynolds stresses were then normalised by the square of the mean wind velocity, at height z, taken from the reference tower for the corresponding period of time (U_{rz}^2). This procedure was the same as for the normalising of the cup anemometer velocity data.

2.5 Measurement of flow direction

The instruments used to obtain flow direction data were *Vector Instruments W200P Potentiometer Windvanes*. These devices respond to airflow guided by a fin which aligns with the wind and permits free-moving continuous rotation. The vanes are reliable when wind speeds are above 0.6 ms^{-1}, and accurate to ±2° when flow exceeds 5 ms^{-1} (Campbell Scientific User Guide, 1988).

The vanes sampled wind direction at z = 0.5 m, level with the lowest anemometer height. As there were insufficient vanes to instrument every post at which windspeed measurements were made, vanes were positioned along the transect to ensure a regular coverage of flow direction data throughout the interdune. Before each data run commenced, the vanes were aligned to magnetic north using compass measurements. As a precaution, the vanes were periodically checked during the measurement periods, and the configuration of vanes was verified at the end of the data run to see if flow had led to a misalignment through twisting of the pole. Once operating, the datalogger recorded the wind direction indicated at that instant for each vane at an interval of every 10 seconds.

Mean direction data and directional variability data were processed after collection. For the presentation and analysis of flow directional variability, the spread of compass bearing data was used to create a normalised measure of flow unimodality. This was based on a trigonometric conversion of the direction data from bearing form as produced in the field to scalar co-ordinates. Each period of flow sampling had a resultant vector line with an angle and a length (ω). The angle was the mean direction, and the length represented the constancy of flow indexed for the total number of readings for that run. In this case therefore, the vector length and value ω is the *inverse* of the flow directional variability i.e. a longer line and higher ω value is a flow with a less variably directed flow. An example is shown in Figure 2.9.

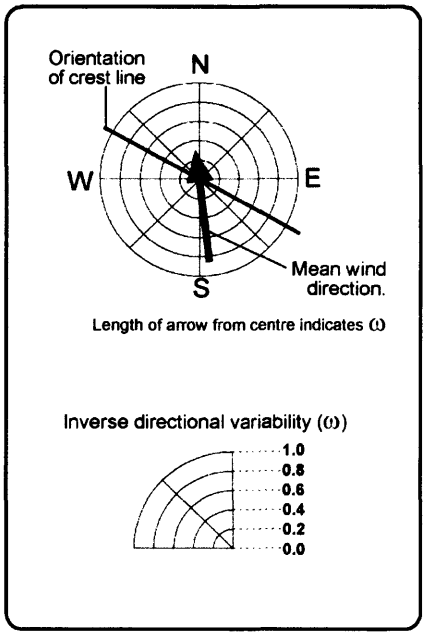

Figure 2.9 Diagrammatic representation of mean direction and flow directional variability (ω) data.

Figure 2.9 shows that a potential ω value of unity (to the outer ring) represents a flow that is purely unimodal and unvarying in flow direction.

As part of the field experiment, flow visualisation was another aspect to the study of flow direction. Marine distress flares with a discharge duration of around 4 minutes were set off when the incident flow was approaching from an angle of interest. Photographs were taken, with the exact times that the flare was ignited and then expired being noted, so flow visualisation periods could be related to transect velocity and vane data. Other successful flow visualisation data have previously been recorded from smoke (Livingstone, 1986) and flags (Walker, 1999).

2.6 The co-ordinate system for data presentation

For ease of reference to direction and distance within the different study sites, a common system of co-ordinates was used when referring to sampling and location within each study setting (Figure 2.10). Distances in the lee of the studied isolated dunes and through interdunes are expressed as length in terms of the equivalent upwind dune heights (h) from the upwind dune crest (x/h = 0). The three axes that relate to the directional components of flow for Reynolds stress are also illustrated in Figure 2.10.

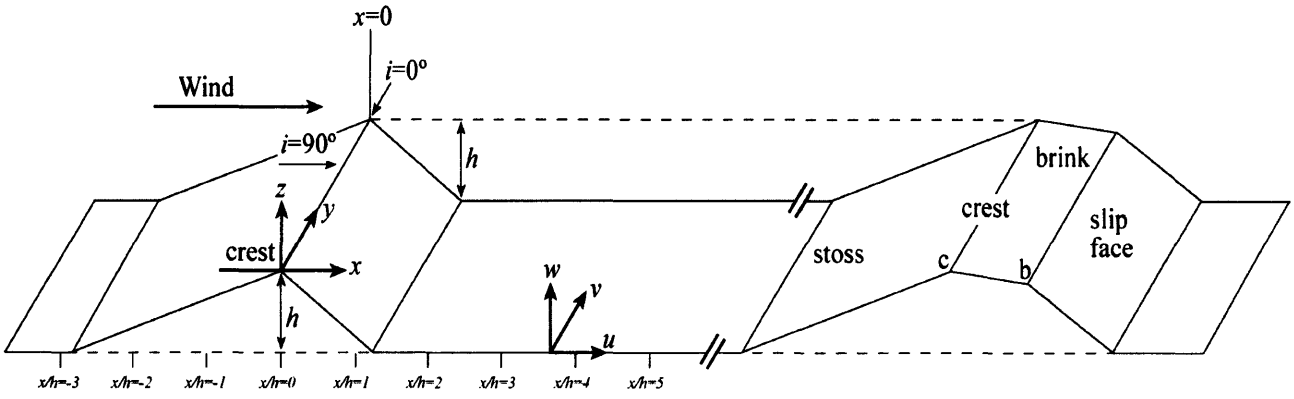

Figure 2.10 Interdune schematic in cross-section, showing height equivalent for horizontal distances from upwind dune crest. Also featured is the co-ordinate system for wind direction, and the relation of the three orthogonal axes (x, y, z) to components of wind direction u (streamwise flow), v (spanwise flow) and w (vertical) for a wind blowing normal to the upwind dune crestline, i =90° (where flow is parallel to the crestline i = 0°). The upwind dune has a unified crest and brink point, the downwind dune demonstrates a separated crest and brink. Key dune features are labelled (note this is illustrative, downwind dune not always crest-brink separated).

Chapter 3
Results and Discussion

3.1 Introduction

This chapter describes and discusses the results of the field investigations conducted initially on isolated barchan dunes, and then within the study interdunes. The results in this chapter therefore serve to fulfil the first stated objective of the study. Data are presented for the changes in flow velocity and directional variability, as well as the different turbulent stresses. Velocity and turbulence are the variables most relevant to sediment entrainment and movement, whilst for a two dimensional study of flow along a transect, the directional variability will clarify observed flow patterns.

The investigation of flow characteristcs within interdunes and isolated bedform lee-sides is also restricted to periods when flow was transverse. Sweet and Kocurek (1990) identified transverse flow as having an incident angle to the upwind crestline of 90 ±20° for a ridge dune, which is 0±20° for a barchan centreline. Flow perpendicular to the crestline again represents the sampling of the simplest type of incident flow, since the lee-side deflection will be minimal (Tsoar, 1983a; Tsoar *et al.*, 1985) which is a requirement for a first order assessment of interdune dynamics. Moreover, for the small quasi-equilibrium forms of the study dunes, a perpendicular wind direction should be the most common wind they receive.

3.2 Characteristics of flow for isolated barchan dune examples

As detailed in Chapter 2, the approach employed to investigate the geomorphologically relevant parameters of airflow within interdunes involved firstly a series of observations on how a single dune influenced key aspects of airflow. These observations were made in order to provide a comparison with the recorded flow patterns within interdunes.

3.2.1 Mean velocity around isolated barchan dunes

3.2.1.1 Upwind of and over the dune

The variation of flow velocity upwind of and over sand dunes is now a well recognised phenomenon. Our understanding of flow on the windward slope is such that the explanations of observed velocity have led to its modelling (e.g. Walmsley and Howard, 1985; Weng *et al.*,

1991; van Boxel *et al.*, 1999) based on earlier meteorological studies of the influence of hills on near-surface boundary layers (Jackson and Hunt, 1975; Hunt *et al.*, 1988).

Figure 3.1 shows the observed velocity variation upwind of and over BARC1. The data here are presented as a fractional speed-up ratio (δs) (Section 2.3.2), but for Figure 3.1 it should be noted that local velocities were derived from the sonic anemometer, and from a sampling height of z = 0.3 m. These original data were then normalised with the lowest reference tower anemometer of z = 0.5 m. This particular fractional speed-up expression demonstrates the effect of a dune on mean velocity, but this combination of data is only used for this isolated dune example. As such, it is not strictly directly comparable to the fractional speed-up velocities presented in the subsequent results.

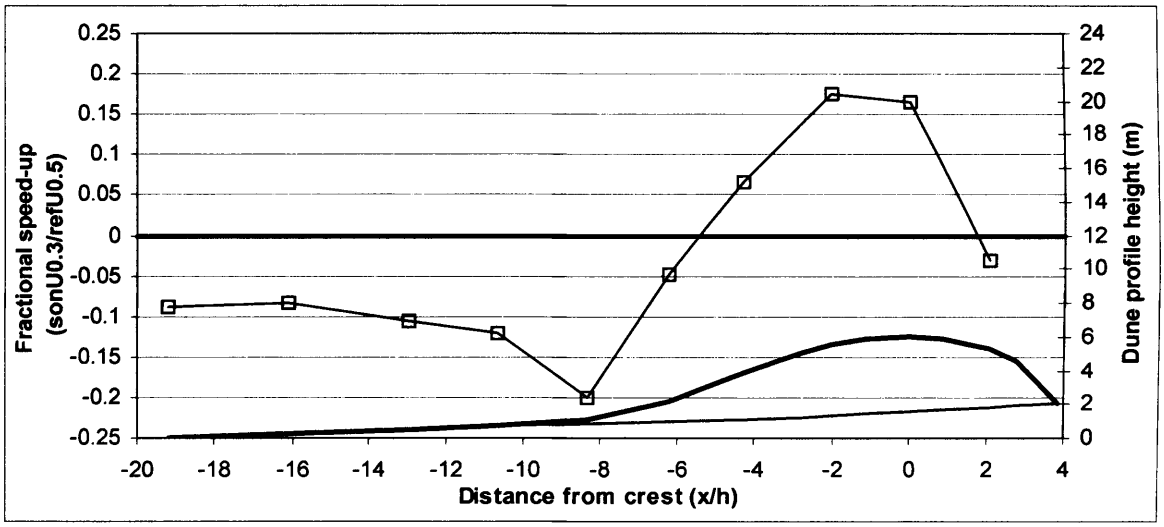

Figure 3.1 Airflow velocity upwind of and over isolated BARC1 at z = 0.3 m. Note that the fractional speed-up in this case is derived from sonic anemometer data collected at z = 0.3 m as a fraction of the velocity at the reference tower for z = 0.5 m. Reference tower is located at x/h = -19.22. Mean flow direction is 3° off dune centreline. Dune height is exaggerated.

The general pattern of velocity perturbation upwind of and over the barchan dune is in good agreement with similar measurements of velocity variation conducted both in the field and wind tunnels (e.g. Mulligan, 1988; Wiggs, 1993; Frank and Kocurek, 1996a). In the unaffected flow region upwind of x/h = -16.12, flow velocity is similar with fractional velocities remaining constant at just less than -0.1 in Figure 3.1. Fractional velocity is not zero for this region because the average speed measured at z = 0.3 m is consistently less than that for the reference speed at z = 0.5 m which it is referenced against. The steadiness of the fractional speed-up however serves to indicate that unperturbed flow exists for x/h = -16.12 and upwind thereof.

As the dune is approached and the positive pressure exerted by the dune body is encountered by the flow, upwind velocities start to show a decrease (Jackson and Hunt, 1975). This is explained by the Bernoulli principle that holds that a pressure rise necessarily induces slow down of flow, and has been applied to flow at the toe of hills (Hunt and Simpson, 1982) (see Section 1.5.1). The deceleration is greatest at the dune toe x/h = -8.34 where δs = -0.20. Thereafter, velocity increases along the windward slope with a speed-up maximum of δs = 0.18 at x/h = -2.09. At this point flow is 0.27 faster than the speed measured furthest upwind. A similar degree of speed-up value is found at the crest probably because of the rather flat summit of the dune. The amplification of velocity measured at the crest is comparable to other studies on dunes (e.g. Lancaster 1985a; see review in Lancaster, 1994). This acceleration up to the crest is due to the well-established influence of streamline compression on the windward slope caused by the negative perturbation in the pressure field near the crest (Jackson and Hunt, 1975). Downwind of the crest but before the dune brink, the convex surface slope encourages flow expansion to occur, and a considerable deceleration is observed to δs = -0.03. This is a reduction of one fifth from the crestal velocity.

The behaviour of velocity measured over BARC1 agrees very well with numerous previous studies reporting on the influence of isolated dunes on mean velocity.

3.2.1.2 Lee-side of the dune

Of significance to the mean velocity patterns that are found within interdune areas is the nature of flow recovery in the lee of the upwind dune obstacle. The response of flow in the lee of a single barchan dune is shown in Figure 3.2 which presents a typical pattern of velocity as measured downwind of the isolated dune BARC1.

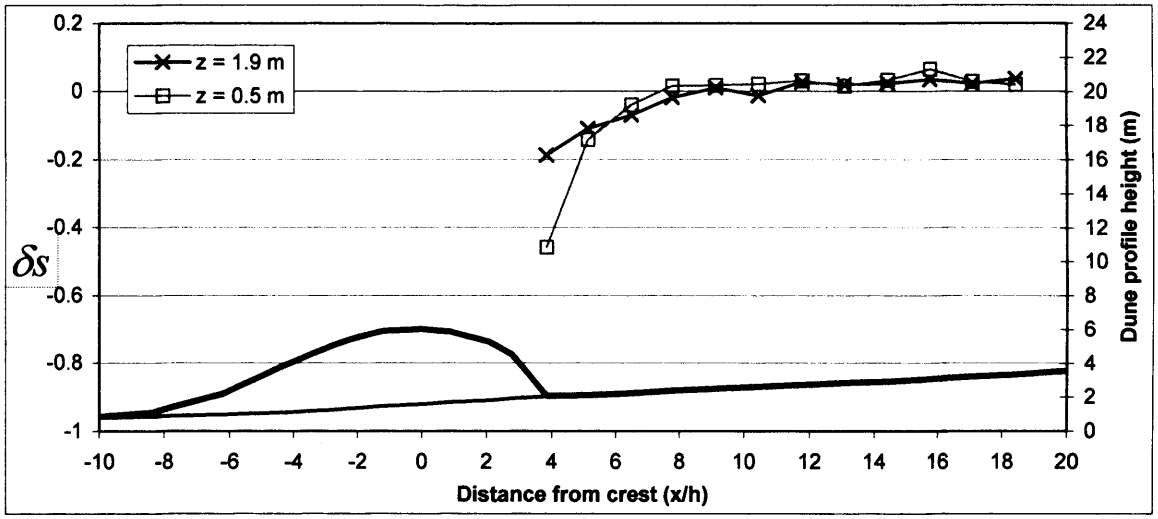

Figure 3.2 Time-averaged normalised velocity in the lee of isolated barchan centreline, BARC1, for the two sampling heights. Incident flow was transverse (4° off dune centreline). Measurement run duration, 34 minutes (Run 2C). Dune height is exaggerated.

The general pattern of the observed fractional speed-up in the lee of the dune is one of velocity recovery. In the immediate lee of the dune (x/h = 3.84) there is a reduction in velocity evident at both heights, with deceleration by almost 20% of the reference velocity (to δs = 0.81) at z = 1.9 m, and nearly half to δs = 0.46 at z = 0.5 m. This overall velocity drop is an expected one, having been recognised in many previous studies of airflow over dunes (e.g. Hoyt, 1966; Sweet and Kocurek, 1990; Sweet, 1992; Walker, 1999). It is a result of one of the most fundamental aspects of dune flow-form interaction, and is attributed to the divergence of streamlines that occurs as flow expands on separation when it detaches from the dune brink. The magnitude of the deceleration observed here is in agreement with other studies on similar types of dune of comparable size (e.g. Lancaster 1989a; Walker, 1999).

The departure between the values of normalised velocity for the two heights in the lee is particularly significant. At the first measurement point in the lee of BARC1 in Figure 3.2 (x/h = 3.84), the airflow at z = 0.5 m is much slower relative to mean reference velocity than is the case for z = 1.9 m height. This difference in speeds is explained by the fact that at z = 1.9 m, the airflow is in close proximity to the faster moving air in the lower wake as illustrated in Figure 1.5. At z = 0.5 m, the first measurement point lies within (or is much closer to) the reduced velocity zone of the separation cell, also shown in Figure 1.5. The velocity difference is indicative of the shear in the flow that exists between these heights along the free shear layer. For flow separation, the downwind limit of this is marked by the point where separated flow becomes reattached to the surface, which is also the point where the IBL begins

developing (McLean and Smith, 1986; Frank and Kocurek, 1996b). Following flow re-attachment, velocities increase throughout the depth of the profile in response to the wake dissipating (downward from above) and the development of the IBL (upward from the surface).

The difference between the normalised velocity values at the two heights for x/h = 3.84 in Figure 3.2 shows that there is a steeper gradient to the velocity profile than would be expected for the profile in an unperturbed boundary layer. Figure 3.3 highlights the difference in velocity gradients between the two sample heights for each of the first five posts in the lee (up to x/h = 9.11) during data Run 2C, and allows comparison with the upwind reference flow profile.

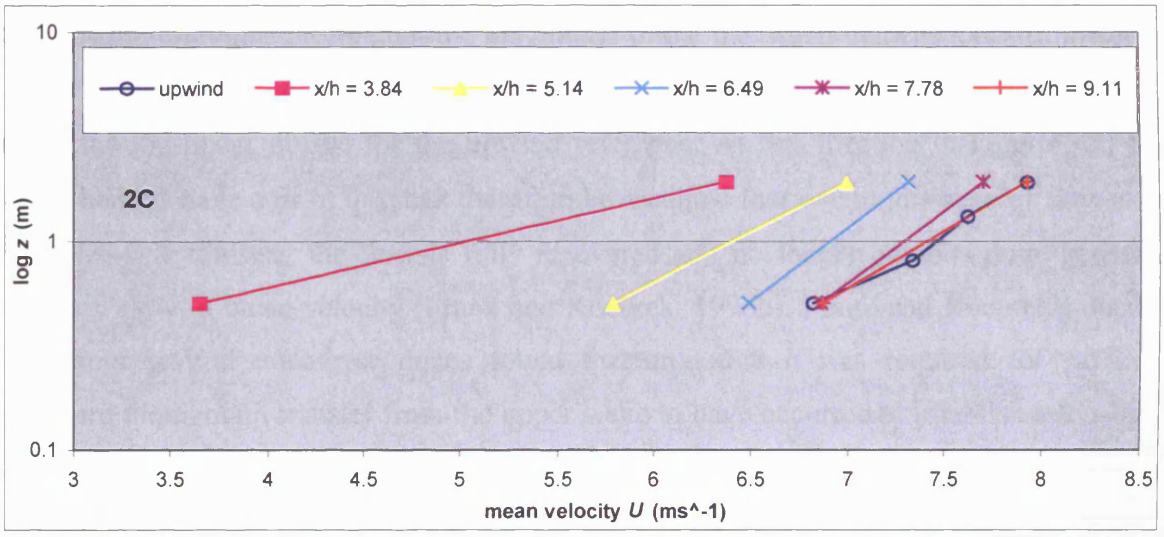

Figure 3.3 Semi-logarithmic profiles of mean velocity upwind and downwind of isolated BARC1. Profiles are from a) four sample height profile at the upwind reference (x/h = -19.22) b) two height (z = 0.5 m and 1.9 m) velocity gradients for the dune lee-side. Flow conditions as Figure 3.2 (Run 2C).

The extent of the gradient between recorded velocities at x/h = 3.84 is indicated in Figure 3.3, which demonstrates the high shear between the slow moving air of the near-surface separation cell, and the flow influenced by the faster wake above it (Frank and Kocurek, 1996b; Walker, 1999). The existence of the considerable shear due to the presence of the separation cell for x/h = 3.84 indicates flow is not yet re-attached to the surface. By x/h = 5.14 however, the relative speed-up at z = 0.5 m suggests that the separation cell does not extend this far downwind, and that flow has re-joined the surface and has begun recovery of its velocity. With further distance downwind of BARC1, the velocity values can be seen to increase at both heights in both the normalised velocity values in Figure 3.2, and as absolute velocities in

Figure 3.3. This recovery is due to flow acceleration in the lower levels of the profile, as momentum is transferred downward from the faster wake with increasing downwind distance. The fact that flow recovery is a balance between the growth of the IBL from the point of re-attachment and the dissipation of the wake is shown in the significant acceleration for z = 0.5 m between x/h = 3.84, and x/h = 5.14, where a speed-up from 3.65 ms^{-1} to 5.79 ms^{-1} is observed.

With the downward transference of turbulent energy, the shear within the flow in the lee is also reduced as velocities equilibrate toward a single vertical velocity profile, similar to the unperturbed reference. This feature of the change in velocity over downwind distance as flow recovers is shown in the decay of the gradient of the measured velocity profiles (Figure 3.3). At x/h = 6.49, the slope of the velocity gradient between the two sample heights is the same as that of the reference profile, but the magnitude of the measured velocities is still lower for both heights. By x/h = 9.11, the velocity differential between z = 1.9 m and z = 0.5 m matches that of the log-linear profile for the upwind reference. At this location in Figure 3.2, both sample heights have a δs of 0. It can therefore be assumed that where this state of flow exists on the lee-side transect, the flow is fully recovered and no longer exhibits dune generated secondary flow in mean velocity (Frank and Kocurek, 1996b). Frank and Kocurek's detailed study from several transverse dunes found that around 8 h was required for sufficient downward momentum transfer from the upper wake to have occurred to establish a log-linear velocity profile. The distance of x/h = 9.11 for BARC1 therefore reveals a good agreement with this, and for other aeolian (up to 10 h in Walker and Nickling, 2002) and sub-aqueous (Nelson and Smith, 1989) bedforms.

However, given that flow separation occurs at the brink of a dune (Lancaster, 1994; Frank and Kocurek, 1996b), the relevant distance for flow recovery downwind of BARC1 may be exaggerated if it is assessed from the dune crest because of the crest-brink separated morphology of the study dune. The mean flow deceleration for the region between the crest and the brink in Figure 3.1 revealed that flow had slowed in this location, but the recorded velocity decrease was not of the magnitude seen immediately downwind of the dune slip face, where separation proper occurs. If the distance for flow recovery in the lee of BARC1 is considered in terms of dune heights from the brink (x/h_{brink}), then the lee-side distance at which the upwind mean velocity profile is matched becomes x/h_{brink} = 6.33. This indicates

that flow becomes re-attached considerably closer to the dune, with this issue being investigated further in the following section.

3.2.1.3 Effect of dune morphology on lee-side flow recovery

The cross profile of BARC1 (Figure 3.2) shows that the crest and brink of this barchan dune are separated. All varieties of transverse dune commonly exhibit forms that exist with a sharp crest where the crest and brink are co-incident (Cooke *et al.*, 1993). Such a difference in the morphology of the dune could be expected to have implications for the distance required for airflow to exhibit recovery in the lee. The pattern of mean velocity in the lee of an isolated dune exhibiting coincident crest and brink (BARC2a) is presented in Figure 3.4.

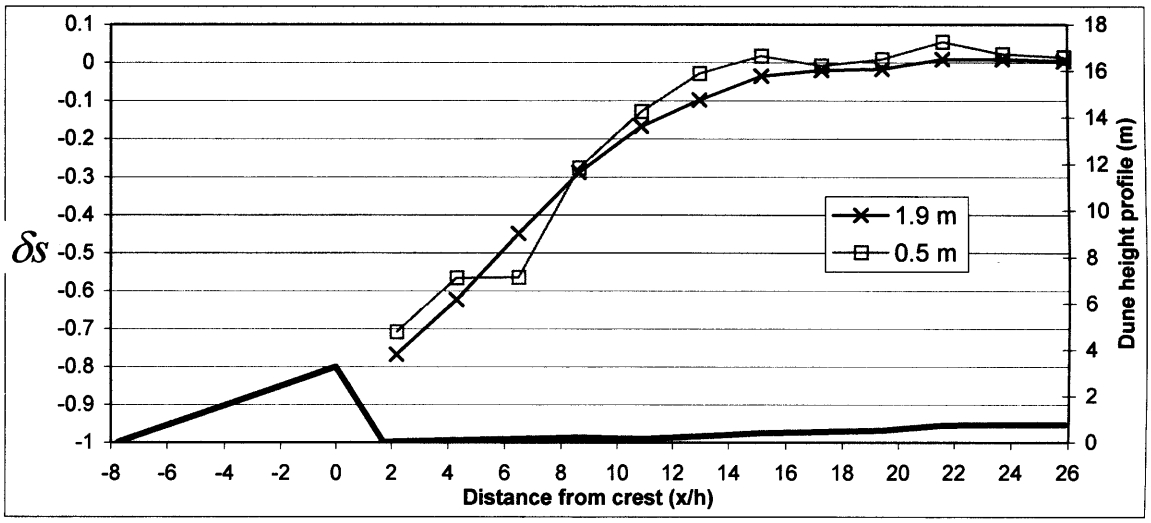

Figure 3.4 Time-averaged normalised velocity in the lee of isolated barchan centreline, BARC2a, for the two sampling heights (Run 6C). Incident flow was transverse (8° off dune centreline). Measurement run duration, 27 minutes.

Comparing Figures 3.2 and 3.4, it is apparent that BARC2a with the unified crest-brink morphology exerts a greater influence on flow downwind of the dune. For the crest-brink unified dune, velocities in the immediate lee (x/h = 2.18) are δs = -0.77 at z = 1.9 m and δs = -0.71 at z = 0.5 m in relation to their respective mean upwind velocities. The effect of the dune shape is particularly demonstrated by the fact that the velocity reduction in the immediate lee is much greater at z = 1.9 m for BARC2a than was recorded for BARC1 (δs = -0.19) (Figure 3.2). This difference indicates that directly downwind of the crest-brink unified dune, the upper sample height is far less influenced by the fast overshooting air that has de-coupled from the dune. The cause of this is that for BARC2a, the flow is projected upward on separation as a consequence of the sharp crest morphology. The fast flow that is present due

to the downward angled flow leaving the rounded crest of BARC1 (Figure 3.5) is therefore absent for BARC2a.

Figure 3.5 Flow visualisation on BARC1. Origin of smoke is in the area between the crest and brink of the dune and shows slope-attached streamlines until the brink where flow separation occurs, but with a downward component towards the surface. Vertical post is 3 m high for scale.

Having been conveyed upward at the brink by the dune morphology of BARC2a, the separated flow also takes a greater distance to re-attach itself with the surface in the lee-side. This is reflected in mean velocities remaining lower for a further downwind distance than for BARC1. The greater extent of the separation cell in the lee is shown by the fractional velocity behaviour measured along the transect at z = 0.5 m. After an initial increase in speed, the velocity at the lower height is steady at δs = -0.56 between x/h = 4.32 and x/h = 6.49, with this constancy suggesting that both of these measurements lie within the slack flow of the separation cell. This fact is confirmed by the data from the wind vanes along the lee-side transect, and in particular the pattern of directional variability of the flow, ω, in Figure 3.6 (see Section 2.5).

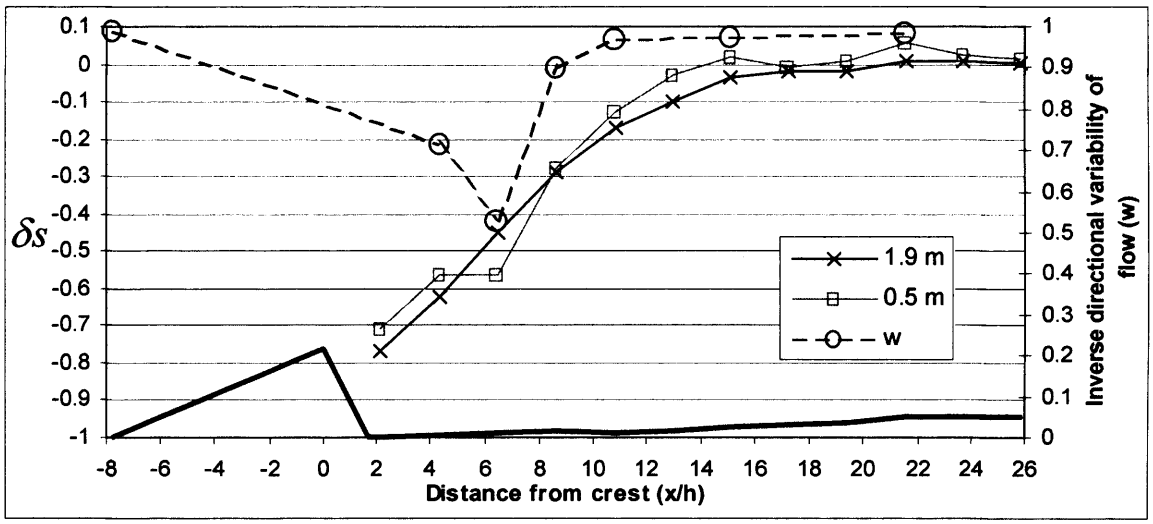

Figure 3.6 Time-averaged normalised velocity in the lee of isolated barchan, BARC2a, for the two sampling heights (Run 6C) as presented in Figure 3.4. In addition is the normalised directional variability of flow (ω), measured at z = 0.5 m. Note inverse scale for directional variability. Dashed line to aid interpretation only.

Downwind of the dune, the point where flow re-attaches to the surface is characterised by the highest directional variability, since this is the location where flow is most erratic as the boundary of the separation cell migrates (Sweet and Kocurek, 1990). It can be seen that direction is most variable at x/h = 6.49, where ω = 0.53. Closer to the slipface at x/h = 4.32, flow direction was relatively more constant with ω = 0.71. Thus the similar velocities at z = 0.5 m for both these points confirms that they were both incorporated within the separation cell, and that flow re-attachment was at least 6.5 h from the crest. Flow direction is considerably more stable by x/h = 8.63 (ω = 0.90), with this decrease in variability pointing to recovery of flow downwind of re-attachment. At this distance there is also the first evidence of the velocities at both heights sharing the same fractional speed-up (δs = -0.27). Thus the greater directional constancy together with the increasing overall velocity (and the change in its gradient) as shown by the δs values are both diagnostic of flow recovery.

From these data, flow is ascertained to be re-attached between x/h = 6.49 and 8.63 for BARC2a, and shows a better concurrence with the suggested 10 h upper limit for separation behind dunes of Walker and Nickling (2002) and the lee-side flow fields modelled by Parsons *et al.* (2004b). At x/h = 10.86 the directional variability of the flow has dropped further to ω = 0.97, a level which is comparable to the constancy of upwind reference values. At this distance δs = -0.17 at z = 1.9 m and δs = -0.13 at z = 0.5 m show that the attributes of primary flow direction recover before mean velocity. Figure 3.6 demonstrates that investigating the velocity data in conjunction with the directional variability of flow greatly assists in the

interpretation of the lee-side secondary flow elements such as re-attachment and subsequent recovery.

Given the greater downwind distance required for flow re-attachment that is imposed by the crest-brink unified dune when compared to the crest-brink separated form, a greater distance also exists before mean velocity values match the unperturbed reference conditions. In Figure 3.4 it is evident that for BARC2a flow in the lee of the dune is closest to the reference profile at x/h = 17.23 (Figure 3.4). This is over twice the distance suggested by Frank and Kocurek (1996b) as necessary for equilibration of velocity profiles. There is an indication that the velocity gradient between the sampling heights, and therefore shear between near-surface flow and that at z = 1.9 m above this, becomes restored at x/h = 8.62, but velocities are still δs = -0.3 less than upwind at both heights. Downwind of this point, there is a relatively greater acceleration in the flow at z = 0.5 m evident from x/h = 10.86 to 15.11. Given flow re-attached in the lee of BARC2a around 7 h, the increased speed-up detected near the surface from 11 to 15 h matches well with a *6 h* distance from re-attachment where Walker and Nickling (2003) noted rapid IBL development at the surface.

The pattern of lee-side secondary flow in the mean velocity data is significantly different between the isolated study dunes due to the effects of their different morphologies. The dune morphology associated with the crest-brink separated form, BARC1, ensures that as air passes the crest, the change in surface attitude is insufficient to cause separation at this point, and whilst undergoing expansion, the flow effectively follows the dune topography. At the brink, where flow de-couples from the dune, the streamlines possess a component of downward deflection which impels re-attachment to the surface. This was evident in flow visualisation experiments (Figure 3.5). For certain crest-brink separated dune situations, the lee-side flow has been found to be capable of remaining attached to the dune surface downwind of both the crest and the brink. This led Sweet and Kocurek (1990) to cite lee-side geometry (slope angle) as a key determinant of near surface lee-side flow type. The crest-brink separated profile also produces negative (convex) streamline curvature, which is recognised to dampen turbulence (Section 3.2.2.4), and has been incorporated in a model of barchan dune morphodynamics (Wiggs *et al.*, 1996) (Figure 1.4). With a sharp crested dune, where crest and brink are co-incident, there is no portion of convex curvature after the crest and the dune does not impart a

downward trend to the detached air. As a result, flow re-attachment and the recovery of flow characteristics to upwind velocities is seen to occur over a longer distance.

3.2.2 Turbulence variation over isolated dune examples

This section shows the variation in the different elements of Reynolds stress measured on the isolated dunes. Turbulence patterns were measured in the lee of both BARC1 and BARC2a dunes where the flow was sampled at a height of z = 0.5 m. In the case of BARC1, the variation in Reynolds stresses upwind of the dune body was also observed and for this transect the sonic anemometer sampled at z = 0.3 m (see Section 2.4.2).

3.2.2.1 Streamwise Reynolds stress component for isolated dune examples

Figure 3.7 shows the observed pattern of the streamwise component of Reynolds stress ($\overline{u'^2}/U_r^2$) upwind of, over and in the lee of the isolated dune BARC1.

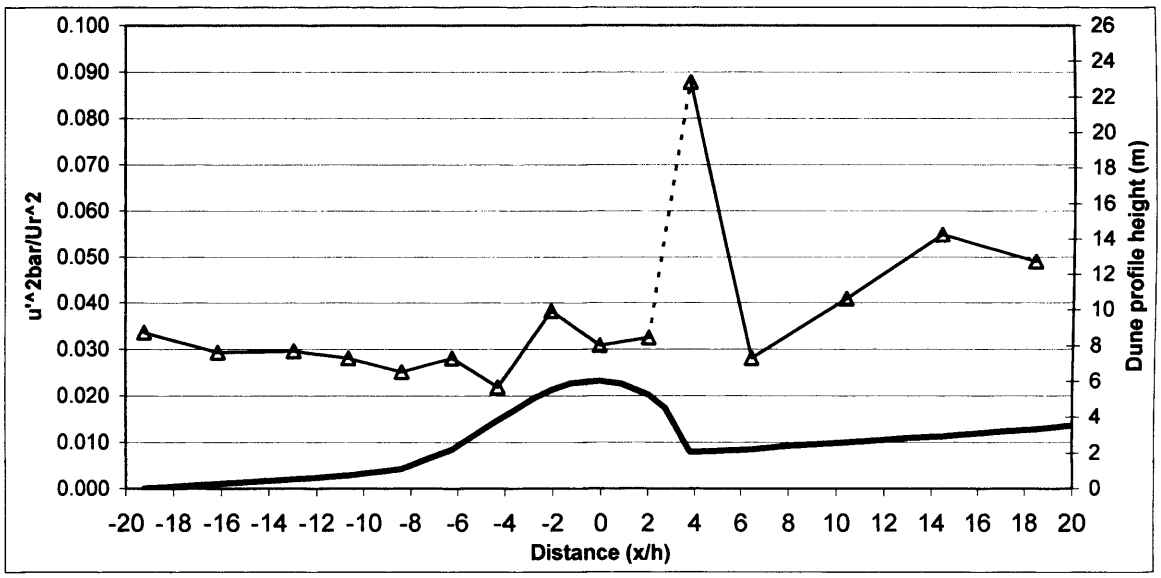

Figure 3.7 Variation in streamwise Reynolds stress ($\overline{u'^2}/U_r^2$) over an isolated barchan BARC1. Dashed line represents abrupt change from upwind to downwind transects. Sampling height z = 0.3 m upwind, z = 0.5 m downwind of brink. Dune height is exaggerated.

At the furthest point upwind of the dune, x/h = -19.22, the streamwise Reynolds stress component is 0.0336, and drops to 0.0294 at x/h = -16.12 where it remains constant until x/h = -12.96. These upwind values are of particular interest since they represent conditions that characterise the streamwise turbulence of unperturbed flow and can be compared to the turbulence patterns observed within the study interdunes. Downwind of the relatively stable streamwise turbulence around x/h = -14.00 there follows a more sustained drop in $\overline{u'^2}/U_r^2$ to

x/h = -8.34 the first measurement on the windward slope, where values are 75% of those at the furthest upwind location. The occurrence of this decrease in streamwise turbulence is coincident with the fall in flow velocity that was seen upwind of the isolated dune toe (Figure 3.1). This measured turbulence decline does not match well-established findings which have shown an increase in streamwise turbulence upwind of hills (Zeman and Jensen, 1987; Finnigan *et al.*, 1990) and a dune centreline in a wind tunnel (Wiggs *et al.*, 1996). On the lower windward slope at x/h = -6.21 however, $\overline{u'^2}/U_r^2$ is seen to rise noticeably toward upwind levels and this suggests there may be a lag in the response of streamwise turbulence to the upwind velocity reduction. The data in Figure 3.7 show a far better fit with the Wiggs *et al.* (1996) $\overline{u'^2}/U_r^2$ observations made furthest from the surface, and along a dune *flank* transect. Furthest above the surface, Wiggs *et al.* similarly detected a peak in the streamwise Reynolds stress for the dune toe that was located on the lower windward slope. The appearance of this peak was therefore downwind of the location of maximum velocity deceleration, as is also the case here.

Considering this turbulence of the flow over the dune, the data in Figure 3.7 continue to show a close similarity to the measurements of streamwise Reynolds stress over a barchan flank conducted by Wiggs *et al.* (1996). In purposely observing flow over a barchan dune flank, Wiggs *et al.* studied the effect of a dune topography profile that incorporated a separated crest and brink. This is instructive since the separation of these features on the dune profile is also the case for the centreline of BARC1. Subsequent to the peak on the lower part of the windward slope (x/h = -6.21) where $\overline{u'^2}/U_r^2$ rises to 0.0282 (discussed above), there is a sharp drop in the middle of the slope. This broadly corroborates the pattern of the Wiggs *et al.* data, although the extent of the observed fall is larger here since turbulence dips to 35% below the furthest upwind value. At x/h = -2.03 streamwise turbulence rises again where it exceeds the extreme upwind value by 15% and establishes a maximum. Further downwind of this peak, at the crest and upwind of the brink, there is a drop in $\overline{u'^2}/U_r^2$ to levels that are around 10% lower than for x/h = -19.22. The turbulence patterns and their geomorphological implications for dunes are explained with reference to streamline curvature and acceleration in Section 3.2.2.4.

In the immediate lee of the dune (x/h = 3.84), $\overline{u'^2}/U_r^2$ peaks dramatically with values just over two and a half times those at x/h = -19.22. The generation of such turbulence has been found to be associated with the separation of flow and the creation of secondary flow structures that produce considerable turbulent stresses. In particular, relatively high streamwise turbulence exists between the sheltered separation cell and the overlying wake region along an area termed the turbulent free shear layer (see Figure 1.5) (Allen, 1994; Bennett and Best, 1995; Keogh and Addison, 1996). The existence of this layer and its proximity to x/h = 3.84 for BARC1 was also portrayed in the gradient between the mean velocity sample heights (Figure 3.4). The turbulence associated with this layer is produced by the shedding of eddies from the layer, with these vortices responsible for the generation of streamwise turbulent elements (Kiya and Sasaki, 1983; Müller and Gyr, 1986). This eddy shedding is certain to be detected at x/h = 3.84 given the proximity of the sampling point to the shear layer. Furthermore, sub-aqueous experiments have found that the surface region where flow becomes re-attached and where the shear layer projects onto the bed tends to display high streamwise turbulence as eddies impact here (Bennett and Best, 1995; Best and Kostaschuk, 2002).

The contribution of the re-attaching flow to the $\overline{u'^2}/U_r^2$ peak at x/h = 3.84 is shown by the fact that the mean velocity data for BARC1 (Figure 3.2) suggested that flow was re-attached before x/h = 5.14. It has also been found that re-attachment itself occurs over a distance of 0.5 h, due to the different size eddies shedding off the shear layer at the surface (Walker and Nickling, 2002). This suggests that turbulence sampling at x/h = 3.84 will not only receive the input of eddies leaving the shear layer, but also those vortices that arrive at the surface, both of which create Reynolds streamwise stress. It is also notable that the similar lee-side streamwise turbulence findings of Best and Kostaschuk (2002) were for a dune with a low angle lee slope (14°) that may have similarities to the crest-brink separated BARC1 with its convex profile downwind of the crest.

As flow recovers with no obstacles downwind of the dune, the streamwise component of Reynolds stress exhibits an increase between x/h = 6.49 and 14.42 where at the latter it is 63% greater than furthest upwind. From x/h = 14.42, values start to drop so that by the furthest downwind extent of the measurement transect (x/h = 18.42), $\overline{u'^2}/U_r^2$ is 46% greater than the value at the upwind extremity. This difference could be attributed to the sonic sampling

height of z = 0.5 m for the lee compared to z = 0.3 m for the upwind and windward transect. Figure 3.8 adds the plot of streamwise Reynolds stress measured in the lee-side of BARC2a, a second isolated bedform for which turbulence data were collected over an extended lee-side distance.

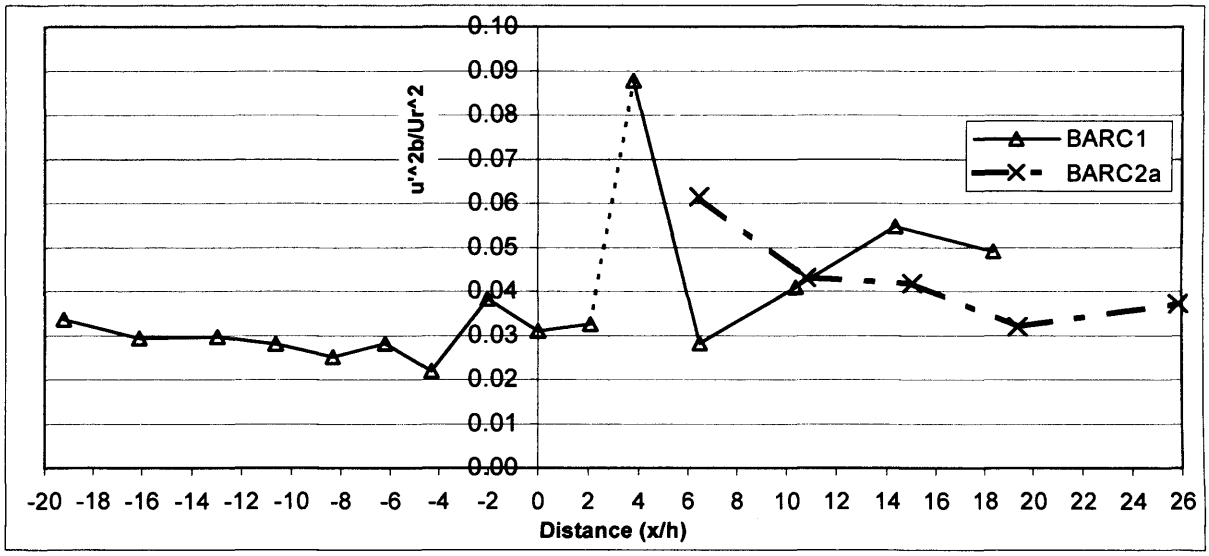

Figure 3.8 Lee-side recovery of streamwise Reynolds stress ($\overline{u'^2}/U_r^2$) downwind of two isolated dune examples. A composite diagram of streamwise turbulence upwind and downwind of the dune crest for BARC1, and an extended downwind portion for BARC2a.

For BARC2a, the maximum value of $\overline{u'^2}/U_r^2$ was again found at the sampling point nearest to the upwind dune body, where the peak was 0.0615 at x/h = 6.49. In Figure 3.8 the normalised horizontal turbulence for BARC2a at this distance is around twice that of BARC1. This difference is ascribed to the greater distance that separated flow is projected by the sharp crested dune morphology of BARC2a, (see Section 3.2.1.3). With separated flow existing over a further lee-side distance, the free shear layer extends further downwind for the crest-brink unified dune and this leads to the production of streamwise turbulence further downwind. The observed $\overline{u'^2}/U_r^2$ pattern again agrees with the mean velocity (Figure 3.6), with a mean flow-reattachment distance of around 6.5 h. As highlighted, this is further than the 4 h found for BARC1, and therefore shares better agreement with Walker and Nickling's (2002) findings of 6-10 h (and Nelson *et al.*, 1995). In the lee-side of the sharp crested BARC2a compared to the rounded BARC1, the influence of flow re-attachment is still evident in the streamwise turbulence signal at x/h = 6.49. Figure 3.8 shows that between 10 and 11 dune heights downwind, there is only a 5% difference in $\overline{u'^2}/U_r^2$ for both dunes.

In the downwind flow recovery zone, there is a difference in the behaviour of streamwise turbulence for the two isolated dunes (Figure 3.8). Whereas the lee-side of BARC1 reveals an increase in streamwise turbulence with distance from the dune before a decline evident at *x/h* = 14.42, the data for BARC2a in Figure 3.8 show an ongoing decrease with distance. Significantly, the BARC2a data extend for a greater downwind distance of over 25 *h*. In doing so, the data show that by *x/h* = 25.87, streamwise turbulence has recovered to within 10% of the furthest upwind values measured for BARC1. Walker and Nickling (2003) reported a similar dimensionless distance for streamwise turbulent stresses to recover to upwind values for a model transverse dune in a wind tunnel. In the Walker and Nickling study however, turbulence demonstrated an increase over the lee-side distance to level off at upwind values. Such increases were also seen from a re-attachment minimum to an equilibrium flow state in fluvial studies downstream of dunes (McLean and Smith, 1986; Nelson and Smith., 1989). The difference between these overall increases and the decrease exhibited in Figure 3.8 is due to the measurement of turbulent stress at the surface by the other studies. In measuring at the surface, turbulence is sampled as it grows under the developing IBL, which is established following flow re-attachment to the surface. At a sampling height of z = 0.5 m for the lee-side of BARC2a in Figure 3.8, the general fall in $\overline{u'^2}/U_r^2$ toward recovered values is more likely to be a result of the lower wake's dissipation as mean velocity profiles recover and flow becomes steadier (Frank and Kocurek, 1996b). As reported, the distance for recovery of streamwise turbulence in this study shows a good similarity to those from others, despite the different trend increases. Certainly by the point at *x/h* = 19.40 for BARC2a, the value of $\overline{u'^2}/U_r^2$ is similar to far upwind of the dune and this would suggest that by this distance, a height of z = 0.5 m was safely well within the IBL originating at re-attachment.

For BARC1, where separated flow has been seen to become re-attached close to the dune due to its crest-brink separated profile (c. 5 *h*), the initial increase for streamwise turbulence between *x/h* = 6.49 and 14.42 could be reflecting an aspect of the IBL development analogous to Walker and Nickling's (2003) findings. Whilst it is acknowledged that z = 0.5 m is unlikely to be inside the IBL so close to the re-establishment of the layer, Walker and Nickling report a rapid rise in shear stress from streamwise fluctuations at the surface within 6 *h* of flow reattachment. The observed increase in $\overline{u'^2}/U_r^2$ to c. 14.5 *h* from the crest at z = 0.5 m may mirror that increase noted for the surface by Walker and Nickling (2003). Generation of turbulence between the growing IBL and the lower wake may also be responsible. Flow

recovery is a combination of wake dissipation from higher regions and internal boundary layer growth from the surface (Frank and Kocurek, 1996b; Walker and Nickling, 2002). The effects of this combination can explain the observed streamwise turbulence patterns in the lee of the isolated dunes where topography does not interfere with airflow recovery. The evidence of the recovery of streamwise Reynolds stress components here also agrees generally with fluvial experiments, at the lower end of the 30-50 *h* range suggested by McLean and Smith (1986).

3.2.2.2 Vertical Reynolds stress variation for isolated dune examples

Figure 3.9 indicates that there is relatively little variation in vertical turbulence from upwind of BARC1 to the crest of the dune.

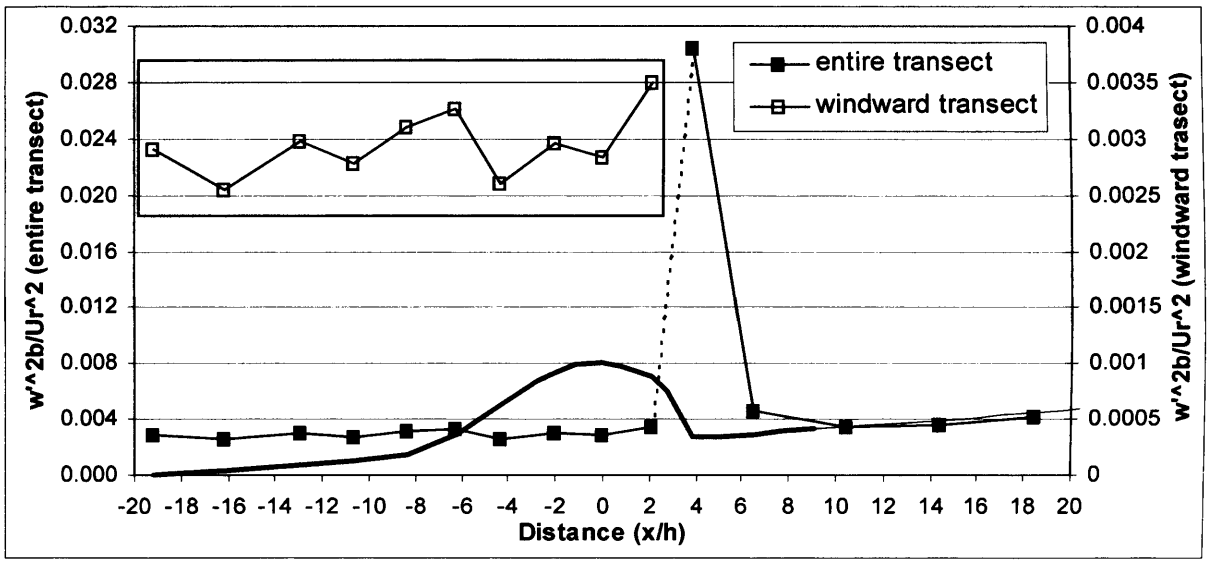

Figure 3.9 Variation in vertical Reynolds stress ($\overline{w'^2}/U_r^2$) over an isolated barchan BARC1. The boxed profile shows the data for the windward portion of the entire transect, plotted on a reduced scale (right hand axis) to show variation for the upwind area. Dune height vertical scale is exaggerated.

Along the windward transect (detail in inset Figure 3.9), $\overline{w'^2}/U_r^2$ is 0.0029 at x/h = -19.22 and the variation up to the dune brink is never more than 20% from this reference value. Over the dune body itself, two peaks are noticeable in the variation of vertical turbulence. The first lies on the lower windward slope at x/h = -6.21, after which there is a sudden drop to below upwind values. A second peak is found in the region between the crest and the brink where the vertical Reynolds stress component reaches 0.0035 (x/h = 2.09). The significance of these peaks is attributed to the effects of streamline curvature and is discussed in Section 3.2.2.4.

The maximum component of vertical Reynolds stress is found in the lee of BARC1 (x/h = 3.84), where values are over 11 times greater than those at x/h = -19.22. Relatively low vertical turbulence has been found to characterise the ground surface of, and the area contained within, the flow separation cell itself. The free shear layer between the separation cell and the wake flow region on the other hand is an area of high vertical turbulence, due to eddy shedding along the length of the layer (Bennett and Best, 1995). The peak in $\overline{w'^2}/U_r^2$ observed here indicates the influence of this shear layer as detected in the vertical turbulence signal. The evidence of the shear layer being near to the surface at x/h = 3.84 also suggests that flow re-attachment must also be near to this point (a supposition reinforced by the high $\overline{u'^2}/U_r^2$ values, Figure 3.8). By x/h = 6.49 vertical turbulence has diminished considerably and is only 61% greater than the furthest upwind measurements. This shows a significant reduction in the influence of the shear layer, since fewer $\overline{w'^2}/U_r^2$ generating eddies conveyed from the shear layer were found to reach this far downwind. At x/h = 10.44, $\overline{w'^2}/U_r^2$ is 0.0034 and has recovered to a value only 17% away from x/h =-19.22, however, by the furthest downwind point on the transect, the vertical turbulence has risen to a level 45% greater. The pattern of the vertical Reynolds stress variation in the lee of BARC2a is shown in Figure 3.10.

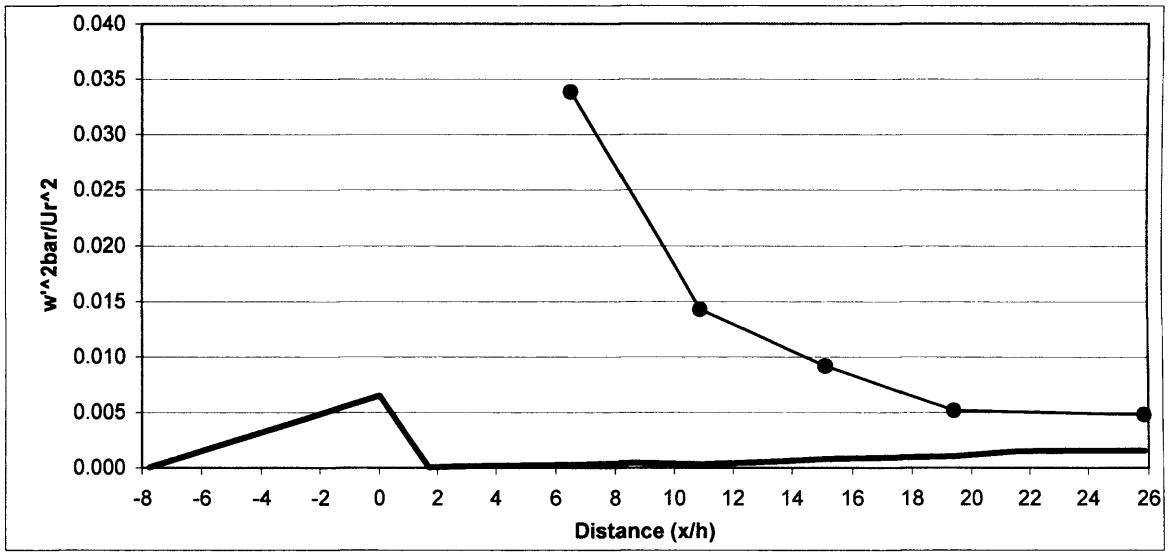

Figure 3.10 Variation in vertical Reynolds stress ($\overline{w'^2}/U_r^2$) in the lee of isolated barchan BARC2a. Dune height scale is exaggerated.

For BARC2a, the leeside peak in $\overline{w'^2}/U_r^2$ is evident again and at *x/h* = 6.49 it is approximately 7 times the minimum value of 0.00484 at *x/h* = 25.87. With increasing distance downwind from the dune, there is a continual decline in the vertical component of Reynolds stress until *x/h* = 19.40, where values are steady to the furthest point downwind. The differences in the vertical turbulence variation measured on the lee-side for the two isolated examples are presented in Figure 3.11.

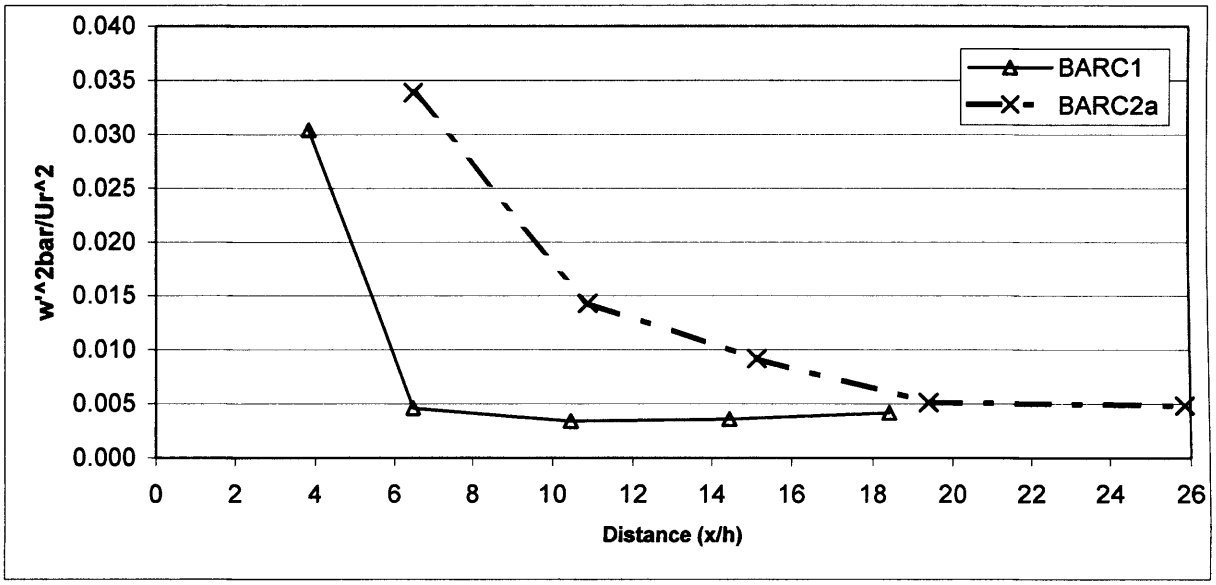

Figure 3.11 Composite diagram of vertical Reynolds stress ($\overline{w'^2}/U_r^2$) recovery on the lee-side of the two isolated barchan dune examples. For dune profiles, see Figure 3.9 and 3.10.

Figure 3.11 presents more evidence to show that the crest-brink unified dune (BARC2a) exerts a more extensive impact on lee-side turbulence characteristics. In the measurements made nearest to the lee slope for BARC2a, the $\overline{w'^2}/U_r^2$ values are of a similar magnitude to BARC1, but they are found to be maintained a further 2.5 *h* downwind at *x/h* = 6.49. This shows that flow separation effects extend to *x/h* = 6.49 since the free shear layer which generates vertical turbulence elements through eddy shedding results in enhanced $\overline{w'^2}/U_r^2$ at this distance. A comparison with the mean flow parameters reinforces this (Figure 3.4). At *x/h* = 10.86 for BARC2a, vertical turbulence is still nearly three times greater than the downwind minimum. In the lee of BARC1 however, $\overline{w'^2}/U_r^2$ demonstrates less than 26% variation from *x/h* = 6.49 to 18.42.

3.2.2.3 Reynolds shear stress variation for isolated dune examples

The variation in Reynolds shear stress for the solitary bedform BARC1 is shown in Figure 3.12.

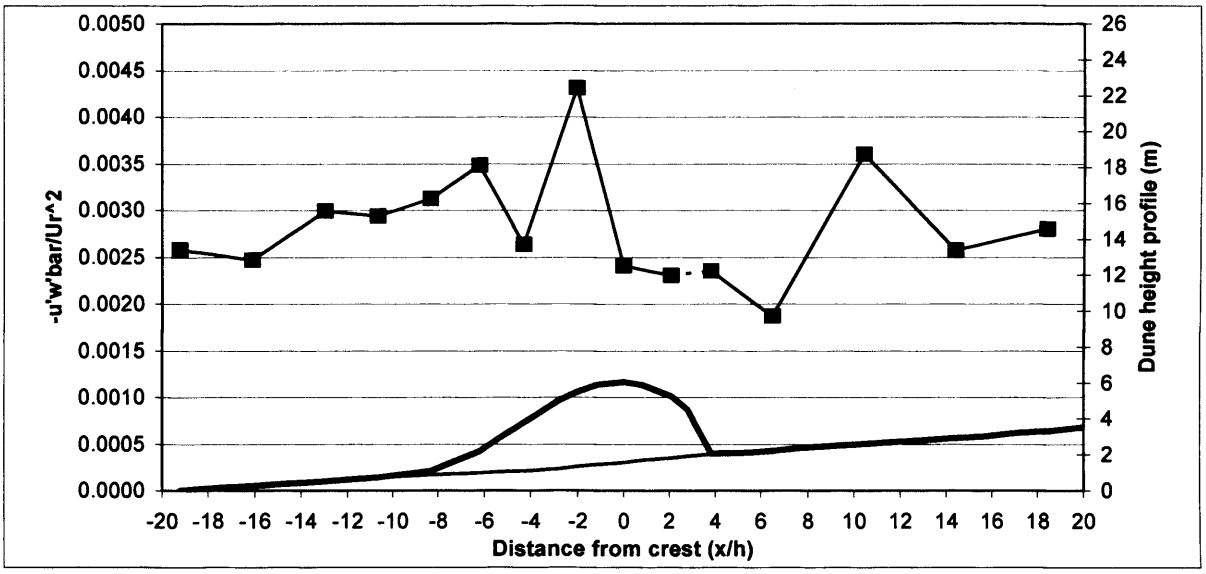

Figure 3.12 Reynolds shear stress ($-\overline{u'w'}/U_r^2$) upwind and downwind of isolated BARC1. Dune height scale is exaggerated.

In relation to an upwind value of 0.0026 at *x/h* = -19.22, values of $-\overline{u'w'}/U_r^2$ show a 16% increase by *x/h* = -12.96. From *x/h* = -10.96 there follows a steady rise in Reynolds shear stress to levels at *x/h* = -6.21 that are 35% greater than those of the upwind reference. This increase in shear stress from the upwind area to the middle of the windward slope is highly significant given that it occurs through a region of significant deceleration of mean flow upwind of the dune (Figure 3.1). For this retardation, it might be expected that shear velocity (u_*) would fall as a result, however it should be remembered that Reynolds shear stress is related to shear velocity through $u_* \equiv \sqrt{-\overline{u'w'}}$ (Equation 2.5) (Wiggs *et al.*, 1996; Walker and Nickling, 2002). Finnigan *et al.* (1990) and others have put forward the positive influence of concave streamline curvature on Reynolds shear stress through the imparting of additional turbulent stresses in order to explain the maintenance of shear in spite of the velocity decrease upwind of hills. The considerable geomorphological significance of this issue for sand dunes is discussed in the following section.

The consistent upwind increase in Reynolds shear stress ceases halfway up the windward slope at x/h = -4.29 for BARC1, where shear stress falls sharply to within 2% of the value at

x/h = -19.22. Following this drop, the maximum value of $-\overline{u'w'}/U_r^2$ then appears at x/h = -2.09, where $\overline{u'^2}/U_r^2$ was also at its greatest on the windward slope, and where mean velocity achieved a maximum too (Figure 3.1). For fluvial studies, the maximum shear stress has been predicted and measured in just such an upper stoss location (McLean and Smith, 1986; Nelson *et al.*, 1993). This suggests that the $-\overline{u'w'}/U_r^2$ peak here is primarily a consequence of flow acceleration effects imparting shear stress (Zeman and Jensen, 1987; Walker and Nickling, 2002). The Wiggs *et al.* (1996) Reynolds shear stress maxima were not found as far upwind of the crest as in Figure 3.12, but the effect of BARC1's broad, rounded crestal area has already been noted for mean flow velocity, where the maximum speed-up was also detected some way before the crest. Furthermore, on the rounded sub-aqueous 'sand wave' bedform investigated by McLean and Smith (1986), the surface shear stress maximum appeared upstream of the elongated crest area. After the maximum value upwind of the crest, shear stress in the crest-brink region (x/h = 0 and 2.09) are both at levels up to 9% less than the upwind reference. This is again attributable to streamline curvature, and the negative turbulence dampening effect that is a consequence of convex flow.

It is noteworthy that time-averaged Reynolds shear stress in the immediate lee of the dune is seen to be relatively low. At x/h = 3.84, $-\overline{u'w'}/U_r^2$ is actually 8% less than for x/h = -19.22. The high values for both the streamwise and vertical components of Reynolds stress seen at this location provided evidence of the turbulent layer bounding the separation cell existing near the surface at x/h = 3.84. However, the mean Reynolds shear stress data for this point do not agree, since shear stress would also be expected to be high if the turbulent layer between separation cell and wake was being sampled for the measurement period (Bennett and Best, 1995). Instead, the low shear stress indicates a low covariance between the streamwise and vertical velocity fluctuations. Multi-directional streamwise velocity readings from the sonic anemometer however reveal that reverse flow ($-u$) directed upwind toward the dune slip face was measured for only 4% of the turbulence sampling time at x/h = 3.84. Such an infrequent reverse flow indicates that x/h = 3.84 was on the very downwind limit of the flow separation zone in the lee of BARC1. This is confirmed by the rapid acceleration in the time-averaged velocity at z = 0.5 m between x/h = 3.84 and 5.14, which is a response to faster flow at the surface occurring after re-attachment (Figure 3.3). Around re-attachment therefore,

$-\overline{u'w'}/U_r^2$ is found to be low as a time averaged value. Whilst the mean is low, the variation in shear stress is great. The co-efficient of variation (CV_τ) for the shear stress expressed as

$$CV_\tau = \sigma_{u'w'}/-\overline{u'w'} \qquad \text{Equation 3.1}$$

where $\sigma_{u'w'}$ is the standard deviation of the $u'w'$ product. This shows that the variation is nearly 25 times the mean value for x/h = 3.84. With both values normalised to U_r, the CV_τ at x/h = -19.22 (for z = 0.5 m) was a sixth of that for x/h = 3.84. This implies intermittent high shear stresses exist at re-attachment and is attributed to the effect of eddies from the shear layer impacting at the re-attachment point (Bennett and Best, 1995; Walker and Nickling, 2003). The low prevalence of reverse flow also indicates that the sample point is not entirely within the mean sepration cell. Were this the case, much more of a reverse flow component would be observed than the 4% here.

Further downwind from the immediate lee, and after a further drop in $-\overline{u'w'}/U_r^2$ to 28% less than the upwind reference, there is a sharp rise in $-\overline{u'w'}/U_r^2$ to levels that are 40% higher at x/h = 10.44. Following this however, at both x/h =14.42 and 18.42, Reynolds shear stress return to values within 8% of those of the upwind reference, suggesting a nearly complete recovery of the shear stress parameter. This occurs as the wake region loses its turbulent energy through its vertical expansion downwind, and eddy shedding (Walker and Nickling 2002). In terms of lee-side recovery distance, the behaviour of Reynolds shear stress at z = 0.5 m measured here mirrors the pattern of surface stress recovery in terms of distance, if not their trend. This is attributed to the fact that when the bed stress is measured, the IBL growth leads to an increase in shear stress from a minimum at re-attachment to values consistent with unperturbed flow, requiring a minimum distance of c. 20 h (e.g. Bradshaw and Wong, 1972; Walker and Nickling, 2003). The lee-side variation in $-\overline{u'w'}/U_r^2$ is explored further in Figure 3.13 which shows the shear stress patterns in the lee of BARC2a.

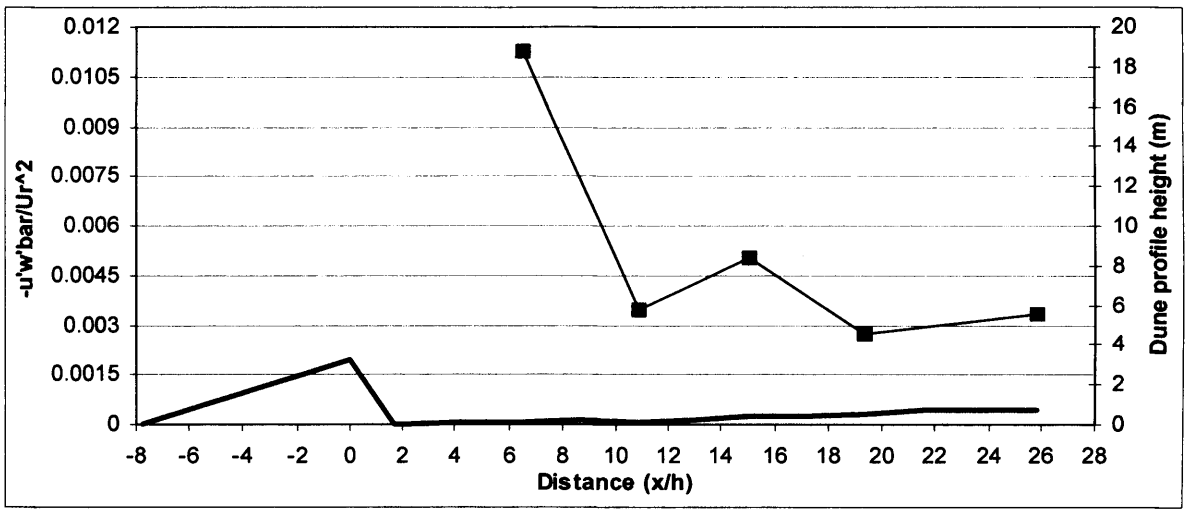

Figure 3.13 Reynolds shear stress ($-\overline{u'w'}/U_r^2$) downwind of isolated BARC2a.

For BARC2a, there is an obvious maximum in shear stress recorded at x/h = 6.49, where the shear is nearly four times greater than the transect minimum located at *x/h* = 19.40. Values for $-\overline{u'w'}/U_r^2$ at *x/h* = 19.40 and 25.87 are within 6% and 28%, respectively, of the Reynolds shear stress upwind minimum observed for BARC1 at *x/h* = -19.22 shown in Figure 3.12. This relatively good agreement suggests that flow has recovered its upwind turbulent characteristics by the end of the transect.

The variations in Reynolds shear stress for isolated bedforms BARC1 and BARC2a are compared directly in Figure 3.14.

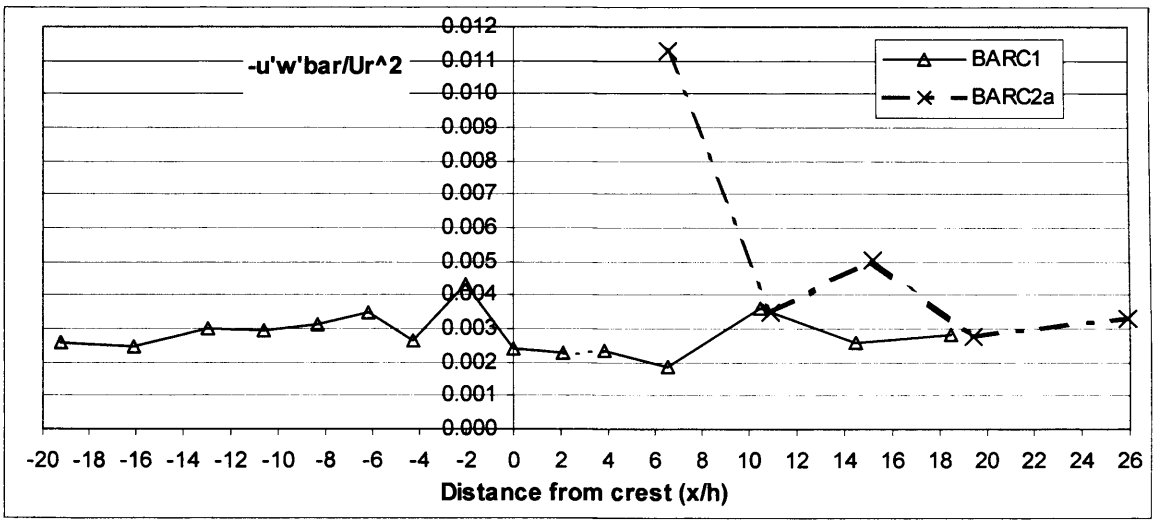

Figure 3.14 Composite diagram of Reynolds shear stress ($-\overline{u'w'}/U_r^2$) variation for the two isolated barchan dune examples. For dune profiles, see Figures 3.12 and 3.13.

The most striking feature in the variation of $-\overline{u'w'}/U_r^2$ for the two solitary study dunes is the absence of a lee-side peak for BARC1, where it was argued a peak might have been expected in association with the shear of the decending limb of the separation streamline. Looking at the reverse flow from the high frequency sonic velocity measurements for x/h = 6.49 of BARC2a, for which there is a significant signal of shear stress, the existence of a back eddy flow toward the dune ($-\bar{u}$) was observed for 20.3% of the run duration. This indicates that for the measurement period, flow separation in the lee of BARC2a extended to beyond x/h = 6.49 for around a fifth of the time. This led to the sample point registering a considerable time-averaged Reynolds shear stress since it periodically came in contact with key flow elements for the generation of shear; the turbulent layer, and the point of flow re-attachment. The reduced reverse flow signal at x/h = 3.84 for BARC1 reveals lee-side separation rarely extended past this distance, and $-\overline{u'w'}/U_r^2$ as a mean was consequently low (though variation defined by Equation 3.1 was high).

There also appears to be interesting behaviour in the recovery of the Reynolds shear stress on the lee-side for both dunes. At x/h = 15.11 in BARC2a, Reynolds shear stresses demonstrate evidence of secondary flow elements since they remain 78% higher than the transect minimum, and for BARC1, a similar but smaller peak (39% higher) in $-\overline{u'w'}/U_r^2$ is evident in the recovering shear stresses at x/h = 10.44. These discrete rises occur at approximately 8-9 *h* downwind of the point of flow re-attachment for each dune if, as evidence would suggest, re-attachment occurs around 3 *h* for BARC1 and 6 *h* for BARC2a. The wake is a region of flow recovery, in which there is downward momentum from the higher speeds of the upper portions of flow as a key element to the recovery of the retarded lower wake (Frank and Kocurek, 1996b). It is suggested that the increases in Reynolds shear stress detected for BARC1 and BARC2a at 8-9 *h* downwind from flow re-attachment represent the distance where the maximum effect of downward momentum transfer from faster moving upper air can be detected at z = 0.5 m (near the base of the lower wake). The distances of 15.11 *h* and 10.44 *h* are beyond, but in loose agreement with a length of 8 *h* found necessary for lee-side velocity profiles to equilibrate between the upper and lower wake (Frank and Kocurek, 1996b) and a distance of 10 *h* for when constant momentum deficit from sub-aqueous upper flow is first achieved (Nelson and Smith, 1989). The estimations are improved for BARC1

when distances are considered as heights from the brink, the point where flow separation actually occurs.

After these identified peaks in the case of both dunes, $-\overline{u'w'}/U_r^2$ is seen to decrease toward unperturbed reference values, and then to exhibit a gradual increase. This behaviour would appear to be a consequence of sampling within the IBL, identifiable in the furthest downwind reaches of the two lee-side transects.

3.2.2.4 Discussion of turbulence variation over isolated dune examples

Distinctive patterns exist for turbulence elements measured for isolated dunes. Several studies have highlighted the influence of streamline curvature on turbulent flow parameters over hills (Gong and Ibbetson, 1989; Finnigan *et al.*, 1990) and more recently over sand dunes as well (Wiggs *et al.*, 1996; van Boxel *et al.*, 1999). For this study, the effect of streamline curvature on the generation of turbulence is evident upwind of and over the isolated study dune BARC1. Figure 3.15 is a plot of the relationship between surface slope and streamline angle over BARC1 from which an appreciation of flow curvature can be ascertained.

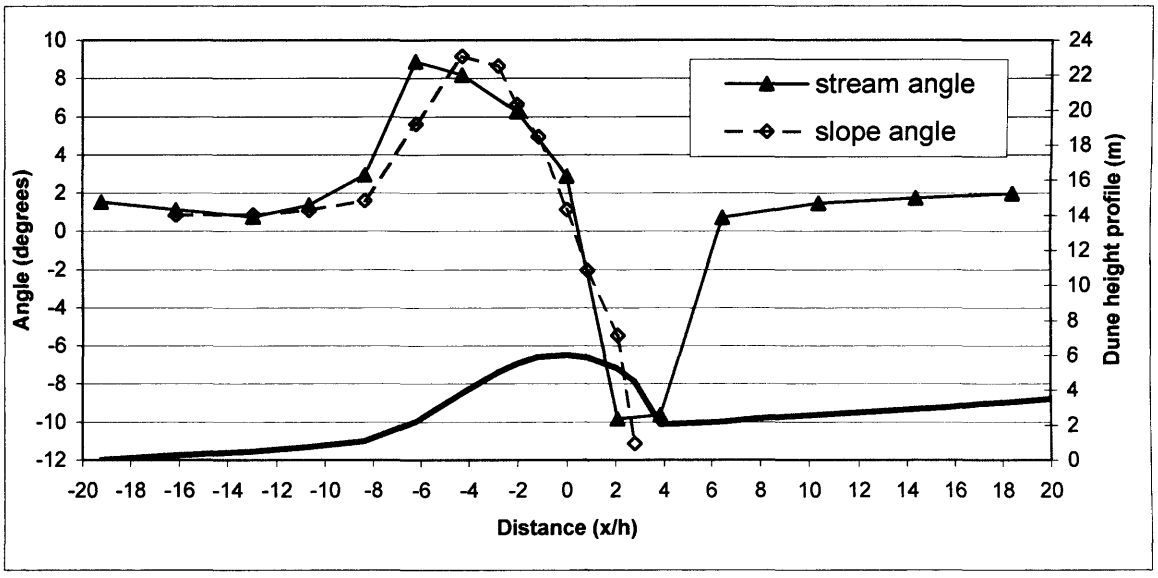

Figure 3.15 Angle of dune surface slope and flow streamline angle at z = 0.3 m over BARC1. Streamlines calculated from sonic anemometer-derived mean horizontal and vertical flow velocities.

Figure 3.15 reveals that the onset of concave streamline curvature at the dune toe occurs at x/h = -10.65, and that concave (positive) curvature can be seen to exist up to the peak in streamline angle, at x/h = -6.29. After this point, the flow angle takes on a convex nature

which leads to negative streamline curvature being evident over the uppermost half of the windward slope and over the crest of the dune as a consequence of its rounded profile.

$\overline{w'^2}/U_r^2$ and $-\overline{u'w'}/U_r^2$ have been found to be turbulent elements that are most sensitive to the effects of streamline curvature (Zeman and Jensen, 1987; Finnigan *et al.*, 1990). Figure 3.15 clearly shows how the area of positive streamline curvature leads to bolstered values of Reynolds shear stress upwind of the dune, despite the recorded drop in mean velocity for this area (x/h = -16.11 to -8.34, Figure 3.1). Concave flow leads to the introduction of extra turbulent structures into the lower velocity portions of the flow profile as vertical motions. These vertical motions increase flow instability, with convex flow producing an opposite effect by imposing stability (Bradshaw, 1969) (Figure 3.16). The addition of these vertical elements is demonstrated by the attendant increase in $\overline{w'^2}/U_r^2$ from x/h = -10.65 to its local peak at x/h = -6.29 (Figure 3.9). This rise in vertical turbulence coincides with the positive stream curvature observed up to the middle of the windward slope.

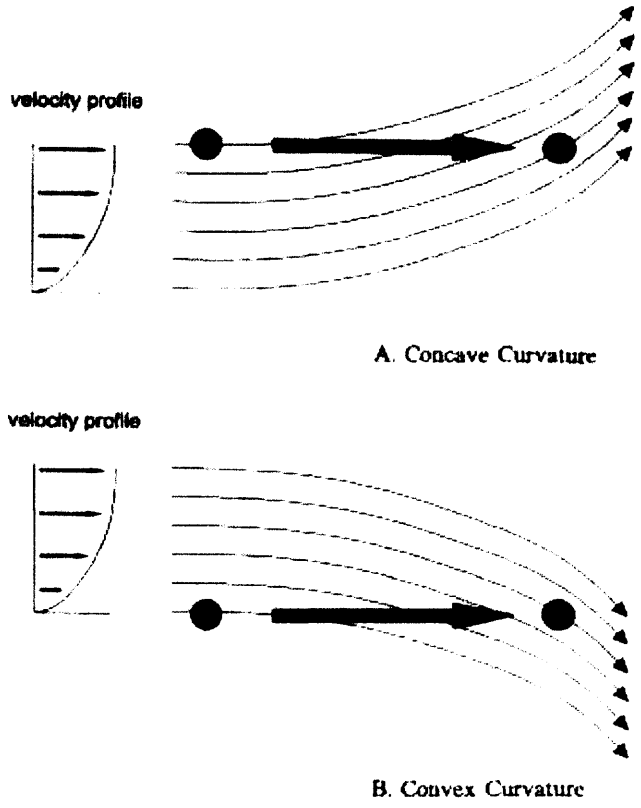

Figure 3.16 The effect of concave and convex streamline curvature on delivering turbulent structures (dots) into different portions of the flow profile, and toward or away from the ground surface (from Wiggs *et al.*, 1996).

The influence of streamline curvature in explaining the turbulence variation over the windward slope of BARC1 is further revealed by the immediate impact that the end of streamline concavity and the onset of streamline convexity brings. Where the positive effects of concavity cease, and where stream curvature has turned negative at *x/h* = -4.29 (Figure 3.15), as the two elements most related to curvature, there is a sudden decrease in $\overline{w'^2}/U_r^2$, and a co-incident drop in $-\overline{u'w'}/U_r^2$ as well. At this point, flow acceleration on the windward slope is the primary factor in the generation of shear stress and, without the turbulent effects of positive streamline curvature, there is an immediate related drop to near upwind levels. Furthermore, the existence of the maximum negative curvature over the top of the dune ensures that $-\overline{u'w'}/U_r^2$ at the crest, and between there and the brink, is severely dampened (Kaimal and Finnigan, 1994). The slight peak for the vertical component of Reynolds stress in this area at *x/h* = 2.09 despite the strong convexity of streamline may well be due to flow expansion which in turn leads to vertical turbulence (Figure 3.9).

Another way of demonstrating the existence of streamline curvature in the sensitive upwind toe region is by examining the flow property of *turbulence intensity* (Stull, 1988; Raupach and Finnigan, 1997), normalised here to the velocity at the reference tower. Turbulence intensity is defined as

$$\alpha = (RMS_{u'}/\bar{u})/U_{r0.5} \qquad \text{Equation 3.2}$$

where α is local turbulent intensity, $RMS_{u'}$ is the root mean square of the fluctuating streamwise velocity component (u'), $\bar{u}$ is local mean instantaneous velocity and $U_{r0.5}$ is mean velocity at z = 0.5 m of the reference tower.

Wiggs *et al.* (1996) argued that where the concave streamline curvature associated with dune topography dominated, flow de-stabilisation would occur since the concavity encourages vertical motion within the velocity profile. This is reflected in increased flow instability, and greater streamwise turbulent intensity due to the contribution of the vertical stresses. Given the positive curvature at the dune toe, enhanced turbulent intensity should be expected for the dune toe, and α measured for BARC1 is shown in Figure 3.17.

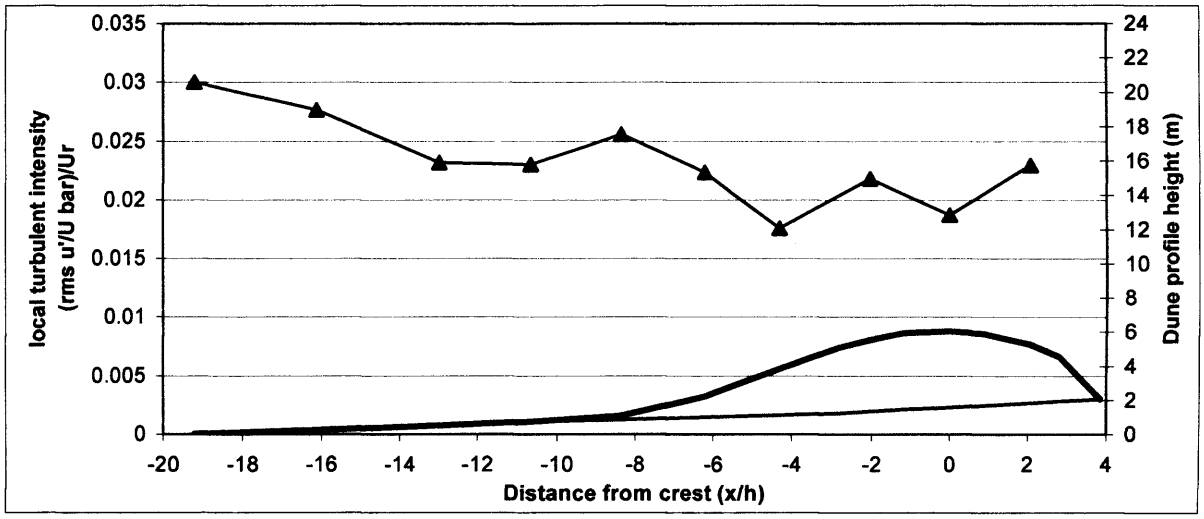

Figure 3.17 Local turbulent intensity (α) over the dune body of BARC1.

Turbulent intensities are initially relatively high in the upwind area, before exhibiting a reduction as the dune is approached. However, there is a significant localised peak in α at the very toe of the stoss slope (x/h = -8.34), where the mean velocity was lowest (Figure 3.1) and the time-averaged streamwise component of Reynolds stress was actually seen to be at a relative low too (Figure 3.7). This peak in turbulent intensity was first noted for dunes by Wiggs *et al.* (1996), and as confirmed in the field study here, it is regarded as indicative of the de-stabilisation of flow at the windward slope toe. The cause of this instability is attributed to the effects of streamline curvature detected in this locality. Along the windward slope, the acceleration of flow due to streamline compression encourages flow stability and there is an attendant dampening of turbulent intensity. The fall in α on the windward slope suggests that turbulence becomes less contributory to shear stress generation compared to forces of streamwise momentum transfer imparted by the ongoing flow acceleration (Walker and Nickling, 2003). Upwind of the crest (x/h = -2.09), there is an upturn in α which was also detected by Wiggs *et al.* (1996) though the magnitude of the gain is larger here, and the further crest-brink rise is due to flow expansion.

The effects of streamline curvature have been suggested to be an important control on the upwind toe area of dunes, one of the most morphodynamically significant parts of the dune. Wiggs (1993) postulated that a rise in turbulence brought about by concave streamline curvature in the toe region has the effect of maintaining sediment transport in the face of the pressure-induced mean velocity reduction (also Wiggs *et al.*, 1996). The effect of positive streamline curvature at the toe leading to a greater $-\overline{u'w'}$, and therefore also shear stress, has

also been modelled for airflow over a dune by van Boxel *et al.* (1999). The findings produced here seem to provide field evidence of the extent to which concave streamline curvature at the toe is sustained, and actually increases.

One problem for the findings here however is that the measured shear stress may not be within the inner layer of Jackson and Hunt's (1975) analytical approach to flow over hills, a region where stress is constant (Wiggs, 2001). This is because that when the flow reaches the windward slope, it might be that a new IBL begins to develop, as suggested by Frank and Kocurek (1996a). However, with measurements at z = 0.3 m, it might be assumed that the eddies detected as generating the extra stress in the toe region here should also be projecting extra stresses at the surface where they will be responsible for enhancing sediment transport.

This possible importance of streamline curvature in controlling sediment transport at the toe of dunes through contributing extra downward vertical stresses to the surface, has important implications for interdunes as well. Given the reduction in mean velocity at the toe, the generation of stresses is necessary at the toe of the downwind dune bordering an interdune in order for the downwind migration of the dune (Tsoar, 1985). The position of the downwind toe therefore partly determines the extent of the interdune, and dune spacing.

3.3 Characteristics of flow velocity within interdunes

In a similar manner to the other descriptions of airflow patterns created by the isolated dunes, the data here for flow within the different interdunes are the patterns formed by winds that are perpendicular to the crest.

3.3.1 Mean velocity pattern in a closely spaced interdune

Figure 3.18 shows the typical pattern of velocity variation for the interdune with the closest spacing (Table 2.1). The toe of the downwind dune windward slope begins at x/h = 4.42 where the surface slope shows considerable concavity in form. At around x/h = 9.5, convexity begins continuing over the rounded crest and towards the brink (x/h = 14.63). Once again, the observed change in velocity at the two heights (z = 1.9 m, z = 0.5 m) through the interdune is well demonstrated when expressed as a ratio of fractional speed-up.

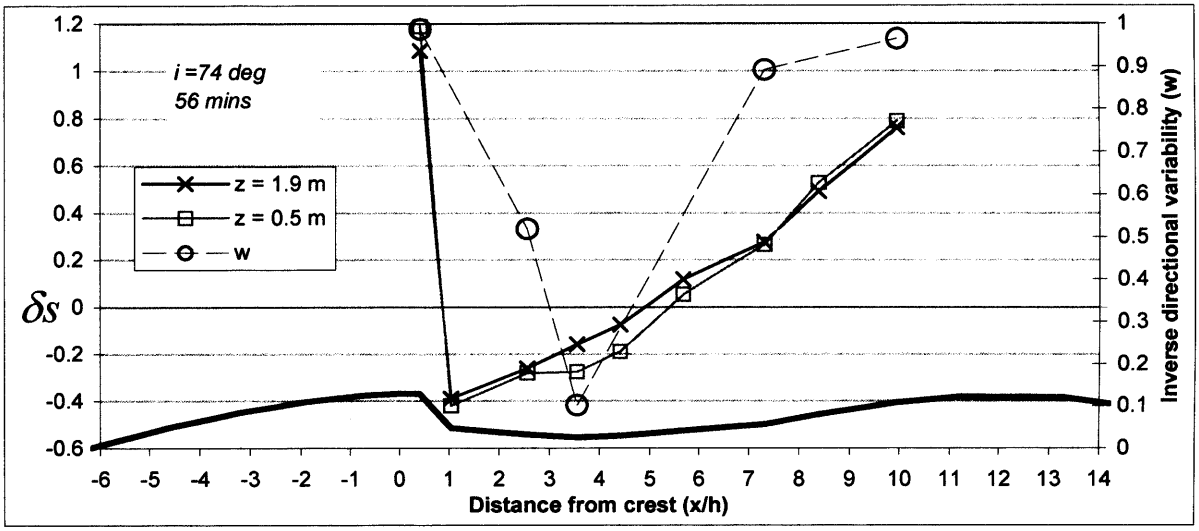

Figure 3.18 Time-averaged fractional velocity in the closely spaced interdune TRANS2 for the two sampling heights (left axis scale) and normalised directional variability of flow (ω), measured at z = 0.5 m (right axis scale). Run i = 74°, duration 56 minutes, mean U_{cr} (crestal velocity) at z = 1.9 m, 7.33 ms^{-1}.

At the crest of the upwind dune, high velocity values are found due to the streamline compression and acceleration of flow over the windward slope, as was also seen for the isolated BARC1 (Figure 3.1). Relative to the reference tower within the interdune (positioned approximately x/h = 6), velocity on the upwind dune crest in Figure 3.18 has increased to δs = 1.09 at z = 1.9 m and δs = 1.19 at z = 0.5 m, therefore over double the speeds observed at the same heights at the interdune reference.

The velocity pattern associated with flow expansion beyond the brink, and the formation of the separation cell in the immediate lee of the upwind dune is broadly similar to that seen for the isolated dune BARC2a in Figure 3.4. At x/h = 1.03 in Figure 3.18 there is a significant drop to δs = -0.39 at z = 1.9 m and δs = -0.42 at z = 0.5 m. It should be noted here that the magnitude of the lee-side decrease in terms of fractional velocity is not as great as that seen for the isolated dune, where for BARC2a, deceleration was less than δs = -0.7 for both heights at x/h = 2.18. This difference is due to the reference tower being placed within the interdune where actual velocities were lower than those of the unperturbed free stream sampled as the reference for the isolated dunes. Whilst the actual speeds for all heights on the reference tower were comparatively less when it was placed in the interdune, the log-linear distribution of velocity with height still conforms to the law of the wall (Equation 1.5), which permits a meaningful reference for fractional velocities. As an example, the velocity profile at the reference tower for the flow period shown in Figure 3.18 is shown in Figure 3.19.

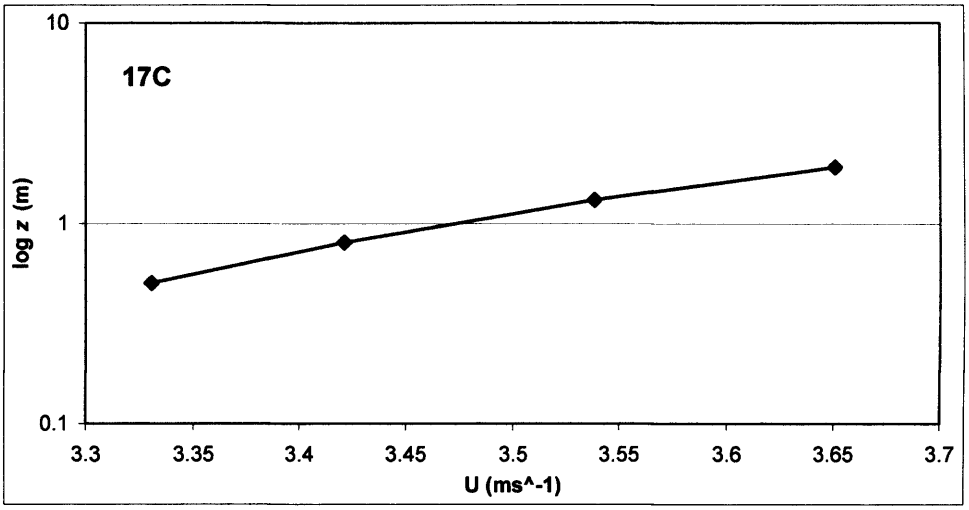

Figure 3.19 Velocity profile of time-averaged actual windspeed from the reference tower in the closely-spaced interdune of TRANS2. Data for the 56 minute measurement run shown in Figure 3.18 (Run 17C).

Following the initial severe drop in windspeed, Figure 3.18 shows that at x/h = 2.56 and 3.54, the velocity at z = 0.5 m remains reduced and also relatively stable at δs = -0.29 and -0.28 for these distances respectively. The existence in this region of steady, reduced velocity near the surface in the lee provides evidence for the existence of a flow separation cell. The directional variability data presented alongside the velocity observations confirms this (Figure 3.18). At x/h = 2.56 the flow direction displays an increased variability of ω = 0.52, which was also seen to be associated with the presence of a separation cell and back eddy in the lee of both isolated crescentic dunes. By x/h = 3.54 in Figure 3.18, the directional variability of flow is at its greatest for the transect (ω = 0.10). This peak in variability is indicative of proximity to the downwind limit of the separation cell since the point of flow re-attachment is associated with the highest directional variability for two reasons. First, greater variability in direction is caused by the turbulent eddies that impact at the surface where flow re-attaches. Secondly, the fluctuation in the extent of the separation cell around its mean distance, a variation which occurs over a length of about 0.5h (Walker and Nickling, 2002) leads to the erratic switching between occurrences of down-transect and up-transect flow. This in turn introduces further variability to the direction observed in the area where flow becomes re-attached to the surface.

It is significant that at the next velocity measurement after the peak in direction variability, at x/h = 4.42, the z = 0.5 m velocity shows an acceleration by 9% to δs = -0.19. This increase is a result of the flow having become re-attached to the surface by this point, and indicates the onset of flow recovery for near the surface. For the typical flow pattern within TRANS2

shown by Figure 3.18, the distance by which flow recovery is detected is seen to agree well with the 4 *h* mean length of separation suggested by Frank and Kocurek (1996b).

Turning to the variation in velocity at z = 1.9 m for the near lee area of the TRANSB2 example (Figure 3.18), the windspeed pattern at this height reflects the behaviour of part of the wake zone in the lee of the upwind dune. For z = 1.9 m, there is a continued rise in the speed downwind from the minimum at x/h = 1.03. The velocity gradient between z = 1.9 m and 0.5 m is low for the first two lee-side posts which suggests that the upper height is not influenced by the fast overshooting air above the separation cell and is therefore actually sheltered. The shear between heights can be seen to increase at x/h = 3.54 where there is significant departure in the fractional velocities of the two heights. The relative increase for the upper height here shows that by this distance downwind, velocity at z = 1.9 m is strongly influenced by the 'lower wake' zone (shown in Figure 1.5), whereas at z = 0.5 m flow remains within the separation cell. In the lower wake region, wind speeds undergo an increase as they receive momentum transferred from the faster moving air above. Frank and Kocurek (1996b) report that in the lower wake, the increase in speed is greater in the top part of this layer, and this is evident after flow re-attachment in that at both x/h = 4.42 and 5.69 there is a greater relative velocity for z = 1.9 m than 0.5 m. The occurrence of flow separation and the initial development of the lower wake in the lee of the upwind dune of TRANS2 was observed in Figure 3.20.

Figure 3.20 Flow visualisation of secondary flow in the lee of the TRANS2 upwind dune using smoke. Separation of flow from the surface is evident at the brink, followed by the illustration of the horizontal and vertical growth of the lower wake region (Figure 1.5). Faster overshooting air leaving the dune lies above this wake, and the separation cell below it. Posts in the lee from left to right are at x/h = 2.56 and 1.03 (0 m and 4.9 m from slipface base, respectively). Flow is right to left in photograph.

With a symptomatic acceleration at z = 0.5 m detected between x/h = 3.54 and 4.42 (Figure 3.18), there is evidence that flow has become re-attached by this latter distance for the time-averaged flow. For the interdune setting of TRANS2, the toe of the downwind windward slope starts at x/h = 4.42, with the first measured point on the actual slope taken at x/h = 5.69. As such there is only a limited distance in which velocity recovery occurs before the influence of the downwind dune is exerted on the speed-up pattern. Of significance in Figure 3.18 is that there is no evidence of the drop in velocity that was measured upwind of the windward toe of the isolated dune (Figure 3.1), a flow feature which has also been recognised in many other experimental and theoretical studies on isolated dunes (e.g. Tsoar, 1985; Wiggs, 1993). The detection or not of this characteristic 'stagnation effect' of the flow upwind of the downwind dune body in the interdunes of this study is dealt with in more detail in the subsequent Section 3.3.2.

Momentum transfer toward the surface from the faster wake portions above is the main contributor to the velocity increase from re-attachment (by x/h = 4.42) to the lower windward slope where δs = 0.12 at z = 1.9 and 0.05 at z = 0.5 m for x/h = 5.69. Velocity increase in this region will be enhanced by the start of the topographic compression of streamlines as well. As overall speeds increase further up the windward slope due to a greater compression effect, the gradient between velocity at the two heights also changes, with the difference in fractional velocity between the sample heights reducing. By x/h = 7.31, a δs = 0.25 exists for both heights which suggests that the velocity gradient of the reference profile (Figure 3.19) is reproduced with speeds 25% greater than the reference tower values. This distance is in good agreement with Frank and Kocurek's (1996b) limit of 8 h for recovery in the profile of flow. Recovery of the velocity profile through a decrease in the gradient between the heights is caused by a greater relative speed-up for z = 0.5 m than z = 1.9 m over x/h 4.42 to 7.31. This change shows the role of the downwind dune in encouraging recovery of the flow profile for the TRANS2 interdune. The greater speed-up seen for the lower height in this region agrees with the windward slope 'amplification layer' detected by Burkinshaw *et al.* (1993). This flow layer of greater acceleration was found a few tens of centimetres above the windward surface for study transverse dunes of a comparable size, and is a response to the growth of an IBL on the windward slope (McLean and Smith, 1986; Frank and Kocurek, 1996a). The role of the IBL in driving windward slope dune dynamics and its relationship with interdune dynamics is

discussed in Section 4.2. Higher up the windward slope of the downwind dune, the pattern of velocity shows continued acceleration. For Figure 3.18, at x/h = 8.4 and 9.95 there is further evidence of greater speed-up near the surface as fractional velocities at z = 0.5 m are δs = 0.53 and 0.79 compared with δs = 0.49 and 0.76 at z = 1.9 m.

3.3.2 Mean velocity pattern in a selection of other interdunes

All the other interdunes in which flow was investigated had quite different interdune extents and forms than the case of TRANS2 described in detail above. These other situations included both the bare study interdunes where dune windward slopes rest on the flat non-erodible substrate, and a sandy interdune of contrasting form to TRANS2.

Another example of mean velocity in an interdune for near-perpendicular incident winds is shown in Figure 3.21. Significantly, this case represents a typical flow situation for where a more appreciable distance exists between the point of flow re-attachment and the start of the downwind dune (Figure 3.21), and has noticeable differences to the TRANS2 case.

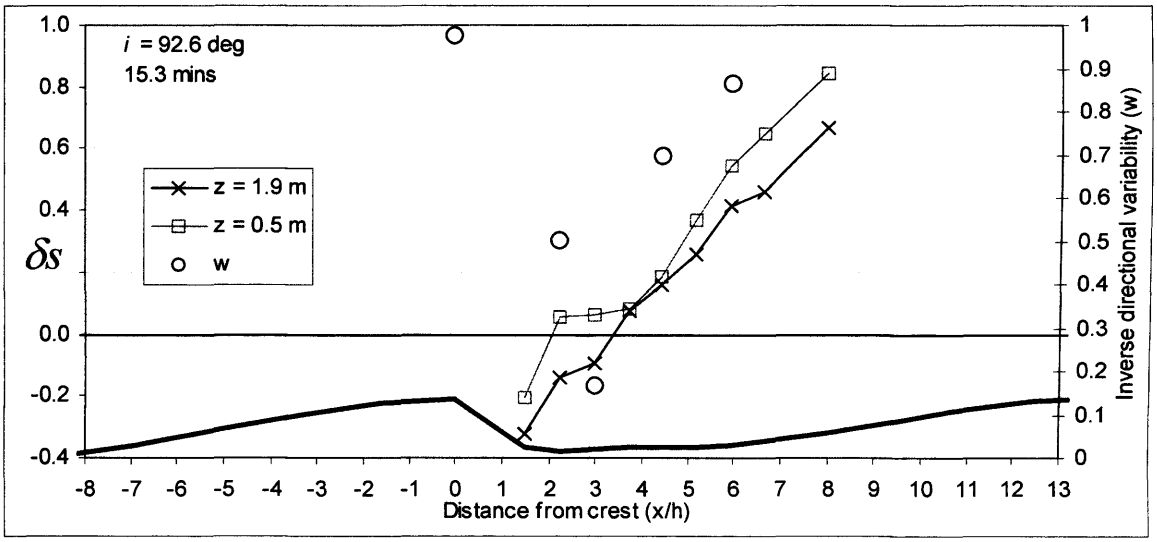

Figure 3.21 Time-averaged fractional velocity in the interdune TRANB2 for the two sampling heights (left axis scale), and normalised directional variability of flow (ω) measured at z = 0.5 m (right axis scale). Upwind crestal δs not included. Run i = 92.6°, duration 15.3 minutes (Run 10C). U_{cr} at z = 1.9 m, 6.18 ms^{-1}. Reference tower not on transect, equivalent distance c. x/h = 4.25.

Once again, the presence of the separation bubble in the upwind dune lee is revealed by a constant flow region of relatively low velocity at z = 0.5 m. The variation in velocity nearest the surface between x/h = 2.22 (δs = 0.05) and 3.72 (δs = 0.08) is only 3%, followed by a sudden increase in velocity of 10% at x/h = 4.45 (δs = 0.18), suggesting that mean flow was re-attached by this point. The pattern of flow directional variability confirms re-attachment

since $\omega = 0.17$ at $x/h = 2.97$, but variability decreases to $\omega = 0.69$ at $x/h = 4.45$ showing the change toward primary flow characteristics across these distances.

With the separation cell ended and flow re-attachment having occurred by c. 4.5*h*, it holds that for the mean flow conditions in Figure 3.21, both sample heights exist within the lower wake region at $x/h = 4.45$ (Figure 1.5). At this distance, the IBL that forms after flow re-attachment is limited in height and will not have developed sufficiently to be detectable at $z = 0.5$ m for this distance downwind of its origin. Since both measuring heights are in the lower wake from $x/h = 4.45$, the continuing overall increase in velocity experienced for both heights thereafter indicates ongoing flow recovery with distance through the interdune. This acceleration reflects the sustained receipt by the lower wake of momentum from the faster flow above, and the effect is also evident in the lowest part of the wake for the near-surface height. At the lower sample height, the speed-up after flow re-attachment throughout the interdune sees an increase of 18% to $x/h = 5.19$ and then by 17% to $x/h = 5.92$, where $\delta s = 0.55$ at the toe of the downwind dune. For $z = 0.5$ m through the interdune from the separation cell to the toe of the next dune, the total magnitude of speed-up is 47% which corresponds to an increase of around 1.0 ms^{-1} for the flow conditions in Figure 3.21.

The data show that there is a steady rate of velocity increase measured near the surface through the interdune (c. 18% each interval) up to $x/h = 5.92$ at the toe of the next dune. Between the toe and the next post on the downwind windward slope, there is a near halving in the observed acceleration since velocity at $z = 0.5$ m increases by only 10% to $x/h = 6.66$. Whilst not generating an actual drop in velocity, this reduction in flow acceleration for the toe region may well be a manifestation of the pressure field induced by the downwind bedform (stagnation effect). Where flow retardation was detected for the isolated dune (Figure 3.1), no effect was evident for the downwind toe or lower windward slope in TRANS2 (Figure 3.18). The reduction in acceleration for TRANB2 in Figure 3.21 is similar to the area of limited velocity increase observed on the lower windward slopes of a reversing dune which was attributed to the stagnation effect (McKenna Neuman *et al.*, 1997). Unexpectedly, the reduction in acceleration is even more apparent for higher above the surface where velocity only increases by 5% between $x/h = 5.92$ and $x/h = 6.66$ in Figure 3.21.

Figure 3.22 shows a selection of other velocity patterns typical for the study interdunes during periods of transverse incident flow. The relationship between directional variability and mean flow is used to infer the area where flow becomes re-attached to the surface.

From Figure 3.22, it can be seen that after the initial retardation, a recurring feature of the velocity pattern in the interdunes when flow is perpendicular to the upwind crest is the lee-side region of stable low-velocity flow at z = 0.5 m. This marks the existence of the separation cell, though the exact pattern of the stable flow region associated with it can vary. For example in Figure 3.22b, flow increases after the immediate retardation from x/h = 1.61 to 3.42, and the area of relatively constant flow within the separation cell is found between this latter point and x/h = 4.32. It is downwind of this stable flow that there is a relatively sudden acceleration for z = 0.5 m (of 9%) from x/h = 4.32 to 5.22 which is diagnostic of flow re-attachment. The noticeable increases in velocity at z = 0.5 m that are indicative of the onset of flow re-attachment occur between x/h = 3.72 and 4.45 (9% acceleration) for TRANSB2 (Figure 3.22a) and between x/h 4.43 and 5.34 (11% acceleration) for TRANS1 (Figure 3.22c).

Figure 3.22 also demonstrates the consistent relationship of directional variability with the near surface velocity pattern associated with flow re-attachment. In particular, the speed-up at z = 0.5 m which marks the downwind boundary of re-attachment is found nearly co-incident with (Figure 3.22a), but always downwind of (Figure 3.22 b and c), the location of the measured maximum of directional variability. Using the velocity and flow variability criteria, there is more evidence of agreement with the 4 h mean limit for flow re-attachment, with inferred areas of re-attachment being within 1 h of this.

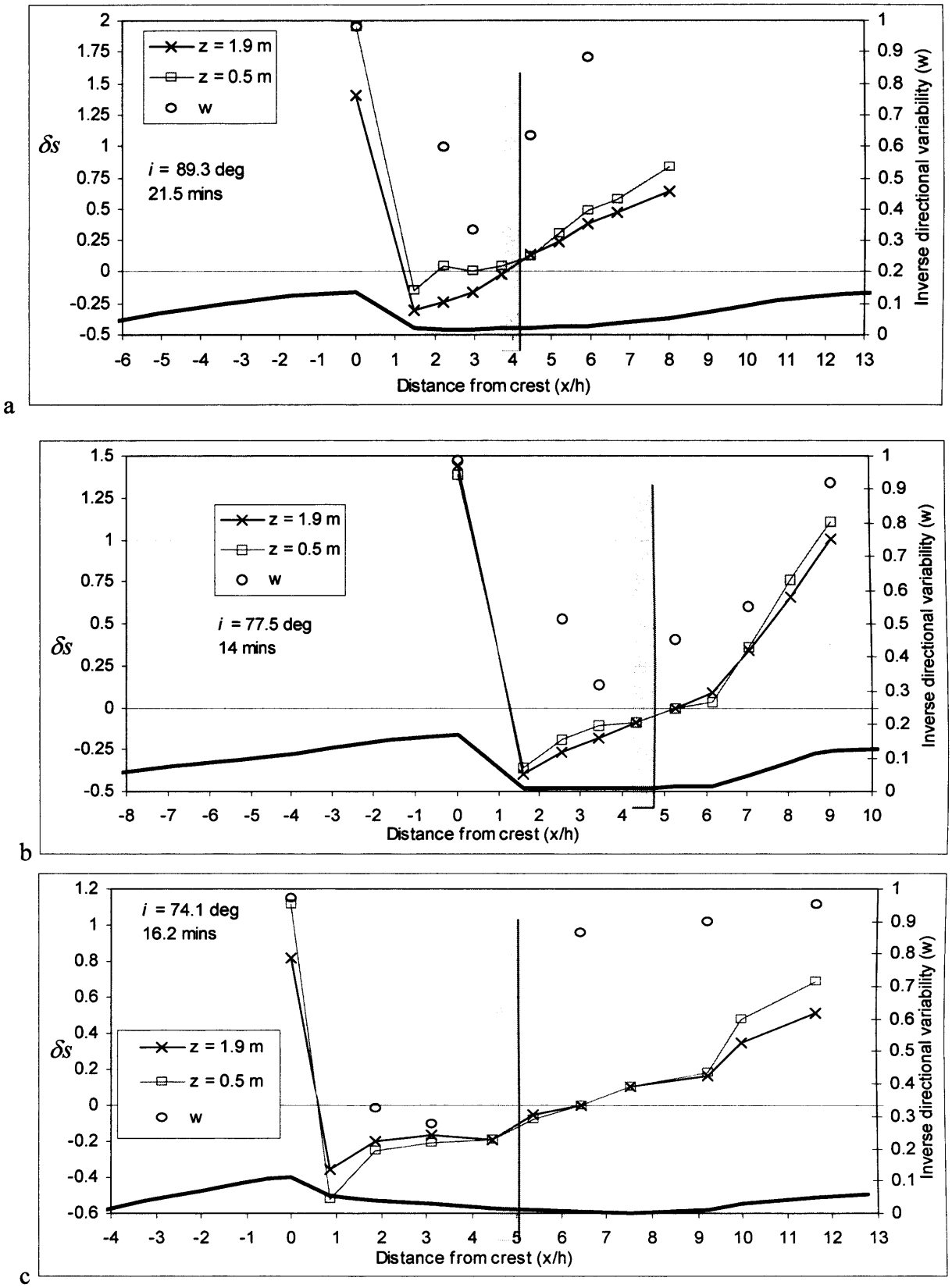

Figure 3.22 Time-averaged fractional velocity in selected interdunes for the two sampling heights and normalised directional variability of flow (ω), for periods of perpendicular incident flow. Shaded areas indicate inferred region of re-attachment. a) TRANB2 i = 89.3°, duration 21.5 minutes, U_{cr} at z = 1.9 m, 6.12 ms^{-1} Run 11B. b) TRANB1 i = 77.5°, duration 14 minutes, U_{cr} at z = 1.9 m, 9.22 ms^{-1} Run 9B. c) TRANS1 i = 74.1, duration 16.2 minutes, U_{cr} at z = 1.9 m, 5.65 ms^{-1} Run 15B. Note different scales δs and x/h scales. Dune height same scale.

In the case of TRANS1 presented in Figure 3.22c, flow accelerates from δs = -0.19 for both sample heights at the edge of the separation cell (x/h = 4.43) to δs = 0.17 (z = 1.9 m) and 0.19 (z = 0.5 m) at the toe of the downwind dune. This is an increase of 36% and 38% respectively. In TRANB2 (Figure 3.22a) the increase between x/h = 3.72 and 5.92 is 35% for the upper sample height and 41% for the lower. There is also an overall increase in velocity for both heights in TRANB1 (Figure 3.22b), where between x/h = 4.32 and 6.12 the δs of flow increases by 18% at z = 1.9 m, and 12% at z = 0.5 m. In this near-surface velocity variation for TRANB1 however, it is apparent that there is a reduction in the velocity increase at x/h = 6.12. At this point, flow accelerates by only 3% from x/h = 5.22, so the observed velocity increase is two-thirds less than for the previous interval. Located at the base of the downwind dune windward slope, this reduction in the rate of acceleration is likely to be caused by the pressure-induced retardation at the toe.

While it is significant that the pattern of the z = 0.5 m velocity data is relatively consistent for the different examples, what is noticeable is that the behaviour of flow at z = 1.9 m varies considerably more between the different interdune situations shown in Figure 3.22. Figure 3.18 showed that the development of the lower wake was important in explaining the velocity variations for the upper sample height. In Figure 3.22, the observed difference in the velocity patterns at z = 1.9 m is accounted for by the characteristics of the upwind dunes of each interdune. With a fixed sampling height of z = 1.9 m, the speeds observed for this height had a variable relationship with the lower wake, whose vertical extent was determined by the upwind dune size and shape. Since the top of the lower wake is bounded by the height of the upwind dune crestline (Figure 1.5, Frank and Kocurek, 1996b), both anemometers were measuring within the lower wake for all of the different interdunes, and data from these measurement points demonstrate the development of this layer.

In the case of the TRANB1 example (Figure 3.22a), actual velocities are very similar for the z = 0.5 m and 1.9 m sample heights up to a downwind distance of x/h = 3.42, as is shown in Figure 3.23.

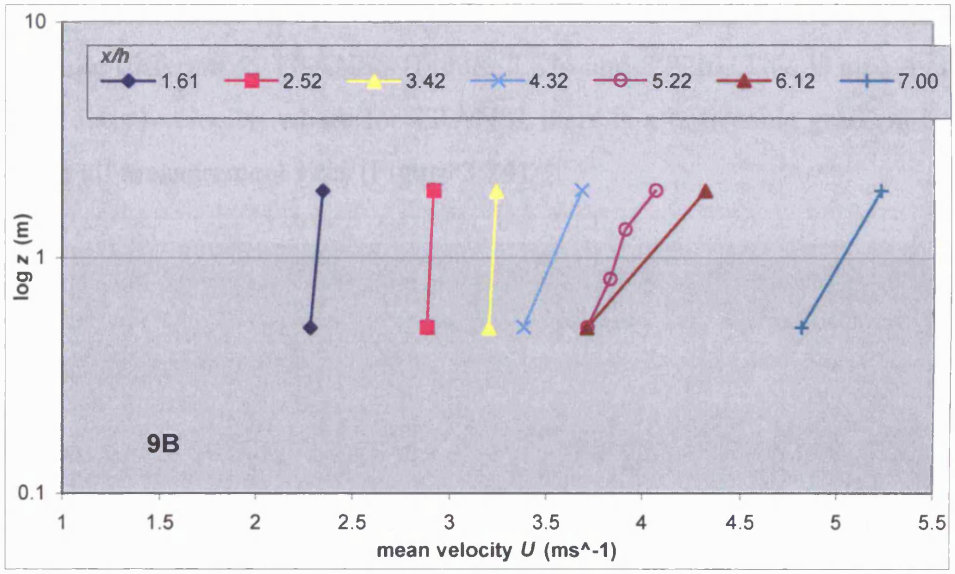

Figure 3.23 Semi-logarithmic profiles of mean velocity within interdune TRANB1 (Run 9B). The reference profile with four sample heights was located at x/h = 5.22. Fractional velocities and flow conditions as Figure 3.22b.

Given flow was inferred to re-attach between x/h = 4.32 and 5.22, the data show that for x/h = 3.42 and upwind, both sample heights were located within the separation cell for TRANB1. This is explained by the sheltering effect of the upwind dune height (6.36 m, Table 2.1) relative to the uppermost sampling height of z = 1.9 m.

The velocity gradient between the two heights increases noticeably at x/h = 4.32 since it is here that the downward expansion of the lower wake is sufficient to be detected at z = 1.9 m. This is reinforced further by the reference profile at the next point which shows an obvious kink in the profile caused by greater velocity at the highest measurement point. At x/h = 6.12, the gradient between upper and lower height velocities is greater still as momentum continues to descend through the entire lower wake. This downward momentum transfer accelerates the flow at z =1.9 m and 0.5 m, but more momentum is received at the upper height increasing the gradient. Furthermore, the speed-up perturbation caused by the presence of the downwind dune is clearly shown by the reduced acceleration and almost equal velocity for z = 0.5 m at x/h = 6.12 and 5.22 (c. 3.70 ms^{-1}). This point also marks the extent of speed-up occurring through the interdune. The influence of flow compression on the windward slope is shown by the large overall velocity increase at x/h = 7.00 and a reduction in gradient with greater acceleration for z = 0.5 m.

The pattern of fractional speed-up for z = 1.9 m in the immediate lee and the interdune of TRANS1 is quite different to TRANB1 (Figure 3.22c and 3.22b). This is also manifested in the profiles of actual velocity, where for TRANS1 there is a noticeable gradient between the two heights for all measurement sites (Figure 3.24).

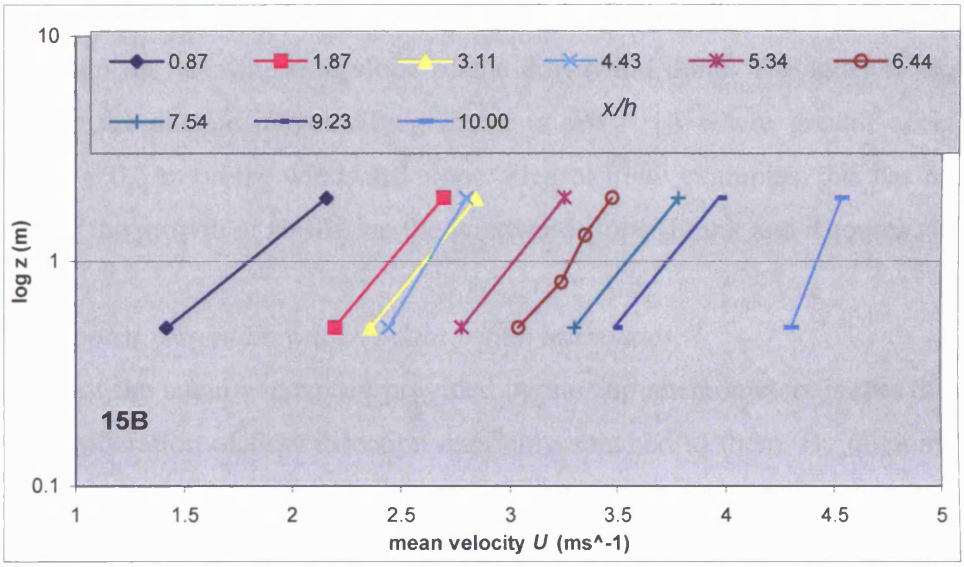

Figure 3.24 Semi-logarithmic profiles of mean velocity within interdune TRANS1 (Run 15B). The reference profile with four sample heights was taken at x/h = 6.44. Fractional velocities and flow conditions as Figure 3.22c.

The relatively small brink height of the upwind dune in TRANS1 (2.28 m) means that the faster element of the wake is near enough to be detected by the upper sampling height. The velocity measurements at z = 1.9 m for the immediate lee-side ($\leq x/h$ = 4.43) all show this influence, while velocities in the separation cell at z = 0.5 m remain low. A similar relationship for velocity between the two heights was also evident where the flow at the upper anemometer was associated with the lower wake, and the lower anemometer with the separation cell in the lee of isolated BARC1 (Figure 3.3). In TRANB1 (Figure 3.23), a velocity gradient between the two heights only became marked after a significant downwind distance, due to the larger sheltering effect of the upwind dune.

The profile gradients observed for TRANS1 are reflected in the relatively similar fractional speed-up values for both upper and lower heights throughout the interdune from x/h = 4.43 to 9.23 (Figure 3.22c). δs values are similar for both heights since Figure 3.24 shows that the velocity profile at the reference tower (x/h = 6.44) has a comparable gradient to the profiles observed across the interdune. Thus there is evidence that the flow profile recovers soon after re-attachment in TRANS1 (around x/h = 5.34), and some way before the $8h$ distance

suggested by Frank and Kocurek (1996b). At z = 0.5 m from the downwind boundary of the separated flow to the windward toe of the next dune, the recovery of flow sees velocity increase by 1.05 ms^{-1}.

Divergence in the fractional velocities is seen in the lee due to the influence of the separated region, and again on the windward slope of the downwind dune. The latter is expressed in Figure 3.23 by the change in velocity gradient at x/h = 10 where greater acceleration is measured for z = 0.5 m on the windward slope. Present in all examples, this has been argued to be a result of the growth of an IBL on the windward slope (Frank and Kocurek, 1996a).

3.3.3 High temporal resolution velocity data within interdunes

One limitation of the mean windspeed provided by the cup anemometers is that these data do not have a consideration of flow direction explicitly attached to them. By aligning the sonic anemometer parallel with the sampling transect in the interdunes, the sonic-based measurement of velocity in the streamwise plane (u) allowed another aspect of the velocity within interdunes to be investigated. The high temporal resolution of the data from the sonic anemometer enabled the calculation of the intermittency of flow reversal (χ) from the time series of instantaneous streamwise velocity. χ is defined as the percentage of the total velocity meaurements where streamwise horizontal flow was directed in a negative (reversed) direction ($-u$) (Best and Kostaschuk, 2002). The time series for selected interdune locations in TRANS1 is shown in Figure 3.25.

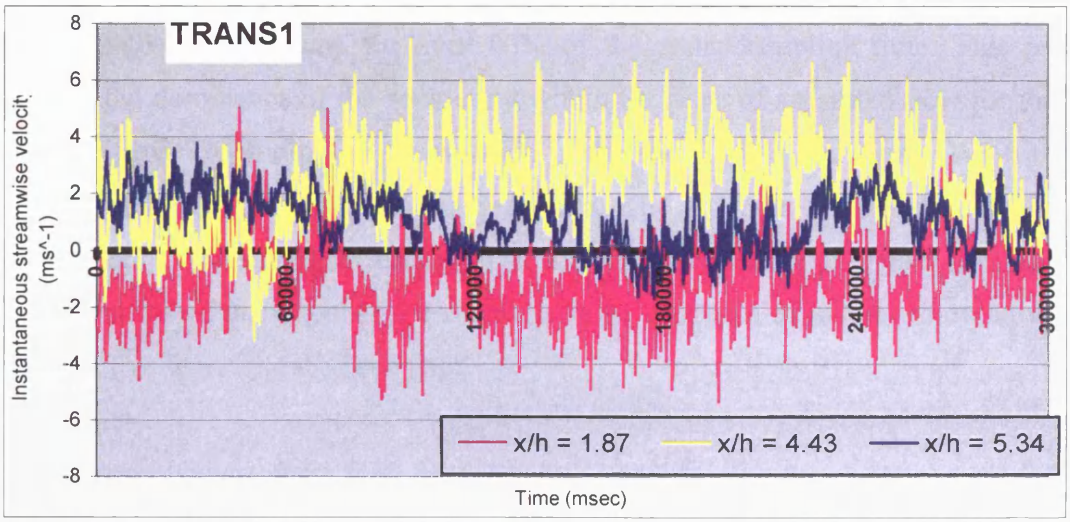

Figure 3.25 Time series for instantaneous measurements of streamwise velocity (u) over five minute sample periods at three downwind locations within interdune TRANS1.

Values for χ were obtained for the interdunes at points along the transect where the sonic was deployed, and are shown with mean sonic derived velocity for the two interdunes in which turbulence was studied in Table 3.1. These high resolution data aid interpretation of the cup anemometer data for the interdunes.

Table 3.1 Intermittency of flow reversal (χ) as a percentage of total sonic measurement run time and sonic derived mean velocity ($\overline{u}$) for interdunes TRANB2 and TRANS1.

Study interdune	Distance downwind (*x/h*)	χ (%)	$\overline{u}$ (ms^{-1})
TRANB2	2.22	88.8	-1.581
	3.72	34.4	0.755
	5.19	3.7	2.500
	6.66	0.9	3.255
TRANS1	1.87	81.1	-1.082
	4.43	6.0	2.420
	5.34	13.9	1.110
	6.44	2.1	2.421
	7.54	0.6	1.999
	9.23	0	2.798

For both interdunes in Table 3.1, mean velocity data from the sonic anemometer reveal areas where the time averaged flow is reversed for the measurements taken closest to the upwind dune ($< x/h = 2.5$). At these points, the observations from the sonic also indicate that flow was directed back toward the dune for over 80% of the sonic sampling time. This provides evidence for the dominance of the back-eddy within the zone of separated flow for the sonic measurement runs. Depending on the position in the lee, Kadota and Nezu (1999) report a maximum χ = 95% for sub-aqueous model dunes. The strength of the return flow is not determined from χ here since any reading of $-u$ is taken as indicative of reverse flow and there is no consideration of the extent of the spanwise flow. Evidence of reversed flow however is highly instructive regarding the flow field.

The intermittency factor of the flow further helps in ascertaining the re-attachment length in the interdune. A value of χ = 50% for any given point indicates that the sampled flow had a positive and negative streamwise direction for an equal number of observations, or, that flow had an element back towards the upwind dune as well as dominantly down the transect

equally for half the run time. Thus a 50% value at a given location is analogous to the lowest directional variability (ω) as measured from the wind vanes, and is therefore associated with the area of flow re-attachment. For TRANB2, the data show that χ was nearest to 50% at x/h = 3.72, where χ = 34.4%. When compared to the pattern of mean velocity in the interdune from cup anemometers for the period of the sonic run, the χ = 34.4% value is found to have an excellent agreement with the speed-up patterns related to flow re-attachment (Figure 3.26).

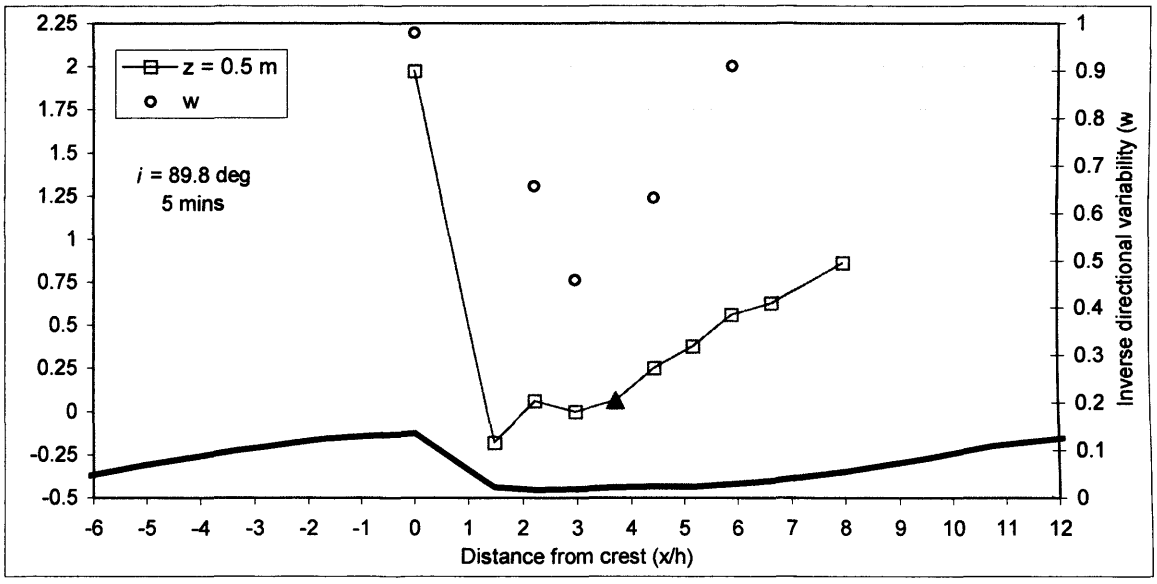

Figure 3.26 Time-averaged fractional velocity (δs) at z = 0.5 m through interdune TRANB2 for the five minute period where the sonic anemometer sampled at x/h = 3.72 (location marked as triangle). Normalised directional variability of flow (ω) also shown. U_{cr} at z = 0.5 m, 6.64 ms^{-1}.

It can be seen in Figure 3.26 that at x/h = 3.72, the velocity z = 0.5 m has begun to undergo an increase (to δs = 0.07) from the relatively constant and reduced upwind values (δs = 0.00). This pattern has consistently been taken to suggest that the mean flow for the measurement period shows re-attachment to the surface by this distance downwind. That the mean flow re-attachment distance was less than x/h = 3.72 for the period of sonic observation at this point is reinforced by the value of χ = 34.4%. This value reveals that flow was directed back toward the upwind dune for approximately a third of the sample time and that *mean* flow experienced at x/h = 3.72 was re-attached since the flow direction here is predominantly positive in the streamwise direction. The proximity of x/h = 3.72 to the mean flow re-attachment distance is implied by the separation cell length periodically exceeding this distance, producing reverse flow 34.4% of the time. This is so, given that χ is only 15.6% less than the maximum possible variation in the sign of u. Recovery of the near-surface flow from the effect of the upwind dune through the interdune TRANB2 is shown in Table 3.1. With increasing distance downwind, the χ signal continues to decrease, and $\bar{u}$ increases downwind of x/h = 3.72. Since

the sonic anemometer measures positive and negative values of u, mean velocity at flow re-attachment will be zero for the surface.

In Table 3.1, following the dominance of time-averaged reverse flow at x/h = 1.87, for TRANS1 there is a discrepancy in the greater duration of return flow measured at x/h = 4.43 than 5.34. For these distances, χ values are 6% and 13.9%, respectively. The suggestion here that flow reversal is more frequent further downwind demonstrates the variable extent of the separation length with time. These data are explained by the fact that the posts were not sampled simultaneously, and there is no normalisation against a reference velocity for the time series data from which χ was calculated.

For the five minute sample run when the sonic anemomenter was deployed at x/h = 4.43 in TRANS1, the downwind extent of the lee-side separation cell was considerably less than its usual length. The cup anemometer and wind vane data provide evidence that for the sampling period at x/h = 4.43, flow was re-attached before 3 h downwind. This was the distance where flow directional variability was low enough to suggest flow had re-coupled with the surface (ω = 0.808). With mean flow re-attachment occurring around 1.5h upwind of x/h = 4.43 therefore, this accounts for the infrequent observation of reversed flow at that post (χ = 6%). When the sonic anemometer sampled at x/h = 5.34, the mean length of flow separation during this run was nearer to a distance of around 4.5-5 h (this more typical re-attachment length is shown in Figure 3.22c). Given that this mean re-attachment distance was considerably closer to the sampling point at x/h = 5.34, there were more instances where reversed flow was detected and so χ = 13.9%. This is also illustrated in Figure 3.25, where the streamwise trace at x/h = 5.34 crosses the zero velocity axis far more frequently than is detected for x/h = 4.43. As such $\overline{u}$ of 1.110 ms^{-1} at x/h = 5.34 is also closer to the zero of pure flow re-attachment.

By x/h = 6.44 in TRANS1, reverse flow was detected for only 2.1% of the time series (6.3 seconds), and this decreased further through the rest of the interdune. The mean velocity from each sonic run in TRANS1 (Table 3.1) is not normalised for the effect of varying overall flow strength, but it still shows general recovery with the maximum (2.80 ms^{-1}) found at the downwind margin of the interdune (x/h = 9.23).

The analysis of the streamwise velocity time series data to show the intermittency factor of reverse flow (χ) for a given point is useful in indicating the distance to flow re-attachment in

an interdune and flow recovery. The time series data here for TRANS1 show the changing length of the separation cell that occurs over time, but also help to confirm the mean flow pattern of the interdune shown in Figure 3.22c. The conformity of streamwise time series data with the mean cup anemometer and wind vane observations is even more apparent for TRANB2 which exhibited a more constant separation cell for the total period that the sonic anemometer sampled within the interdune. The evidence of the temporal variation in the size of the separation cell in the interdunes, together with the time series data in Table 3.1 are returned to when the turbulence patterns for the interdunes are explained in the next section (Section 3.4).

3.4 Characteristics of turbulence within interdunes

Presented here are the variations in Reynolds stress turbulent elements observed through the two interdunes. For all of these observations, the data were collected at a height of z = 0.5 m and the data are normalised to enable comparison along transects and between different interdune situations.

3.4.1 Streamwise Reynolds stress variation within interdunes

Figure 3.27 shows the patterns of streamwise Reynolds stresses observed in the two interdunes.

For TRANB2 (Figure 3.27a), the nearest measurement in the lee of the dune for $\overline{u'^2}/U_r^2$, at x/h = 2.22 is 0.289. This is over 8 times greater than the value for streamwise turbulence seen in undisturbed flow nearly 20 h upwind at the reference for isolated dune BARC1 (0.033). x/h = 2.22 for TRANB2 is located firmly within the separated flow cell as shown by the mean velocity patterns (Figure 3.22a) and the reverse flow (χ) data for the sonic runs (Table 3.1). In comparison to the measurement immediately upwind at x/h = 3.72 there is a large increase by nearly 75% to the maximum streamwise Reynolds stress recorded within TRANB2, $\overline{u'^2}/U_r^2$ = 0.49. The mean anemometer and sonic velocity data suggest that for the interval of the sonic measurement run, x/h = 3.72 was at a point just downwind of where mean flow re-joined with the surface. There is also evidence that the separation cell showed periodic extension beyond this distance, since χ = 34.4% at this position. As such, the intense streamwise mixing of the free shear layer would be intermittently experienced at that point (Allen, 1994). The large $\overline{u'^2}/U_r^2$ peak observed for x/h = 3.72 therefore reveals that the area of flow re-attachment,

including its downwind margin, is associated with a local high in time-averaged streamwise turbulence. This agrees well with Bennett and Best (1995) who found the same results, including a notable high just downstream of the mean re-attachment point for a detailed flow field produced over sub-aqueous bedforms in a flume. The presence of considerable streamwise turbulence in the lee was also attributed to re-attaching flow for the isolated dune examples (Figure 3.8).

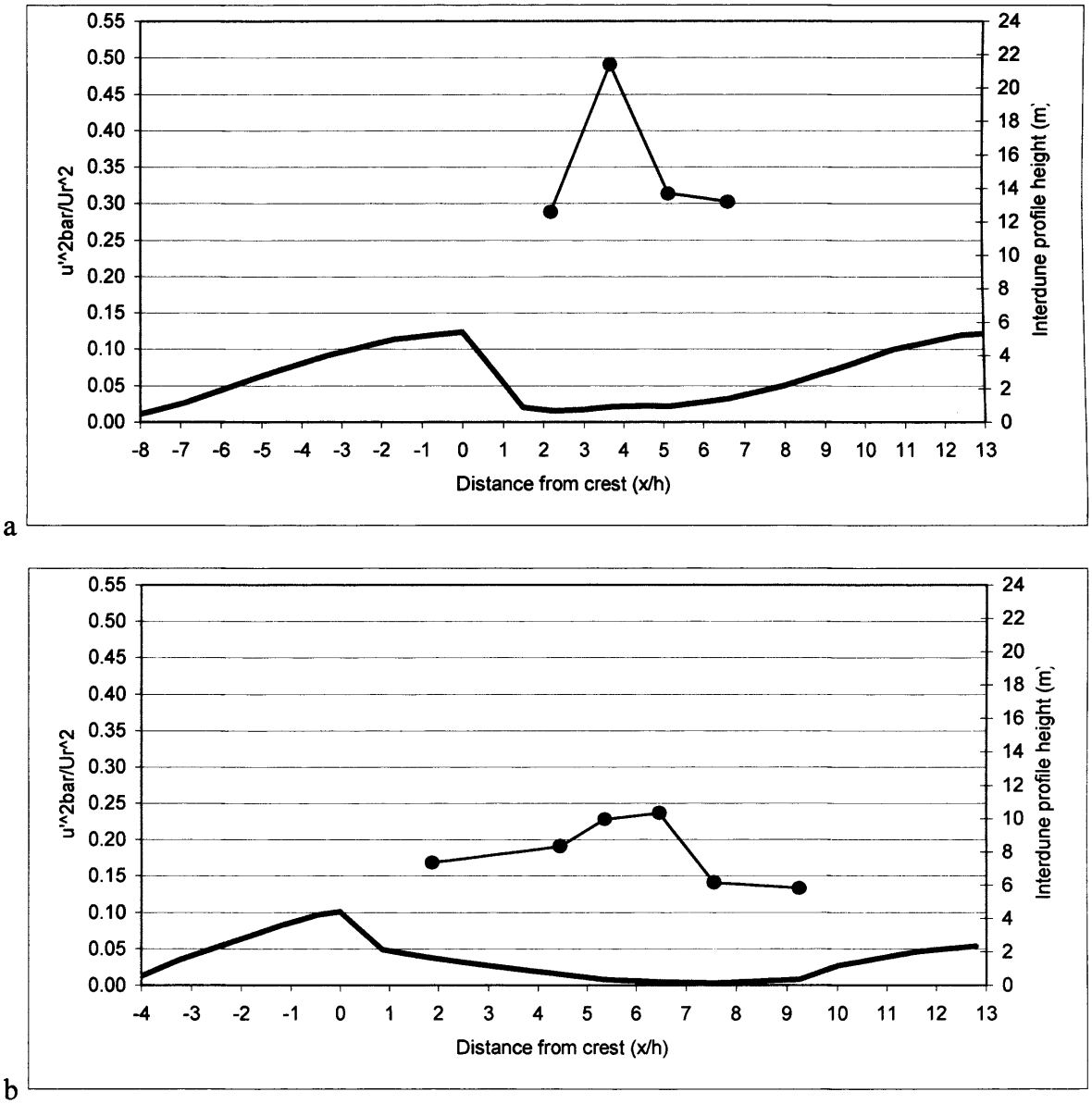

Figure 3.27 Variation in streamwise Reynolds stress ($\overline{u'^2}/U_r^2$) at z = 0.5 m for a) interdune TRANB2, and b) interdune TRANS1. Note same vertical scales for each example.

For TRANB2 (Figure 3.27a), the observed peak in $\overline{u'^2}/U_r^2$ associated with flow re-attachment is a relatively discrete feature within the interdune since by x/h = 5.19, streamwise

Reynolds stresses are seen to drop again. This decline sees streamwise turbulence levels return to those detected within the lee eddy. The evidence in Table 3.1 reveals that separation and return flow was still evident at x/h = 5.19 (χ = 3.7%), and the effect of this is sufficient to generate levels of time-averaged streamwise Reynolds stress that are still around 7.5 times greater than for unperturbed flow. A further decrease in $\overline{u'^2}/U_r^2$ is seen for the remaining portion of the interdune, where values drop by 4% from x/h = 5.19 to 6.66 which is on the base of the windward slope.

In the case of TRANS1 (Figure 3.27b), there are certain noticeable similarities in the exhibited pattern of streamwise Reynolds stress through the interdune. At x/h = 1.87 in the separation cell, $\overline{u'^2}/U_r^2$ is once again considerably higher than that for undisturbed flow since at 0.168 it is 5 times the reference value (0.033). The streamwise Reynolds stress component increases from here until a plateau peak is evident for TRANS1, where at x/h = 5.34 values are 36% greater than at x/h = 1.87 and by 40% at x/h = 6.44, both around 7 times the undisturbed flow. In TRANB2 (Figure 3.27a), this $\overline{u'^2}/U_r^2$ peak was attributed to turbulence introduced by eddy shedding from the shear layer which is nearer the surface when flow re-attaches.

Flow was reversed for 13.9% of the sampling run at x/h = 5.34 in TRANS1 (Table 3.1), indicating this point was generally downwind of mean flow re-attachment, but that the migrating separation cell limit did exceed it sporadically. The mean distance of separation was close enough in order for enhanced time-averaged streamwise Reynolds stresses to be recorded at x/h = 5.34. The peak for $\overline{u'^2}/U_r^2$ observed in TRANB2 was greater because in that interdune, x/h = 3.72 was closer to mean re-attachment point, as shown by χ being nearer to 50% (34.4%), therefore the impact of the eddying was greater. It is suggested that the maintenance of relatively high $\overline{u'^2}/U_r^2$ for x/h = 6.44 shows that the area of turbulence generation caused by flow re-attachment can be maintained downwind of where separation ends (e.g. Bennett and Best, 1995). This is probably a distance over which eddies shed from the re-attaching shear layer still have a positive impact on turbulent flow.

Referring back to Table 3.1, it was explained in Section 3.3.3 that for the sonic anemometer run conducted at x/h = 4.43 in TRANS1, the separation cell was particularly limited in its

downwind extent, with re-attachment occurring some way before x/h = 4.43 (c. 3h). As such, the measured value of $\overline{u'^2}/U_r^2$ = 0.190 at x/h = 4.43 is believed to be unusually low compared to the value that would be expected had re-attachment occurred nearer to this point. This explains the peak in streamwise Reynolds stress that is most related to flow re-attachment appearing at x/h = 5.34.

Following the peak in TRANS1, the time-averaged streamwise Reynolds stress then drops to 0.141 at x/h = 7.54 and a further slight decrease of 5% occurs over the remainder of the interdune to x/h = 9.23. This reduction in $\overline{u'^2}/U_r^2$ matches that seen in TRANB2. Upwind of the isolated dune, streamwise Reynolds stress was also seen to decline, though that was explained by the mean velocity reduction at the dune toe (Figure 3.7). For the case of the fall in $\overline{u'^2}/U_r^2$ as the downwind dune is approached within both the interdunes however, this is attributed to increased distance from re-attachment and less influence from the shear layer, in other words, the recovery of flow. Streamwise Reynolds stress has been found to be most sensitive to acceleration of flow (e.g. Gong and Ibbetson, 1989). Thus the mean velocity pattern of consistent speed-up through the interdunes after re-attachment for the sonic sampling height (z = 0.5 m) might also be expected to contribute to the observed turbulence pattern in the downwind portions of the interdunes. Since the streamwise component of Reynolds stress declines in this area of the interdune however, it seems that wake dissipation effects are dominant over those generative ones for $\overline{u'_2}$ derived from flow acceleration. Furthermore, streamwise turbulence stemming from the shear layer is experienced throughout the interdune because its levels still remain considerably higher at the end of the interdune than for unperturbed flow (Figure 3.7). At x/h = 6.66 in TRANB2 and at x/h = 9.23 in TRANS1, $\overline{u'^2}/U_r^2$ is 9 and 4 times the reference value respectively.

Direct comparison of the streamwise Reynolds stress plots for the two interdune situations is presented in Figure 3.28 where the turbulence data are plotted together in the context of their respective interdunes.

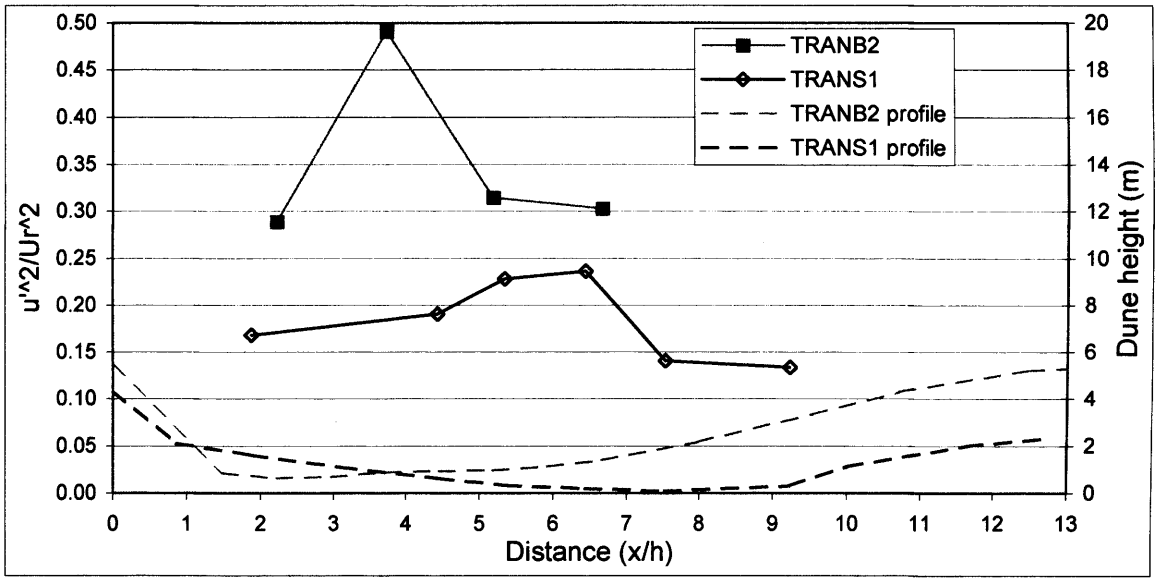

Figure 3.28 Variation in streamwise Reynolds stress ($\overline{u'^2}/U_r^2$) at z = 0.5 m in interdune TRANS1 and TRANB2. Broken lines represent the superimposed profiles for each interdune.

Figure 3.28 shows the reduced extent of the peak $\overline{u'^2}/U_r^2$ (approximately half) in TRANB2 and its appearance at a greater relative downwind distance than for TRANS1. The study by Bennett and Best (1995) between two closely spaced sub-aqueous dunes identified that streamwise turbulence values returned to those within the free stream at a length of around 0.6 λ (where λ is dune crest-crest wavelength). 0.6 λ for both study interdunes is the equivalent to approximately 7.8 dune heights. It can be seen that at this distance, $\overline{u'^2}/U_r^2$ remains far greater than the measured unperturbed values (0.030), but that the occurrence of relatively steady streamwise Reynolds stresses is seen within both interdunes before x/h = 7.8 (Figure 3.8). For the closely spaced bedforms in Bennett and Best (1995), this suggests the importance of flow on the windward (upstream) slope in encouraging recovery of streamwise turbulence.

3.4.2 Vertical Reynolds stress variation within interdunes

Profiles of the vertical Reynolds stress component through each of the interdunes are shown in Figure 3.29.

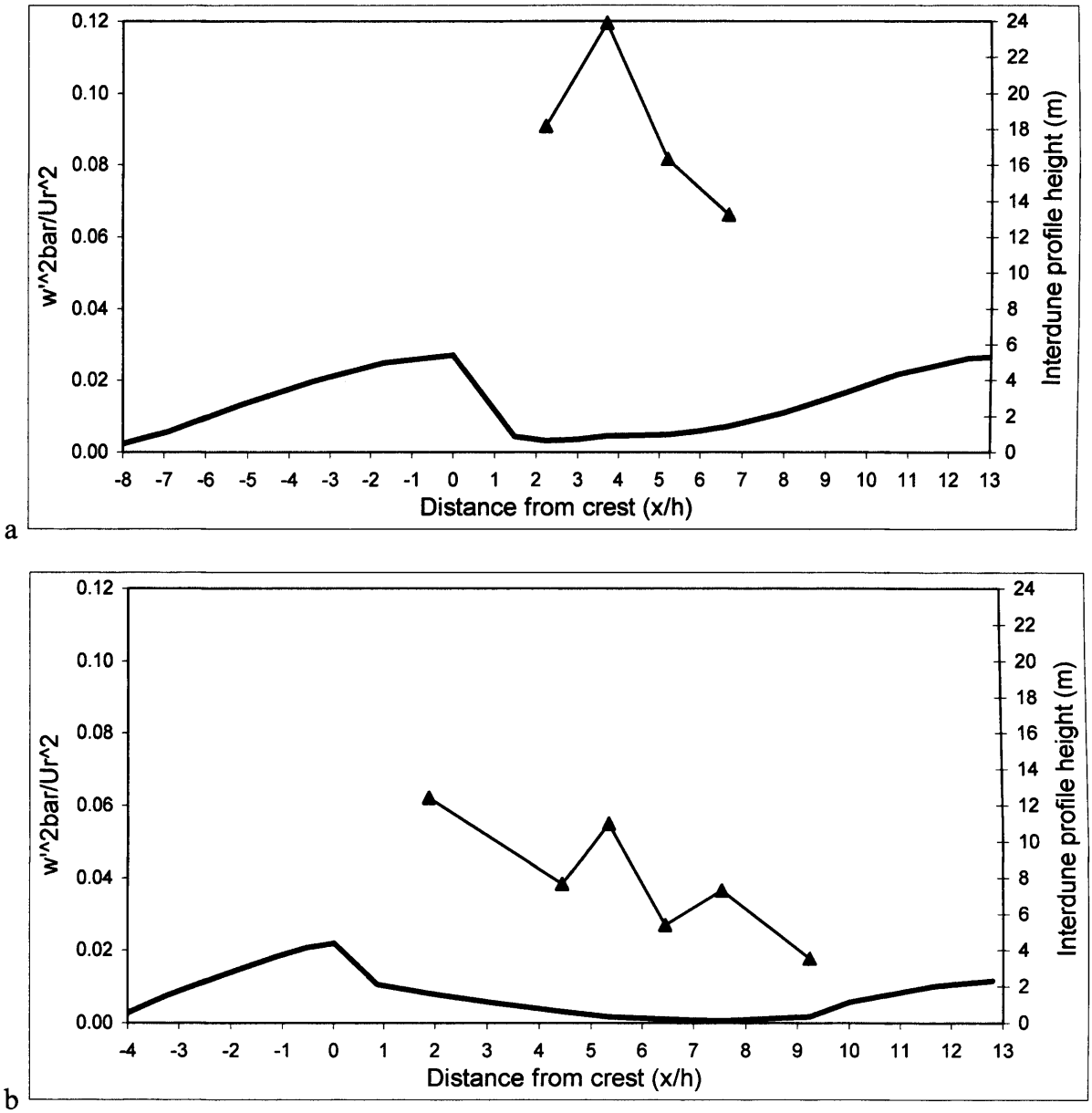

Figure 3.29 Variation in vertical Reynolds stress ($\overline{w'^2}/U_r^2$) at z = 0.5 m for a) interdune TRANB2, and b) interdune TRANS1. Note same vertical scales for each example.

The pattern of vertical turbulence variation displayed in TRANB2 is similar to that seen for the other normal Reynolds stress ($\overline{u'^2}/U_r^2$) in Figure 3.28a. Levels of $\overline{w'^2}/U_r^2$ at x/h = 2.22 however are nearly thirty times those observed for the unperturbed boundary layer, with this increase again a result of increased turbulence in the separation region. Enhanced vertical turbulence should be expected along the free shear layer due to vortex production (Bennett and Best, 1995). More usefully as a comparison therefore, the value for x/h = 2.22 is approximately three times the lee side $\overline{w'^2}/U_r^2$ peaks that were measured for both isolated dunes (Figure 3.11). In TRANB2, where the shear layer comes into closer proximity with the

sampling point at x/h = 3.72 due to mean flow re-attachment occurring nearby, the $\overline{w'^2}/U_r^2$ measured at that point is greater still. At this distance it shows an increase by 30% from x/h = 2.22 to 0.119. With increasing distance from the downwind limit of separation and the eddy source, the vertical Reynolds stress component falls. Such a decline in the intensity of vertical turbulence is also described by Nelson *et al.* (1995) for downstream of a negative step and McLean *et al.* (1994) for a bedform. By x/h = 5.19, $\overline{w'^2}/U_r^2$ has dropped by a third of its transect maximum, and has fallen further to 0.066 on the base of the downwind dune slope at x/h = 6.66.

In TRANS1, similar elements of the vertical turbulence are repeated (Figure 3.29b). $\overline{w'^2}/U_r^2$ is greatest within the separation cell at x/h = 1.87, where the influence of eddies propagating downward from the shear layer above is reflected in terms of the time-averaged vertical turbulence. At x/h = 5.34, located downwind of mean re-attachment (Table 3.1), the component of vertical Reynolds stress remains high since it experiences periodic extension of separated flow which leads to the introduction of vertical turbulence. Here $\overline{w'^2}/U_r^2$ values are 17 times the upwind reference. The relative low in vertical Reynolds stress for x/h = 4.43 is once again explained by, and provides further evidence for, the limited downwind extent of the separation cell for the duration of sampling with the sonic anemometer. The poorly developed separation cell that existed when the device was at x/h = 4.43 resulted in fewer eddies contributing to vertical turbulence at that point. At x/h = 6.44, vertical Reynolds stress is half the value at x/h = 5.34, and after a slight rise, the minimum value for TRANS1 is found at the end of the interdune where at x/h = 9.23 $\overline{w'^2}/U_r^2$ is 0.018. This matches the declining trend in the vertical component of Reynolds stress seen after the re-attachment peak in TRANB2.

The evolution of $\overline{w'^2}/U_r^2$ observed for the downwind portions of both interdunes is interesting. From meteorological studies over hills (Gong and Ibbetson, 1989; Kaimal and Finnigan, 1994) and from the observations discussed for the windward slope of BARC1, the vertical component of Reynolds stress has been found to be sensitive to streamline curvature. However, at the downwind edge of both interdunes, despite the fact that concave curvature is detected in response to the presence of the next dune, no attendant increase is seen in $\overline{w'^2}/U_r^2$

for either case. The local mean streamline angle is 5.8° at x/h = 9.23 in TRANS1, and is 1.9° at x/h = 6.66 for TRANB2. By way of an explanation, it can be seen for BARC1 in Figure 3.9 that the increase in vertical Reynolds stress recorded in conjunction with streamline concavity was relatively small. The pattern for TRANB2 and TRANS1 beyond re-attachment suggests that in the downwind region of interdunes, the overall decline in vertical turbulence with reduced vortex input exerts more of an effect on $\overline{w'^2}/U_r^2$ levels than the positive effects for turbulence of streamline concavity. The generative influence of positive streamline curvature for vertical Reynolds stress may be shifted onto the body of the dune, as was also seen for the variation of this turbulent stress on the windward side of BARC1. Finally, it is worth noting that even without a stream concavity-induced enhancement, $\overline{w'^2}/U_r^2$ values at the downwind edges of the interdunes remain considerably higher than for unperturbed flow conditions.

3.4.3 Variation of Reynolds shear stress within interdunes

The Reynolds shear stresses observed in TRANB2 and TRANS1 show considerable variation in Figure 3.30.

For TRANB2 in Figure 3.30a, the time-averaged Reynolds shear stress measured within the separation cell at x/h =2.22 was found to be almost zero (0.0007). This low mean shear stress is found despite the fact that both the normal Reynolds stresses (vertical and streamwise) measured at x/h = 2.22 were seen to be far in excess of their reference values. The CV_τ = 102.6 (Equation 3.1) showed massive variability for this point though, questioning the value of the derived mean (Section 3.4.4). Following the low values within the separation cell, a negative mean shear stress is seen at x/h = 3.72 as the nearest point taken to mean re-attachment. Here, the normalised Reynolds shear stress is -0.0314, thus the magnitude is high (around 10 times undisturbed values) but with a negative sign. In many other studies of flow turbulence caused by bed perturbations, the separation cell, the shear layer region and the area where separated flow returns to the surface have all been recognised to be areas of enhanced mean shear stress (e.g. Bradshaw and Wong, 1972; McLean *et al.*, 1994; Bennett and Best, 1995). The explanation for the detection of anomalous low and negative average shear stresses for these regions in TRANB2 lies with the dominance of certain turbulent structures in the flow. These structures vary in their contribution to Reynolds shear stress as expressed by $-\overline{u'w'}$, and further attention is given to this in the next section (3.4.4). For x/h = 5.19 in

TRANB2, $-\overline{u'w'}/U_r^2$ has returned to a positive value and is 0.0104. The shear stress then undergoes an increase by 39% of this value for the measurement located at x/h = 6.66, with this rise coinciding with streamline concavity.

a

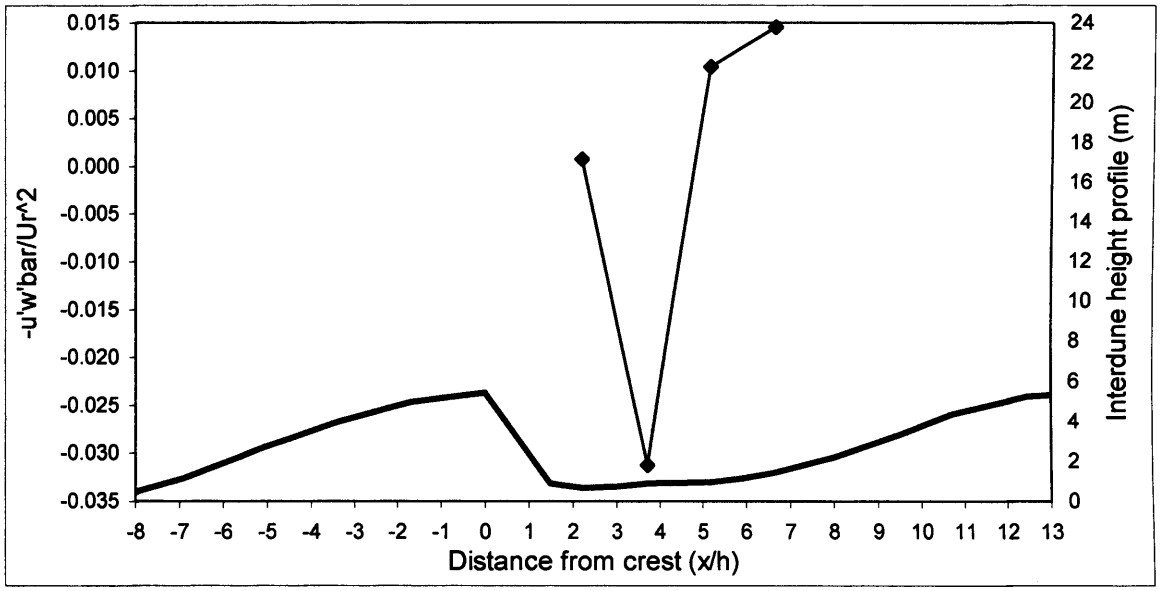

b

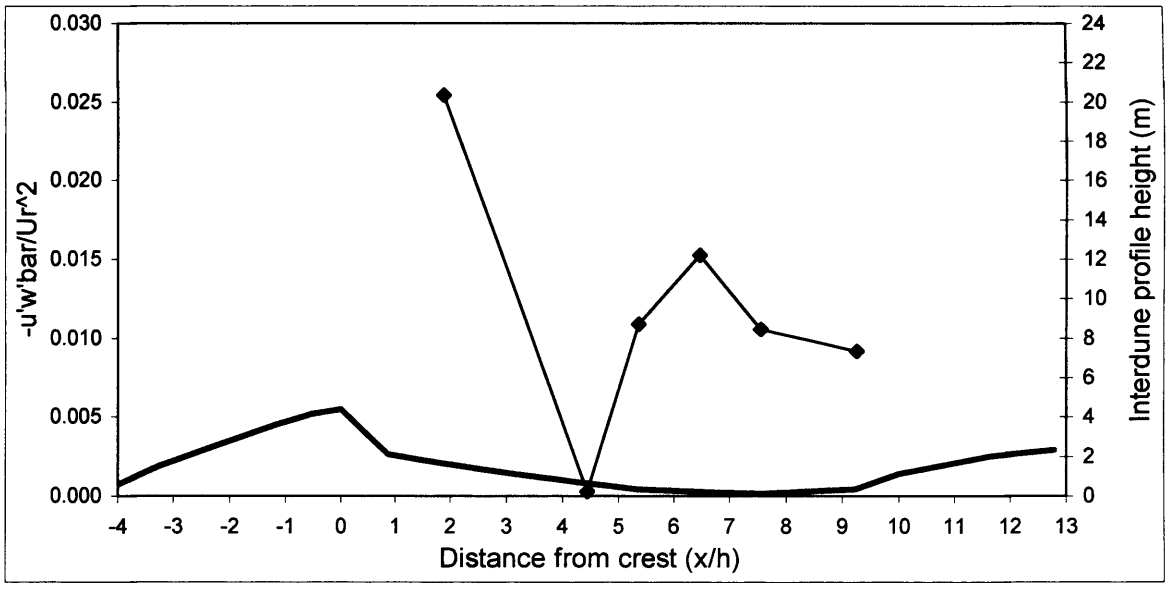

Figure 3.30 Variation in Reynolds shear stress ($-\overline{u'w'}/U_r^2$) at z = 0.5 m for a) interdune TRANB2, and b) interdune TRANS1. Note different vertical scales for observed stress in each example.

For TRANS1 there are two areas in the interdune with identifiable peaks in mean Reynolds shear stress (Figure 3.30b). The first shows compliance with the observed high values for the two normal Reynolds stresses, where a high in mean shear stress is seen at x/h = 1.87 and $-\overline{u'w'}/U_r^2$ is 0.0254. This is a level 8.5 times that found to characterise the undisturbed

boundary layer at the same height from the surface, and the mean shear stress conditions here illustrate the shear layer effect on $-\overline{u'w'}$ better than that seen in TRANB2 (at x/h = 2.22). After this peak, there is a sharp drop to a nearly zero mean shear stress at x/h = 4.43, which was also characterised by large variability (CV_τ). Downwind of this, $-\overline{u'w'}/U_r^2$ is seen to be considerably higher by x/h = 5.34 (0.0109). This region was also more frequently surpassed by the limit of separation (Table 3.1), and thus more subjected to eddies. A further rise in the mean Reynolds shear stress establishes a second peak at x/h = 6.44 where the local value was five times the reference value. Through the remainder of the interdune to the toe of the downwind dune and over a distance of roughly 3 h, $-\overline{u'w'}/U_r^2$ exhibited an overall drop to levels at the end of the interdune (x/h = 9.23) that remained three times that of the reference.

Once again, the region of the downwind dune toe is of special interest for Reynolds shear stress variation through interdunes since streamline curvature is topographically induced here (Section 3.4.2), and such curvature effects have been shown to produce enhanced $-\overline{u'w'}$ at the upwind base of hills (Finnigan *et al.*, 1990). The morphodynamic implications of curvature-enhanced shear stress at the upwind dune toe have been discussed by Wiggs *et al.* (1996) for an isolated dune, and are significant in the case of an interdune since the flow dynamics of the toe area control this boundary of the interdune (Section 4.2).

3.4.4 Discussion of Reynolds shear stress variation in interdunes

It was highlighted in the previous section that low and even negative values for mean Reynolds shear stress existed near to and upwind of re-attachment in TRANB2, and at x/h = 4.43 in TRANS1. This particular pattern of shear stress can be explained by using quadrant analysis to identify turbulent structures from the data series of the streamwise and vertical velocity (Lu and Willmarth, 1973; Clifford and French, 1993). This approach investigates the co-variance of the fluctuating velocities that make up the instantaneous $u'w'$ product in terms of the possible combination of the signs. The four types of possible turbulent 'events' are defined by the quadrants in Figure 3.31.

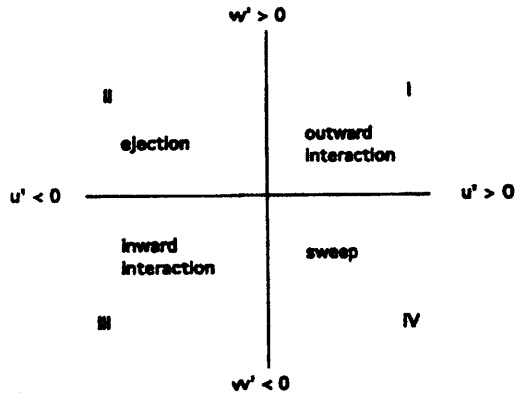

Figure 3.31 Quadrant plot of the four structures of momentum exchange, or turbulent events, defined by the relative signs for the streamwise vertical and fluctuating components i.e. u' and w'. Roman numerals indicate quadrant (Q) number 1-4 (after Sterk *et al.*, 1998).

It can be seen that Q1 (where $u' > 0$ and $w' > 0$) and Q3 (where $u' < 0$ and $w' < 0$) events, the outward and inward interactions respectively, actually contribute negatively overall to shear stress when it is expressed as Reynolds shear stress $-\overline{u'w'}$ due to their transport of momentum upward and away from the surface (where $-u'w' < 0$) (Sterk, 2000). In the case of Q3 events in particular, detailed studies of turbulent structures have found that the negative stress magnitude of these outward interactions is similar to the positive stress created by ejections (Q2) (Nelson *et al.*, 1995). Ejection events however are usually dominant in frequency though, thus ensuring that an overall positive value of $-\overline{u'w'}$ is the general case (Clifford and French, 1993). Where the frequency of outward interactions is found to be increased however, values of mean shear stress are low as a consequence, since the negative effects of outward interactions are dominant. Where the frequency of Q1 events is found to be overriding, a negative effect is consequently exerted on the average Reynolds shear stress. The relative occurrence of each turbulent event type for the sampling points through TRANB2 is shown in Table 3.2.

Table 3.2 Analysis of negative shear stress contributing interaction-type events (Q1, Q3) in TRANB2

Distance from crest *(x/h)*	Q1 and Q3 events (% of total events)	*u'w'* correlation coefficient
2.22	49.7	-0.0046
3.72	53.6	0.129
5.19	44.9	-0.0647
6.66	44.7	-1.03
-19.22 (Reference)	41.2	-0.291

Table 3.2 indicates the prevalence of Q1 and Q3 events (53.6% of total events) at x/h = 3.72 in TRANB2, a fact which is also represented in the overall positive correlation between streamwise and vertical fluctuations there. Unperturbed flow (the reference from x/h = -19.22) shows the least influence by outward interactions (41.2%), and this has the strongest negative coefficient (leading to positive -$u'w'$). Thus the negative $-\overline{u'w'}$ at x/h = 3.72 is explained by the skewed distribution toward Q1 and Q3 interactions, with Q1 events as the most commonly detected for the five minute measurement run at x/h = 3.72. Bennett and Best (1995) also observed local concentrations of these outward interaction events near flow re-attachment (as x/h = 3.72 is). They attributed this to the influence of upward and outward deflection of the re-attaching flow after it had 'rebounded' from the surface, giving the flow an upward transport of momentum. Given the proximity to re-attachment here, this explanation would fit for the unusually high presence of Q1 at x/h = 3.72 in TRANB2. The near-zero positive value seen at x/h = 2.22 in TRANB2 (Figure 3.30a) is shown by the very weak correlation between $u'w'$ (-0.0046), and the relatively high contribution of Q1 and Q3 events which reduces the time-averaged shear stress value.

A further significance of the turbulent structures is that despite contributing negatively to shear stress, Q1 events have not been found to produce a corresponding reduction in the local sediment transport rate, but rather an enhancement of it. This has been ascertained by high resolution turbulent flow and transport sampling experiments (Nelson *et al.*, 1995). The suggested mechanism for this is that the positive streamwise velocity component of the outward interaction encourages drag on particles, and the positive upward velocity acts to move the entrained sediment upward and into faster velocities that exist at height, thereby increasing the transport rate (Bennett and Best, 1995). At re-attachment therefore, the low time averaged Reynolds shear stress are compensated for in terms of sediment transport by the effect of high-magnitude low-frequency events.

It should be noted that in this level of quadrant analysis no threshold was applied to the effect of an event (Bennett and Best, 1995; Sterk *et al.*, 1998). The analysis is based only on the appearance of an event as a combination of signs for the instantaneous velocities with no consideration for magnitude (Clifford and French, 1993). Despite this, the findings show how a consideration of coherent flow structures at a point is vital in terms of understanding turbulence variation, and the way that flow separation instigated by dunes is effective at

generating this micro-turbulence. In fact, the link between mean Reynolds shear stress and sediment transport is now questioned (Sterk *et al.*, 1998) especially where flow is complex as affected by bedforms. Fundamentally, it is the detailed near-surface turbulence that controls sediment transport because these fluctuations control lift and drag (McLean *et al.*, 1994).

Chapter 4

Implications of Interdune Dynamics

4.1 Introduction

The results of the fieldwork have been described and explained in Chapter 3, where the information that was gained from the study of interdune dynamics was related directly to achieving the first objective of the study, as set out in Section 1.6. This chapter takes a detailed look at the typical patterns of dynamics that were observed in the different interdunes in order to tackle the second objective of the project. To fulfil this second objective, the implications of the experimental results are examined firstly to characterise the observed dynamics for the interdune types. Following the characterisation of the different dynamics, the geomorphological significance of the different interdune types is then considered.

4.2 Characterising the different interdune dynamics

4.2.1 The closely-spaced interdune setting

Section 3.3.1 described in detail the typical flow patterns within TRANS2, the sandy-floored interdune with the shortest interdune length. The data show consistent evidence of flow separation at the brink, and then subsequent re-attachment of flow to the surface, with a mean distance between 3.54 and 4.42 h (Figure 3.18). Following re-attachment, the flow near the surface was seen to accelerate immediately. This speed-up was attributed to the increased momentum reaching nearer the surface since the end of the separation cell allowed the quicker wake flow to expand downward to the bed (Figure 1.5). Measuring at z = 0.5 m so closely downwind of re-attachment means the sampling will be outside the newly formed IBL, which will be closer to the surface. Despite the lack of evidence from the data here, from the detail of other studies (e.g. Nelson and Smith, 1989; Nelson *et al.*, 1993) it is well-established that underneath the wake, an IBL does begin to develop from the point where the separated flow re-couples. With this as the case, in TRANS2, the re-development of the IBL therefore occurs in conjunction with the presence of the windward slope of the downwind dune, where the toe of the slope was at x/h = 4.42 and where re-attachment is detected just before this.

Part of the second objective of this study was to characterise the interdune dynamics observed and discussed in Chapter 3. For the case of the processes operating in TRANS2 as described above, it is argued here that the particular relationship between the topography and the near-surface flow is characteristic of the flow response model to predict flow over bedforms (McLean and Smith, 1986).

Further evidence for the notion that it is flow response elements that explain the dynamics of TRANS2 is shown by the effect of the change from erosional to depositional stages that is central to the flow response model (Section 1.3.3). This change is reflected in the form of the downwind windward slope in TRANS2. The evolution from erosion to deposition predicted by the flow response model occurs due to the contrasting wake (positive) and IBL growth (negative) effects balancing out by a certain distance downwind of the dune. When a second dune is present downwind, the response of the flow to initial separation and then re-attachment occurs on the downwind windward slope. The resultant erosion pattern on this slope tends to create a windward form characterised by a gently convex profile starting from around mid-slope (Cooke *et al.*, 1993). The concavity in the form of the TRANS2 slope exists until around $x/h = 7.5$ (Figure 3.18) where the onset of convexity suggests that the stress and transport are distributed through the interdune in the way prescribed by the flow response model.

4.2.2 The "extended" interdune setting

Where it was argued in the previous section that the typical flow in TRANS2 was suggestive of the occurrence of the flow response model, the dynamics of the other studied interdunes are less well characterised by this particular response model. This is the case for both the study interdunes with bare, eroded surfaces, as well as for TRANS1, the sandy example that has the longest interdune length from the sample of interdunes (Table 2.1). In particular within these "extended" interdunes (where there is an identifiable, often flat, interdune area extending beyond re-attachment (Frank and Kocurek, 1996b)) the IBL that develops where flow re-attaches is not associated immediately with the subsequent bedform windward slope. In other words, even with an erodible bed (TRANS1), the shear stress variation that the IBL establishes does not instigate the next bedform as the flow response model would suggest. Figure 3.21 and the selection in Figure 3.22 show that mean re-attachment was some way upwind of the downwind dune.

Furthermore, the near-surface speed-up data examples where the interdune was relatively extensive (especially Figures 3.22b, 3.22c and 3.23) specifically also demonstrate the way flow reacts to the downwind dune in "extended" interdunes - identifiably a result of the adverse pressure gradient, or stacking effect, at the toe of the obstacle (Hunt and Simpson, 1982). Actual reductions in velocity caused by the pressure at the upwind toe were rarely observed (cf. Figure 3.23 $z = 0.5$ m), rather, decreased accelerations were more often seen for the toe region (McKenna Neuman *et al.*, 1997). The infrequency of detecting overall retardation at the toe was attributed partly to the $z = 0.5$ m sampling height. However, the most pertinent aspect is that flow was observed as undergoing a reaction to the presence of the next dune at the downwind edge of the "extended" interdunes. Such a mean velocity change is not seen in the flow response model, or in Figure 3.18, since the flow acceleration from re-attachment negates any adverse pressure build-up from the almost downwind adjacent stoss slope. In their study (with lowest anemometers at $z = 0.1$ m), Frank and Kocurek reported, "Whenever an interdune flat was present, there was a drop in near surface wind speeds immediately upwind of the next downwind dune" (1996b: p. 454). Where flow seems to be reacting to the presence of the downwind dune in the "extended" interdunes, it is visible to a varying degree that pure flow response does not appear to be occurring, which is the case except in the closely spaced TRANS2.

Whereas the elements of the well-accepted mechanism of flow response (McLean and Smith, 1986) (Figure 1.3) were offered to explain the flow in TRANS2, for the case of the "extended" interdunes, a new conceptual model is proposed in order to characterise the dynamics of interdunes with that form (Section 3.3.2). Such an approach was validated by the recurrence of particular flow patterns through the "extended" interdunes under transverse flow. This new model represents a large step towards achieving the study's second objective; the characterisation of the dynamics for this type of interdune.

4.2.3 A conceptual model for flow in "extended" interdunes

Firstly, it should be borne in mind that the interdunes to which this descriptive model applies are not rigorously defined here. Instead, they are put forward only in the broadest sense. It is certainly not possible to attach a critical physical length for the "extended" interdune in order for the dynamics to behave differently to pure flow response. Rather at this stage, the new conceptual model serves only to explain the flow features, and their geomorphological significance, for the situations of wherever these particular flow features appear within an

interdune. The examples here are TRANB1, TRANB2 and TRANS1, where the dunes bounding the interdunes are not closely spaced. Walker (1999) and Walker and Nickling (2003) studied dunes with what they termed a "close spacing", where the interdune length was 0.5 *h*. Table 2.1 confirms the smallest spacing excluding TRANS2 (3.8 *h*) was TRANB2 where the interdune length was 4.4 *h*.

Based on the nature of the variation in the patterns of near-surface flow (velocity, direction and turbulence), a series of zones are identified across the "extended" interdune in an attempt to characterise it. These zones are named, and the distinguishing processes for each one are described. Furthermore, the geomorphological significance of the flow characteristics ascertained for each zone is provided. The geomorphological significance of the flow in interdunes is discussed in terms of the changes in potential sand transport capacity that occurs with the change in windflow. To guide this, the general relationship that has been found to link potential sediment transport and the wind, through the shear velocity of flow, u_* (where u_* is proportional to the gradient of the log-linear velocity profile) is considered.

$$q \approx u_*^3 \qquad \text{Equation 4.1}$$

Thus sediment flux (*q*) is described approximately by the cube of the shear velocity (Bagnold, 1941; see review in Greeley and Iversen, 1985). Accurate determination of shear velocity from vertical velocity profiles however poses numerous problems. Moreover, the approach is invalidated entirely when profiles are not log-linear, as is the case in the complex flow in the lee-side of a dune, where flow is recovering or when accelerating on the windward slope (Mulligan, 1988; Walker, 1999). As such, the velocity change at z = 0.5 m throughout the interdune is used in place of actual shear velocity, where near surface velocity is assumed to vary as the shear velocity does. Given the problems of shear velocity determination, this method now sees greater advocacy in aeolian geomorphology (Wiggs, 2001). It is acknowledged that velocity and sand transport are not perfectly linked (Watson, 1987; Stout and Zobeck, 1998), but it is argued here that the near surface velocity can adequately inform a conceptual model for "extended" interdunes. This study also includes direct Reynolds shear stress data, although as a result of the complex flow and a variable vertical profile of stress in the inner region with stress measured away from the surface, again this variable cannot be linked directly with sediment flux potential. This fact is further reinforced by the Reynolds shear stress data presented for the interdunes (Figure 3.30) and in other dedicated studies that

have shown that mean shear stress itself does not have a straightforward link with sediment flux in disturbed flows. This is due to the large variations about the mean and the intermittent contribution to transport by turbulence structures (Nelson *et al.*, 1995; Sterk *et al.*, 1998). Turbulence does however compliment the conceptual model, and whilst a definitive method for predicting sediment transport in complex flows is lacking, mean velocity and turbulence are the most relevant factors and will permit estimations of varying transport potential. Guided by this, a descriptive model is advanced for conditions of perpendicular flow within aeolian transverse dune interdunes, where the interdune is of an "extended" nature (Table 4.1).

4.2.3.1 Zone of separation

In the area upwind of the mean point of flow re-attachment, mean velocities are reduced greatly in the immediate lee as a result of streamline expansion beyond the dune brink and the separation of flow from the surface. After the severe initial drop, cup anemometers indicate an area of reduced velocity for the near-surface flow that is relatively constant within the cell forming the *zone of separation.* Near surface sonic anemometer velocities show low speeds with a negative mean. This is reinforced by the wind direction, which shows the occurrence of reversed flow with a sufficient constancy to indicate it is regularly the dominant component.

Normal Reynolds stresses tend to be high, since they are influenced by the free shear layer between the separation cell and the lower wake, with its eddy shedding and high shear. Where influenced by the shear layer, Reynolds shear stresses are also high, but time-averaged shear stress nearer and actually at the surface is considerably lower than the maximum in the shear layer (also Bennett and Best, 1995). This is the first indicator that the height of at-a-point sampling is an important control on the observed turbulence patterns, compared with the detail of the vertical profile of stress variation measured in the wind tunnel or flume (e.g. Zeman and Jensen, 1987; Maddux *et al.*, 2003a, 2003b).

Table 4.1 A conceptual model for flow dynamics in the "extended interdunes" of transverse dunes under conditions of perpendicular incident flow. Interdune zones progress downwind. Explanation in text.

Interdune Zone	Flow Characteristics			Geomorphological significance
	Velocity	*Flow Direction*	*Near-surface turbulence*	
SEPARATION	Low, and relatively constant Negative component in streamwise plane	Mean direction toward upwind dune ω relatively constant	High Reynolds normal stress in shear layer Shear stress variable with *z*	Zero to low erosive potential Related to upwind dune?
RE-ATTACHMENT	Low velocity Zero velocity in streamwise plane	Mean direction highly variable Maximum ω	High Reynolds normal stress in shear layer Shear stress variable	Highly intermittent erosive potential
RECOVERING FLOW	Beginning marked by onset of acceleration Continued overall increase through zone	Decreasing ω Mean direction often crest parallel in upwind part of zone	Declining Reynolds normal stress Decline in non-surface shear stress	Increasing erosive potential/transport competence
RECOVERED FLOW	Steady velocity	ω equal to primary flow Mean equal to primary	Declining Reynolds normal stress Declining/steady shear stress	Steady transport competence
INTERACTION I	Relative slowing or retardation	ω equal to primary flow Mean equal to primary	Possible increase in shear stress (streamline curvature induced)	Maintenance of transport competence
II	Acceleration on windward slope	ω equal to primary flow Mean equal to primary	Increasing surface shear stress Normal Reynolds stresses curvature/acceleration controlled	Increase in actual erosion on downwind dune

The low speeds and mean shear stress indicate that this area is one of low transport potential. Furthermore, under certain flow conditions, there may be a sediment input due to grain fallout from the separated flow (Nickling *et al.*, 2002). Walker (1999) has measured appreciable sediment movement back toward the slipface in the separation cell. He stresses a transport contribution to the slipface and the maintenance of dune form. Uncertainty remains over that component, but the small geomorphological significance for this interdune region therefore is restricted to the upwind dune shape, including the possible effect of longitudinal flow along the slipface (Walker and Nickling, 2002) which creates enhanced sand trapping (Momiji and Warren, 2000).

4.2.3.2 Zone of re-attachment

In terms of the downwind distance for the location of this dynamic zone, estimates for separation length within the extended interdunes range from around 3.5 *h* to 5.5 *h*, which agrees well with the lower estimates of other aeolian and sub-aqueous studies (e.g. Engel, 1981; Nelson and Smith, 1989; Frank and Kocurek, 1996b). The true point of flow re-attachment at the surface will be characterised by a zero average velocity for flow purely in the streamwise plane (with a sonic anemometer). For cup anemometers, as a result of time-averaging, the flow re-attachment is best marked by the point before the onset of acceleration that ends the area of constant flow representing the separation cell. The migration of the separation length over time by a distance of about 0.5 *h* (Walker and Nickling, 2002) is also supported here. The inconsistency of the point of flow re-attachment over this small distance means flow directional variability is greatest for the *zone of re-attachment*. Further upwind, ω is enhanced as reversed flow is relatively constant, and downwind, ω grows as flow recovers toward its primary conditions. The high variability means mean direction is actually unrepresentative of any real preferred flow direction in this zone.

Since the free shear layer is projected onto the bed in the *zone of re-attachment* as the separation streamline descends, there are high normal Reynolds shear stresses found here. Mean (Reynolds) shear stress is highly variable as a result of turbulent fluctuations caused by eddy impact at the bed. For a near-surface height, turbulent structures exert control on the shear stress including overall negative contributions to $-\overline{u'w'}$ (Figure 3.30), though the link with surface sediment transport is complicated since these negative shear stress events do not necessarily inhibit transport (Nelson *et al.*, 1995). With a low velocity and mean shear stress,

the mean sediment transport potential is accordingly limited in the *zone of re-attachment* but there is evidence that it is intermittently enhanced at turbulent time scales. The occurrence of transport at all points is strongly controlled by the occurrence of turbulent events. These are remarkably efficient in terms of transport however since, over time, the *zone of re-attachment* is not an area for deposition, and the erosive ability there is sufficient to maintain the re-attachment area as sand free in the bare interdunes.

4.2.3.3 Zone of recovering flow

With the onset of recovery beginning with flow re-attachment and the development of an IBL at the surface, the *zone of recovering flow* is the region within the interdune where the return of the flow to primary conditions is seen to take place. One of the most apparent and important characteristics of the dynamics here is the ongoing increase in near-surface velocity throughout the zone (e.g. Figures 3.23 and 3.24). Re-attachment is indicated by the onset of acceleration in the time-averaged data, and this acceleration continues for the whole zone due to the wake dissipation and downward momentum extraction. Driven by the accelerating flow, directional variability undergoes a continued decrease with distance in this zone, and ω will reach upwind values before velocity does (Figure 3.22a, 3.22b and 3.22c). With the improvement in direction constancy, mean direction also consistently changes towards the general flow conditions. For the upwind end of the zone, direction is found to have moved from dominantly reversed in the separation cell to nearer that of the free stream, often sub-parallel to the upwind dune crestline.

Over distance in the *zone of recovering flow* there is a decrease in the streamwise and vertical Reynolds stress, as well as shear stress. The free shear layer is by far the primary source of all turbulence in the wake and with distance downwind from this source, the extent and frequency of elements influencing turbulent airflow will recede (Table 4.1). It is important to note that this overall decline in turbulence pertains to the case of sampling at the near-ground, that is away from the surface, but securely within the wake (z = 0.5 m). At the surface, shear stress actually increases from a minimum at flow re-attachment as shown in Bradshaw and Wong (1972) and Walker and Nickling (2003). Both these studies are especially relevant since they sampled surface stress variation behind a backward-facing step and an isolated dune respectively. These are similar to the situation that exists in the "extended" interdune scenario, until the downwind dune influences on turbulence are manifested.

The geomorphological significance for this region is one of erosive potential. The increasing velocity means that, when the re-attaching flow is strong enough, flow in the *zone of recovery* will be capable of eroding throughout the whole of the zone. Speed-up increases transport capacity so that sediment entrained upwind as well as sediment downwind can be moved. This mechanism accounts for the existence of bare interdunes, as also recognised in terms of the interdune sediment budget by Frank and Kocurek (1996b). Furthermore, under the IBL (not sampled here) the pattern of increasing surface shear stress complements the increasing velocity in suggesting that the *zone of recovering flow* is one of erosion. Turbulence at the near-surface (z = 0.5 m) instead reflects the general trend of recovery of the airflow.

As possible further evidence for the geomorphological significance of this interdune region, the form of lee-side dune aprons is suggested. These aprons are sand piles that are found attached to many dune slipfaces (Cooke *et al.*, 1993). It is seen in this study that the downwind extent of an apron is co-incident with the instigation of flow recovery in sandy interdunes (TRANS1, Figure 3.22c). This situation was also the case in Sweet and Kocurek (1990) but was not commented on. Significant differences therefore exist for the *zone of recovering flow* as seen within the "extended" interdunes model and the original model of flow response. This point concerning the difference in the interdune types is returned to in Section 4.3.

4.2.3.4 Zone of recovered flow

This zone is shaded in Table 4.1 to indicate that it is not always present within the "extended" interdune, and may only appear in certain large interdunes, or under non-transverse incident flow conditions, where flow angle effectively extends the interdune length. In cases where this zone is evident (no examples in this study), the flow velocity is steady throughout the zone, having recovered to primary flow levels and direction attributes. As such, the presence of a *zone of recovered flow* within an interdune is effectively analogous with the recovered flow downwind of an isolated dune (e.g. Figure 3.2 or 3.3), but with another dune ultimately downwind. The *zone of recovered flow* only ends when the impact of the downwind dune is felt. Where the downwind dune has an impact on the flow before the flow is recovered, as was the case for all interdune situations reported here, the zone is non-existent for an "extended" interdune. Distances of 10 h for a return to unperturbed velocity (Lancaster, 1989a) and 16-18 h for BARC2a this study (Figure 3.4) attribute a possible minimum length scale before the recovered flow zone starts.

Whilst the velocity is constant at a recovered level in this zone, it is unlikely the flow will be recovered in terms of turbulence. Turbulent elements are likely to remain higher than the unperturbed boundary layer conditions. The isolated dune studies showed that for all of the turbulence components measured, an enhanced signal persisted even when flow speed was recovered (Figures 3.1, 3.8 and 3.14). This is reinforced by the similar (and further, up to 50 *h*) downwind distances from perturbation in the literature (e.g. Walker and Nickling, 2003; McLean *et al.*, 1996). A truly recovered flow zone in terms of turbulence as well is therefore a theoretical case.

The geomorphological significance of this zone is debatable given its rarity. In actual fact, similarities with the wake dissipation and IBL growth over the distance necessary for the *zone of recovered flow* to occur can be drawn with the flow response model and the mechanism of that model for initiating dunes (as described in Section 1.3.3). This is not the flow-form control on arrangements of bedforms that already exist which the flow response model also suggests, which in turn is seen in the interdune of TRANS2 and schematically in Figure 1.3.

4.2.3.5 Zone of interaction

This region is found at the downwind part of the interdune and is marked by the detection of the influence on flow exerted by the next downwind dune. Where a *zone of recovered flow* is not present in an "extended" interdune, the *zone of interaction* follows the *zone of recovery.* For the case of a flat interdune, the interaction of flow with the downwind dune is two-part, and this effectively splits the *zone of interaction* into an upwind (I) and downwind (II) part.

Zone of interaction I is where a negative effect on near-surface velocity is seen. This negative change is manifested as either a reduction in the rate of flow acceleration, or an actual retardation of flow, and is due to the adverse pressure created by the upwind dune, or stacking effect. The extent of the stacking effect on velocity is variable though, and a physical decrease in speed-up is not always apparent. The examples in Figure 3.22 show several different magnitudes of velocity change within the interdune at the downwind dune toe. With a *zone of recovered flow* present in an interdune, or the nearer that flow had got to a recovered state, the more the observation of actual retardation at the windward toe is likely. This is because in the upwind part of the *zone of interaction*, there is a balance between three important influences on flow. These are the growth of the IBL from re-attachment, the dissipation of the wake

(both of which occur through the *zone of recovery*) and finally the influence of the downwind dune. The observed velocity change at the toe will reflect this interaction (plus sampling height with reference to the height of the developing boundary layers).

In terms of the geomorphological significance of *zone of interaction I*, the fall in velocity suggests a reduction in sediment transport competence. However, in one interdune case (TRANB2, Figure 3.30a) and in the case of the isolated dune (Figure 3.12), concave flow and shear stress increases were seen for the upwind toe region, thus supporting the streamline curvature dune model of Wiggs *et al.* (1996). This holds that positive streamline curvature at the toe can promote shear stress that will compensate for the velocity drop and possible reduction in flux. The absence of deposition for the upwind toe provides more evidence to reinforce the positive role of turbulence for transport.

Zone of interaction II is characterised by acceleration caused by streamline compression on the downwind dune, and it effectively marks the end of interdune in terms of process. The merger of speed-up caused by the windward slope together with flow that is accelerating in the interdune due to flow recovery, means it is often difficult to completely segregate the two effects. A key feature of the "extended" interdune, however, is that a second IBL in effect forms at the base of the windward slope of the downwind dune (Frank and Kocurek, 1996a, 1996b) (discussed further in Section 4.3). The shear stress increase under this IBL drives the sediment transport on the dune slope necessary for equilibrium form (Tsoar, 1985; Lancaster, 1985a), but the layer is beneath the sampling range of cup anemometers (Frank and Kocurek, 1996a; Wiggs *et al.*, 1996).

All forms of turbulence begin to be controlled by the interplay of acceleration and streamline curvature on the windward slope (Kaimal and Finnigan, 1994). However, a rise in shear stress that is seen as a lagged event for the isolated dunes may be present (Figure 3.12). A key control on the detection of this shear stress increase will be the height of measurement of the at-a-point sampling in relation to the inner layer (Section 1.5.1) (Jackson and Hunt, 1975; Wiggs, 2001).

4.3 Geomorphological significance of the different interdune types

By recognising the occurrence of distinctive flow response behaviour within TRANS2, and then by introducing a new model in order to explain the different flow dynamics that were

common to all the "extended" interdunes, the observed interdune dynamics have been split into two. Each of these interdune types is described by a model.

Following the characterisation of each interdune type with reference to their model, and in order to further tackle the study's second objective, a brief comparison is made between the models in order to highlight their different geomorphological significance. Table 4.2 re-states the geomorphological significance for the "extended" interdune zones offered in Table 4.1. Alongside this in Table 4.2 is the geomorphological significance inferred in the same terms for the model of flow response (based on McLean and Smith, 1986).

Table 4.2 Comparison of geomorphological significance for the interdunes described by the "extended" interdune and flow response models.

Interdune Zone	Extended interdune model	Flow response model
SEPARATION	Zero to low erosive potential Related to upwind dune?	Zero to low erosive potential
RE-ATTACHMENT	Highly intermittent erosive potential	Highly intermittent erosive potential
RECOVERING FLOW	Increasing erosive potential/transport competence	Onset of flow-form interaction, and ACTUAL transport
RECOVERED FLOW	Steady transport competence	NO EQUIVALENT
INTERACTION I	Maintenance of transport competence	NO EQUIVALENT
II	Increase in actual erosion on downwind dune	Continued actual erosion on downwind dune

Thus, Table 4.2 explores the geomorphological significance for the interdune spaces in the two different interdune types, where the zones identified for the "extended" interdunes are imposed onto the flow response model to provide a spatial framework for the comparison.

There is essentially no difference between both models in terms of the geomorphological significance of *separation* and *re-attachment*. Given both models are related to bedform spacing, the distance for flow re-attachment effectively establishes a minimum distance for spacing, creating a control that is common to both types of interdune. This minimum spacing

point is fixed geomorphologically due to the limited erosion within the separation cell, and the high intermittent transport at the mean point where flow re-couples. It follows, and is seen, that for flow response situations, the minimum spacing governed by mean re-attachment length will also be close to the spacing actually exhibited (Engel, 1981; Nelson and Smith, 1989).

The fundamental difference between the models is located in the *recovering flow* zone. Here, for the setting of "extended" interdunes, there is recovery in the wake airflow following the separation perturbation due to momentum receipt in the lower wake, and the IBL development for near the surface. For the flow response model however, the recovery of flow occurs in conjunction with the windward slope of the next dune. The effects of topographic forcing as well as flow recovery are combined, meaning flow-form interaction is incorporated. With the IBL growth occurring over the windward slope, it also means that actual erosion can occur (with sufficient wind strength) since a sediment supply is guaranteed. The geomorphological difference between the models in this respect is that the onset of windward slope flow-form interaction in the dynamics of the "extended" interdune model is not exhibited until further downwind, and the *zone of interaction (II)*.

Furthermore, when flow-form interaction with the downwind dune does occur in "extended" interdunes, the nature of the interaction is significantly different to that for the case of the pure flow response model. This is reflected by the extended interdune showing a two-part *zone of interaction*, where flow has an element of slow-down at first. For closely spaced dunes, the upwind stacking effect is not evident (e.g. Nelson *et al.*, 1993; Bennett and Best, 1995; Walker, 1999). In the downwind part of *interaction* for flow response interdune situations, the IBL that grows and leads to an increase in shear stress on the windward slope is the same one that formed at flow re-attachment. In "extended" interdunes, however, a second IBL has been suggested to form on the windward slope (Frank and Kocurek, 1996a, 1996b). As such, the "flow reaction model" might be a suitable term for the characterisation of dynamics in "extended" interdunes. The imposition and development of the second IBL in turn controls the morphodynamics on the windward slope and the downwind dune.

On this last point, the significance of the different behaviour of IBLs between the models for flow response and "extended" interdunes has further implications for the controls on transverse dune spacing. The flow response model, developed for sub-aqueous bedforms,

assumes an erodible bed. The IBL at re-attachment therefore leads to the development of a bed in direct response to the variation in surface shear stress caused by flow recovery from the perturbation. Within "extended" interdunes, the same pattern of recovering shear stress will be found at the surface, yet spacing of the dunes for the same height may be different to where sediment uninhibited flow response operates. This introduces the control of sand availability on bedform spacing, and spacing arrangements as an expression of this (Lancaster, 1988). In "extended" interdunes, where speed-up of flow is seen throughout the interdune, the increasing erosive potential of the interdune flow has a geomorphological role in that it can account for the presence of sand-free stretches between dunes. However, where dune development is occurring in an area of limited sand availability, it seems that with respect to the sediment control, the dynamics of the interdune flow may be much more "dynamically neutral". This is in terms of the role the dynamics have in fixing spacing, especially when compared with their role when sediment is readily available.

Chapter 5
Conclusions and Future Research

This project had an overall aim to increase our understanding of the geomorphological significance of a variety of interdune types in transverse sand dune areas.

To achieve this aim, the variation in geomorphologically relevant aspects of airflow has been investigated within a selection of transverse dune interdunes. The approach employed for this investigation of interdune dynamics was driven by the need for the collection of such data, given their recognised utility in advancing our understanding of dunes.

Relating back to the particular objectives of the research, the first objective was:

1. To obtain data on geomorphologically relevant variables within transverse dune interdunes. In particular, the measurement of flow velocity, direction and turbulence.

From this first objective, three primary conclusions are drawn from the considerable amount of data that was collected by field experiments conducted when flow was perpendicular to the crest.

i- The expected velocity patterns for the lee-side of the upwind study dunes were seen (Frank and Kocurek, 1996b). This led to the detection of flow separation, reversal and the quantification of the mean re-attachment length (3.5 h to 5.5 h), thereby determining the extent to which separated flow occupied the different interdunes. Dune shape is an important control on re-attachment length. High temporal resolution streamwise velocity data proved highly effective at detecting the extent to which flow was reversed, and the proximity to the mean re-attachment point for a given sampling run.

ii- After re-attachment, mean near-surface velocity was found to undergo overall increases throughout all interdune settings. The influence of the downwind dune on interdune velocity patterns was variable and was influenced by the type of interdune. No 'stacking effect' was seen for closely spaced dunes, but negative changes in velocity were apparent in interdunes that had an "extended" nature i.e. where the interdune was relatively longer than the separation length.

iii- Turbulence measured through the interdune at a height near the surface (z = 0.5 m) is dominated by flow recovery in the (lower) wake downwind of re-attachment. This was manifested through a decline in streamwise, vertical and Reynolds shear stresses, with downwind distance from the shear layer, indicating the importance of the layer as the dominant source of turbulence throughout the interdune. Variability in shear stress was enhanced at re-attachment. By the downwind margin of the interdunes, all turbulence remained far in excess of unperturbed boundary layer values, which suggested turbulent flow does not recover to free stream levels, further showing the influence of the wake at this sample height. Furthermore, at the downwind dune toe of the interdune, the turbulence generated by the wake appears to mask the change in turbulence at the toe which was seen in the isolated dune investigation, and was attributed to streamline concavity (Wiggs *et al.*, 1996).

The second objective of the study was:

2. To use the results from (1) above to characterise observed interdune dynamics and investigate the geomorphological significance of the various interdune types.

With regard to the attempts to characterise the dynamics for the study interdunes, and their significance, the following conclusions are highlighted.

i- Mean flow patterns, interdune topography and the close relationship between these two variables was seen as symptomatic of the flow response model (McLean and Smith, 1986) for an interdune with a closely-spaced dune arrangement and a sandy bed.

ii- The measured field situations also showed cases where the lengths of interdunes were considerably greater than the mean flow re-attachment length, and the downwind dune of the interdune pair could therefore not be associated with the IBL forming where flow re-coupled with the surface. Thus the flow response model did not appear to describe the interdune spacing. The dynamics of these "extended" interdunes were characterised by a new descriptive model. The fundamental difference between the interdune types is the nature of the flow-form interaction. Some other conclusions are based on that.

iii- Frank and Kocurek (1996a, 1996b) supposed that a second IBL formed at the base of the windward slopes of dunes that were preceded by an "extended" interdune, and that the stress variation set up by this layer accounted for the individual morphodynamics

for that dune. For the "extended" interdunes in this study, significance is attached to the reaction by the flow to the downwind dune which is missing in the model based solely on flow response. A *zone of interaction* was suggested to incorporate the different velocity behaviour at the downwind dune.

iv- Returning to Ahlbrandt and Fryberger's (1981) classification for interdunes, whilst it was only a simplistic tool, the assumption that depositional processes dominate sandy interdunes might be especially misleading. Sandy-floored interdunes may well be undergoing net erosion, or be transporting sand without any net change.

v- For controls on dune spacing, the separation length of flow fixes a minimum distance to establish a minimum spacing between dunes.

Finally, it is possible to highlight some directions that would be profitable for the future study of interdunes, and also how this course of action would be worthwhile for aeolian geomorphology. This study of interdune dynamics was based on the undertaking of key process measurements, and it is believed that there will remain utility to this approach. Some of the most informative aeolian studies recently have coupled detailed field and wind tunnel studies (e.g. Wiggs *et al.*, 1996; Walker and Nickling, 2003), with the latter study actually looking at a closely-spaced dune setting. Surface shear stress variation is inherent in the flow response model for both initiating dunes and acting as a subsequent control on their form. Problems remain with attempts to sample turbulence in the wind tunnel due to equipment limitations (e.g. pressure artefacts and Irwin probes, Walker and Nickling, 2003), and the sonic anemometer used here has been found to be a robust tool for field application in aeolian environments. On the other hand, wind tunnel and flume studies can re-create vertical profiles of turbulence, approaching to very near to surface (e.g. Nelson *et al.*, 1993), where sonic anemometers are at-a-point measuring devices from which detailed turbulence fields would be hard to produce. Using the benefits of an allied wind tunnel and field study, there is the possibility to make a detailed examination of flow elements within a range of interdunes of different dune spacings.

In terms of studies of interdune dynamics, it should be remembered that the only analysis presented here was for perpendicular flow patterns. Flow from different incident angles has been seen to create different lee-side flow patterns on dunes, and especially linear varieties (Tsoar, 1983a; Tsoar *et al.*, 1985), which may change effective interdune length, or fetch. In

addition, longitudinal flow along transverse dunes has been overlooked (Walker, 1999). Crestline sinuosity has implications for transverse dune dynamics, and it might be that the interdune stretches behind linguoid or barchanoid elements may have greater relative significance. These elements suggest a lateral variation in interdune dynamics. In the field in the Skeleton Coast, the occasional adjoining linguoid portions between crescentic ridges seemed to form active pathways for preferential transport of sediment between the ridges. Field studies dedicated to investigating the airflow and transport patterns of these specific areas would appear to be a profitable direction.

Furthermore, it is inevitable that our modelling of all aspects of the sand dune system will continue to improve. There has recently been a whole suite of different kinds of numerical models for the dune field scale especially recently (Section 1.4; see Bishop *et al.*, 2002). Some of these models deal explicitly with transverse dunes (e.g. Schwämmle and Herrmann, 2004). This modelling cannot fail to be assisted by further field-based dune studies, where it has been found that even the most complex systems-based simulations have benefited from modification in the light of physically observed processes. It may be in turn that modelling will permit the study of the macro-influences (e.g. sand supply and wind regime) on dune spacing that cannot be appreciated by field studies alone.

Bibliography

Ahlbrandt, T.S. and Fryberger, S.G. (1981) Sedimentary features and significance of interdune deposits. In *Recent and Ancient Nonmarine Depositional Environments: Models for Exploration*, Ethridge, F.G. and Flores, R.M. (eds.). Society of Economic Palaeontologists and Mineralogists, Tulsa, Oklahoma: 293-314.

Allen, J.R.L. (1968) The nature and origin of bed-form hierarchies. *Sedimentology*, 10: 161-182.

Allen, J.R.L. (1994) Fundamental properties of fluids and their relation to sediment transport processes. In *Sediment Transport and Depositional Processes*, Pye, K. (ed.). Blackwell Scientific, Oxford: 25-60.

Anderson, R.S. (1996) The attraction of sand dunes. *Nature*, 379: 24-25.

Arens, S.M., van Kaam-Peters, H.M.E. and van Boxel, J.H. (1995) Airflow over foredunes and implications for sand transport. *Earth Surface Processes and Landforms*, 20: 315-332.

Ash, J.E. and Wasson, R.J. (1983) Vegetation and sand mobility in the Australian desert dunefield. *Zeitschrift für Geomorphologie*, Supplementband, 45: 7-25.

Bagnold, R.A. (1941) *The Physics of Blown Sand and Desert Dunes*. Methuen, London.

Bagnold, R.A. (1953) The surface movement of blown sand in relation to meteorology. *Desert Research, Proceedings of the International Symposium, Research Council of Israel, Jerusalem*: 89-93.

Barnes, J. (2001) Barchan dunes on the Kuiseb River Delta, Namibia. *South African Geographical Journal*, 83: 283-292.

Bennett, S.J. and Best, J.L. (1995) Mean flow and turbulence structure over fixed, two-dimensional dunes: implications for sediment transport and bedform stability. *Sedimentology*, 42: 491-513.

Best, J.L. and Kostaschuk, R. (2002) An experimental study of turbulent flow over a low-angle dune. *Journal of Geophysical Research*, 107(C9): 3135-3154.

Bishop, S.R., Momiji, H., Carretero-Gonzalez, R. and Warren, A. (2002) Modelling desert dune fields based on discrete dynamics. *Discrete Dynamics in Nature and Society*, 7: 7-17.

Bradshaw, P. (1969) The analogy between streamline curvature and buoyancy in turbulent shear flow. *Journal of Fluid Mechanics*, 36: 177-191.

Bradshaw, P. and Wong, F.Y.F. (1972) The reattachment and relaxation of a turbulent boundary layer. *Journal of Fluid Mechanics*, 52: 113-135.

Breed, C.S. and Grow, T. (1979) Morphology and distribution of dunes in sand seas observed by remote sensing. In *A Study of Global Sand Seas*, McKee, E.D. (ed.). United States Geological Survey, Professional Paper 1052: 253-303.

Brimelow, J.C. and van Heerden, J. (1996) Surface temperature and wind fields over the Skeleton Coast (Namibia) and adjacent interior during SAFARI-92. *Journal of Geophysical Research*, 101(D19): 23767-23775.

Bullard, J.E., Thomas, D.S.G., Livingstone, I. and Wiggs, G.F.S. (1995) Analysis of linear sand dune morphological variability, southwestern Kalahari Desert. *Geomorphology*, 11: 189-203.

Burkinshaw, J.R. and Rust, I.C. (1993) Aeolian dynamics on the windward slope of a reversing transverse dune, Alexandria coastal dunefield, South Africa. In *Aeolian Sediments Ancient and Modern*, Pye, K. and Lancaster, N. (eds.). International Association of Sedimentologists Special Publication 16, Blackwell Scientific, Oxford: 13-21.

Burkinshaw, J.R., Illenberger, W. and Rust, I.C. (1993) Wind-speed profiles over a reversing transverse dune. In *The Dynamics and Environmental Context of Aeolian Sedimentary Systems*, Pye, K. (ed.). Geological Society Special Publication No. 72, London: 25-36.

Campbell Scientific User Guide (1988) Campbell Scientific Instruments, Loughborough.

Castro, I.P. and Wiggs, G.F.S. (1994) Pulsed-wire anemometry on rough surfaces, with application to desert sand dunes. *Journal of Wind Engineering and Industrial Aerodynamics*, 52: 53-71.

Clifford, N.J. and French, J.R. (1993) Monitoring and modelling turbulent flow: Historical and contemporary perspectives, In *Turbulence: perspectives on flow and sediment transport*, Clifford, N.J., French, J.R. and Hardisty, J. (eds.). John Wiley & Sons, Chichester: 1-34.

Cooke, R.U., Warren, A. and Goudie, A.S. (1993) *Desert Geomorphology*. UCL Press, London.

Corbett, I. (1993) The modern and ancient pattern of sandflow through the southern Namib deflation basin. In *Aeolian Sediments Ancient and Modern*, Pye, K. and Lancaster, N. (eds.). International Association of Sedimentologists Special Publication 16, Blackwell Scientific, Oxford: 45-60.

Cornish, V. (1897) On the formation of sand-dunes. *Geographical Journal*, 9: 278-302.

Dong, Z., Liu, X. and Wang, X. (2002) Aerodynamic roughness of gravel surfaces. *Geomorphology,* 43: 17-31.

El-Sayed, M. (2000) The nature and possible origin of mega-dunes in Liwa, Ar Rub' Al Khali, UAE. *Sedimentary Geology*, 134: 305-330.

Engel, P. (1981) Length of flow separation over dunes. *Proceedings of the American Society of Civil Engineers*, 107: 1133-1143.

Finnigan, J.J., Raupach, M.R., Bradley, E.F. and Aldis, G.K. (1990) A wind tunnel study of turbulent flow over a two-dimensional ridge. *Boundary-Layer Meteorology*, 50: 277-317.

Folk, R. (1971) Genesis of longitudinal and oghurd dunes elucidated by rolling upon grease. *Geological Society of America Bulletin*, 82: 3461-3468.

Frank, A. and Kocurek, G. (1996a) Airflow up the stoss slope of sand dunes: limitations of current understanding. *Geomorphology*, 17: 47-54.

Frank, A. and Kocurek, G. (1996b) Toward a model for airflow on the lee side of aeolian dunes. *Sedimentology*, 43: 451-458.

Fryberger, S. G. (1979) Dune forms and wind regime, In *A Study of Global Sand Seas*, McKee, E.D. (ed.). United States Geological Survey, Professional Paper 1052: 137-169.

Fryberger, S. G., Al-Sari, A.M. and Clisham, T.J. (1983) Eolian dune, interdune, sand sheet and siliclastic sabkha sediments of an offshore prograding sand sea, Dhahran area, Saudi Arabia. *American Association of petroleum Geologists Bulletin*, 67: 280-312.

Glennie, K.W. (1970) *Desert Sedimentary Environments*. Elsevier, Amsterdam.

Gong, W. and Ibbetson, A. (1989) A wind tunnel study of turbulent flow over model hills. *Boundary-Layer Meteorology,* 49: 113-148.

Goudie, A.S. (1999) The history of desert dune studies over the last 100 years. In *Aeolian Environments, Sediments and Landforms*, Goudie, A.S., Livingstone, I. and Stokes, S. (eds.). John Wiley & Sons, Chichester: 1-13.

Greely, R. and Iversen, J.D. (1985) *Wind as a Geological Process*. Cambridge University Press, Cambridge.

Ha, S., Dong, G. and Wang, G. (1999) Morphodynamic study of reticulate dunes at southeastern fringe of the Tengger Desert. *Science in China (Series D)*, 42: 207-215.

Hallett, B. (1990) Spatial self-organization in geomorphology: from periodic bedforms and patterned ground to scale-invariant topography. *Earth-Science Reviews*, 29: 57-76.

Hanna, S. R. (1969) The formation of longitudinal sand dunes by large helical eddies in the atmosphere. *Journal of Applied Meteorology,* 8: 874-883.

Hardisty, J. (1993) Monitoring and modelling sediment transport at turbulent frequencies. In *Turbulence: perspectives on flow and sediment transport*, Clifford, N.J., French, J.R. and Hardisty, J. (eds.). John Wiley & Sons, Chichester: 35-60.

Harrison, S. (1999) The problem with landscape: some philosophical and practical questions. *Geography,* 84: 355-363.

Havholm, K.G. and Kocurek, G. (1988) A preliminary study of the dynamics of a modern draa, Algodones, southeastern California, USA. *Sedimentology*, 35: 649-669.

Hersen, P., Andersen, K.H., Elbelrhiti, H., Andreotti, B., Claudin, P. and Douady, S. (2004) Corridors of barchan dunes: Stability and size selection. *Physical Review*, 69: article number 011304.

Hesp, P.A., Davidson-Arnott, R., Walker, I.J. and Ollerhead, J. (2005) Flow dynamics over a foredune at Prince Edward Island, Canada. *Geomorphology*, 65: 71-84.

Hesp, P.A. and Hyde, R. (1996) Flow dynamics and geomorphology of a trough blowout. *Sedimentology*, 43: 505-525.

Hesp, P.A., Illenberger, W., Rust, I., McLachlan, A. and Hyde, R. (1989) Some aspects of transgressive dunefield and transverse dune geomorphology and dynamics, south coast, South Africa. *Zeitschrift für Geomorphologie*, Supplementband 73: 111-123.

Holm, D.A. (1960) Desert geomorphology in the Arabian Peninsula. *Science,* 123: 1369-1379.

Howard, A.D., Morton, J.B., Gad-el-Hak, M., Pierce, D.B. (1978) Sand transport model of barchan dune equilibrium. *Sedimentology*, 25: 307-338.

Hoyt, J. (1966) Air and sand movements to the lee of dunes. *Sedimentology*, 7: 137-143.

Hummel, G. and Kocurek, G. (1984) Interdune areas of the back-island dune field, north Padre Island, Texas. *Sedimentary Geology*, 39: 1-26.

Hunt, J.C.R., Leibovich, S. and Richards, K.J. (1988) Turbulent shear flows over low hills. *Quarterly Journal of the Royal Meteorological Society*, 114: 1435-1470.

Hunt, J.C.R. and Simpson, J.E. (1982) Atmospheric boundary layers over non-homogenous terrain. In *Engineering Meteorology*, Plate, E.J. (ed.). Elsevier, Amsterdam: 1-32.

Inman, D.L., Ewing, G.C. and Corliss, J.B. (1966) Coastal sand dunes of Guerrero Negro, Baja California, Mexico. *Geological Society of America Bulletin*, 77: 787-802.

Jackson, P.S. and Hunt, J.C.R. (1975) Turbulent wind flow over a low hill. *Quarterly Journal of the Royal Meteorological Society*, 101: 929-955.

Kadota, A. and Nezu, I. (1999) Three-dimensional structure of space-time correlation on coherent vortices generated behind dune crest. *Journal of Hydraulics Research*, 37: 59-80.

Kaimal, J.C. and Finnigan, J.J. (1994) *Atmospheric Boundary Layer Flows*: *Their Structure and Measurement*. Oxford University Press, Oxford.

Kennedy, J.F. (1969) The formation of sediment ripples, dunes and antidunes. *Annual Review of Fluid Mechanics*, 1: 147-169.

Keogh, D.P. and Addison, P.S. (1996) Coherent flow structures in open-channel slot flow. In *Coherent Flow Structures in Open Channels*, Ashworth, P.J., Bennett, S.J., Best, J.L. and McLelland, S.J. (eds.). John Wiley & Sons, Chichester: 267-280.

Kiya, M. and Sasaki, K. (1983) Structure of a turbulent separation bubble. *Journal of Fluid Mechanics*, 137: 83-113.

Knott, P. and Warren, A. (1981) Aeolian processes. In *Geomorphological Techniques,* Goudie, A. S. (ed.). Allen and Unwin, London: 226-246.

Kocurek, G. (1981) Significance of interdune deposits and bounding surfaces in aeolian dune sands. *Sedimentology*, 28: 753-780.

Kocurek, G., Townsley, M., Yeh, E., Havholm, K. and Sweet, M.L. (1992) Dune and dune-field development on Padre Island, Texas, with implications for interdune deposition and water table controlled accumulation. *Journal of Sedimentary Petrology*, 62: 622-635.

Kostaschuk, R. (2000) A field study of turbulence and sediment dynamics over subaqueous dunes with flow separation. *Sedimentology*, 47: 519-531.

Kostaschuk, R. and Villard, P. (1996) Flow and sediment transport over large subaqueous dunes: Fraser River, Canada. *Sedimentology*, 43: 849-863.

Kroy, K., Sauermann, G. and Herrmann, H.J. (2002) Minimal model for aeolian sand dunes. *Physical Review*, 66: article number 031302.

Lancaster, N. (1980) The formation of seif dunes from barchans – supporting evidence for Bagnold's hypothesis from Namib Desert. *Zeitschrift für Geomorphologie,* 24: 160-167.

Lancaster, N. (1982a) Dunes on the Skeleton Coast, SWA/Namibia: geomorphology and grain size relationships. *Earth Surface Processes and Landforms,* 7: 575-587.

Lancaster, N. (1982b) Linear Dunes. *Progress in Physical Geography,* 6: 476-504.

Lancaster, N. (1985a) Variations in wind velocity and sand transport on the windward flanks of desert sand dunes. *Sedimentology*, 32: 581-593.

Lancaster, N. (1985b) Wind and sand movements in the Namib sand sea. *Earth Surface Processes and Landforms*, 10: 607-619.

Lancaster, N. (1988) Controls of eolian dune size and spacing. *Geology*, 16: 972-975.

Lancaster, N. (1989a) *The Namib Sand Sea: Dune Forms, Processes and Sediments.* A.A. Balkema, Rotterdam.

Lancaster, N. (1989b) The dynamics of star dunes: an example from the Gran Desierto, Mexico. *Sedimentology*, 36: 273-289.

Lancaster, N. (1989c) Star dunes. *Progress in Physical Geography*, 13: 67-92.

Lancaster, N. (1994) Dune morphology and dynamics. In *Geomorphology of Desert Environments*, Abrahams, A.D. and Parsons, A.J. (eds.). Chapman & Hall, London: 474-505.

Lancaster, N. (1995) *The Geomorphology of Desert Dunes*. Routledge, London.

Lancaster, N. (1996) The role of field experiments in studies of dune dynamics and morphology. *Annals of Arid Zone*, 35: 171-186.

Lancaster, N. and Teller, J.T. (1988) Interdune deposits of the Namib Sand Sea. *Sedimentary Geology*, 55: 91-107.

Lancaster, N., Nickling, W.G., McKenna Neuman, C.K. and Wyatt, V.E. (1996) Sediment flux and airflow on the stoss slope of a barchan dune. *Geomorphology*, 17: 55-62.

Lancaster, N., Schaber, G.C. and Teller, J.T. (2000) Orbital radar studies of palaeodrainages in the central Namib desert. *Remote Sensing of Environment*, 71: 216-225.

Lima, A.R., Sauermann, G., Herrmann, H.J. and Kroy, K. (2002) Modelling a dune field. *Physica A*. 310: 487-500.

Livingstone, I. (1986) Geomorphological significance of wind flow patterns over a Namib linear dune. In *Aeolian Geomorphology*, Nickling W.G. (ed.). Allen & Unwin, Boston: 97-112.

Livingstone, I. (1988) New models for the formation of linear sand dunes. *Geography*, 73: 105-115.

Livingstone, I. and Warren, A. (1996) *Aeolian Geomorphology*. Longman, London.

Livingstone, I., Bullard, J.E., Wiggs, G.F.S. and Thomas, D.S.G. (1999) Grain-size variation on dunes in the Southwest Kalahari, Southern Africa. *Journal of Sedimentary Petrology*, 69: 546-552.

Long, J.T. and Sharp, R.P. (1964) Barchan-dune movement in Imperial Valley, California. *Geological Society of America Bulletin*, 75: 149-156.

Lu, S.S. and Wilmarth, W.W. (1973) Measurements of the structure of the Reynolds stress in a turbulent boundary layer. *Journal of Fluid Mechanics*, 60: 481-511.

Mabbutt, J.A. and Wooding, R.A. (1983) Analysis of longitudinal dune patterns in the northwestern Simpson Desert, central Australia. *Zeitschrift für Geomorphologie*, Supplementband 45: 51-69.

Maddux, T.B., Nelson, J.M. and McLean, S.R. (2003a) Turbulent flow over three-dimensional dunes 1. Free surface and flow response. *Journal of Geophysical Research*, 108(F1): 6009, doi:10.1029/2003JF000017.

Maddux, T.B., Nelson, J.M. and McLean, S.R. (2003b) Turbulent flow over three-dimensional dunes 2. Fluid and bed stresses. *Journal of Geophysical Research,* 108(F1): 6010, doi:10.1029/2003JF000018.

Mainguet, M. (1984) Space observations of Saharan aeolian dynamics and the sand budget. In *Deserts and Arid Lands*, El Baz, F. (ed.). Martinus Nijhoff, The Hague: 31-58.

McKee, E.D. (1966) Structures of dunes at White Sands National Monument, New Mexico (and a comparison with structures of dunes from other selected areas). *Sedimentology*, 7: 1-69.

McKee, E.D. (1979) Introduction to a study of global sand seas. In *A Study of Global Sand Seas*, McKee, E.D. (ed.). United States Geological Survey, Professional Paper 1052: 3-19.

McKee, E.D. (1983) Eolian sand bodies of the world. In *Eolian Sediments and Processes, Developments in Sedimentology* 38, Brookfield, M. E. and Ahlbrandt, T. S. (eds.). Elsevier, Amsterdam: 1-25.

McKenna Neuman, C., Lancaster, N. and Nickling, W.G. (1997) Relations between dune morphology, air flow and sediment flux on reversing dunes, Silver Peak, Nevada. *Sedimentology*, 44: 1103-1113.

McKenna Neuman, C., Lancaster, N. and Nickling, W.G. (2000) The effect of unsteady winds on sediment transport on the stoss slope of a transverse dune, Silver Peak, Nevada, USA. *Sedimentology*, 47: 211-226.

McLean, S.R., Nelson, J.M. and Shreve, R.L. (1996) Flow-sediment interactions in separating flows over bedforms. In *Coherent Flow Structures in Open Channels*, Ashworth, P.J., Bennett, S.J., Best, J.L. and McLelland, S.J. (eds.). John Wiley & Sons, Chichester: 203-226.

McLean, S.R., Nelson, J.M. and Wolfe, S.R. (1994) Turbulence structure over two-dimensional bed forms: Implications for sediment transport. *Journal of Geophysical Research*, 99 (C6): 12729-12747.

McLean, S.R. and Smith, J.D. (1986) A model for flow over two-dimensional bed forms. *Journal of Hydraulic Engineering*, 112: 300-317.

Momiji, H., Carretero-Gonzalez, R., Bishop, S.R. and Warren, A. (2000) Simulation of the effect of wind speedup in the formation of transverse dune fields. *Earth Surface Processes and Landforms*, 25: 905-918.

Momiji, H. and Warren, A. (2000) Relations of sand trapping efficiency and migration speed of transverse dunes to wind velocity. *Earth Surface Processes and Landforms*, 25: 1069-1084.

Müller, A. and Gyr, A. (1986) On the vortex formation in the mixing layer behind dunes. *Journal of Hydraulics Research*, 24: 359-375.

Mulligan, K.R. (1988) Velocity profiles measured on the windward slope of a transverse dune. *Earth Surface Processes and Landforms*, 13: 573-582.

Nagtegaal, P.J.C. (1971) Adhesion-ripple and barchan-dune sands of the recent Namib (SW Africa) and Permian Rotliegend (NW Europe) Deserts. *Madoqua,* Series II, 2: 5-19.

Nelson, J.M., McLean, S.R. and Wolfe, S.R. (1993) Mean flow and turbulence fields over two-dimensional bed forms. *Water Resources Research*, 29: 3935-3953.

Nelson, J.M., Shreve, R.L., McLean, S.R. and Drake, T.G. (1995) Role of near-bed turbulence structure in bed load transport and bedform mechanics. *Water Resources Research*, 31: 2071-2086.

Nelson, J.M. and Smith, J.D. (1989) Mechanics of flow over ripples and dunes. *Journal of Geophysical Research*, 94(C6): 8146-8162.

Nickling, W.G. and McKenna Neumann, C. (1999) Airflow and sediment transport over desert dunes. In *Aeolian Environments, Sediments and Landforms,* Goudie, A.S., Livingstone, I. and Stokes, S. (eds.). John Wiley & Sons, Chichester: 15-48.

Nickling, W.G., McKenna Neuman, C. and Lancaster, N. (2002) Grainfall processes in the lee of transverse dunes, Silver Peak, Nevada. *Sedimentology*, 49: 191-209.

Nielson, J. and Kocurek, G. (1987) Surface processes, deposits and development of star dunes, Dumont dune field, California. *Bulletin of the Geological Society of America*, 99: 177-186.

Nishimori, H., Yamasaki, M. and Andersen, K.H. (1998) A simple model for the various pattern dynamics of dunes. *International Journal of Modern Physics B*, 12: 257-272.

Parsons, D.R., Walker, I.J. and Wiggs, G.F.S. (2004a) Numerical modelling of flow structures over idealized transverse aeolian dunes of varying geometry. *Geomorphology*, 59: 149-164.

Parsons, D.R., Wiggs, G.F.S., Walker, I.J., Ferguson, R.I. and Garvey, B.G. (2004b) Numerical modelling of airflow over an idealised transverse dune. *Environmental Modelling and Software*, 19: 153-162.

Phillips, J.D. (1999) *Earth Surface Systems. Complexity, Order and Scale*. Basil Blackwell, Oxford.

Raupach, M.R. and Finnigan, J.J. (1997) The influence of topography on meteorological variables and surface-atmosphere interactions. *Journal of Hydrology*, 190: 182-213.

Schwämmle, V. and Herrmann, H.J. (2003) Solitary wave behaviour of sand dunes. *Nature*, 426: 619-620.

Schwämmle, V. and Herrmann, H. (2004) Modelling Transverse Dunes. *Earth Surface Processes and Landforms*, 29: 769-784.

Sharp, R.P. (1979) Intradune flats of the Algodones chain, Imperial Valley, California. *Geological Society of America Bulletin*, 90: 908-916.

Simpson, E.L. and Loope, D.B. (1985) Amalgamated interdune deposits, White Sands, New Mexico. *Journal of Sedimentary Petrology*, 55: 361-365.

Slattery, M.C. (1990) Barchan migration on Kuiseb River Delta, Namibia. *South African Geographical Journal*, 72: 5-10.

Stam, J.M.T. (1997) On the modelling of two-dimensional aeolian dunes. *Sedimentology*, 44: 127-141.

Stanistreet, I.G. and Stollhofen, H. (2002) Hoanib River flood deposits of Namib Desert interdunes as analogues for thin permeability barrier mudstone layers in aeolianite reservoirs. *Sedimentology*, 49: 719-736.

Sterk, G., Jacobs, A.F.G. and van Boxel, J.H. (1998) The effect of turbulent flow structures on saltation sand transport in the atmospheric boundary layer. *Earth Surface Processes and Landforms*, 23: 877-887.

Sterk, G. (2000) Flattened residue effects on wind speed and sediment transport. *Soil Science Society of America Journal*, 64: 852-858.

Stone, R.O. (1967) A desert glossary. *Earth-Science Reviews*, 3: 211-268.

Stout, J.E. and Zobeck, T.M. (1997) Intermittent saltation. *Sedimentology*, 44: 959-970.

Stull, R.B. (1988) *Meteorology for Scientists and Engineers*, 2nd Edition. Brookes/Cole, California.

Svendsen, J., Stollhofen, H., Krapf, C.B.E and Stanistreet, I.G. (2003) Mass and hyperconcentrated flow deposits record dune damming and catastrophic breakthrough of ephemeral rivers, Skeleton Coast Erg, Namibia. *Sedimentary Geology*, 160: 7-31.

Sweet, M. L. (1992) Lee-face airflow, surface processes, and stratification types: their significance for refining the use of eolian cross-strata as paleocurrent indicators. *Geological Society of America Bulletin*, 104: 1528-1538.

Sweet, M.L. and Kocurek, G. (1990) An empirical model of aeolian dune lee-face airflow. *Sedimentology*, 37: 1023-1038.

Taylor, P.A., Mason, P.J. and Bradley, E.F. (1987) Boundary-layer flow over low hills. *Boundary-Layer Meteorology*, 39: 107-132.

Thomas, D.S.G. (1986) Dune pattern statistics applied to the Kalahari Dune Desert, southern Africa. *Zeitschrift für Geomorphologie*, 30: 231-242.

Thomas, D.S.G. (1988) Analysis of linear dune sediment-form relationships in the Kalahari dune desert. *Earth Surface Processes and Landforms*, 13: 545-554.

Thomas, D.S.G. (1997) Sand seas and aeolian bedforms. In *Arid Zone Geomorphology*, 2nd Edition, Thomas, D.S.G. (ed.). John Wiley & Sons, Chichester: 373-412.

Tseo, G. (1993) Two types of longitudinal dune fields and possible mechanisms for their development. *Earth Surface Processes and Landforms*, 18: 627-643.

Tsoar, H. (1983a) Dynamic processes acting on a longitudinal (seif) dune. *Sedimentology*, 30: 567-578.

Tsoar, H. (1983b) Wind tunnel modelling of echo and climbing dunes. In *Eolian Sediments and Processes,* Brookfield M.E. and Ahlbrandt T.S. (eds.). Elsevier, Amsterdam: 247-259.

Tsoar, H. (1985) Profiles analysis of sand dunes and their steady state signification. *Geografiska Annaler*, 67A: 47-59.

Tsoar, H. (1989) Linear dunes – forms and formations. *Progress in Physical Geography*, 13: 507-528.

Tsoar, H., Rasmussen, K.R., Sørensen, M. and Willets, B.B. (1985) Laboratory studies of flow over dunes. In *Proceedings of International Workshop on the Physics of Blown Sand*, Volume 2, Barndorff-Nielsen, Møller J.T., Rasmussen K.R. and Willetts B.B. (eds.). University of Aarhus, Aarhus: 327-350.

van Boxel, J.H., Arens, S.M. and van Dijk, P.M. (1999) Aeolian processes across transverse dunes. I: Modelling the air flow. *Earth Surface Processes and Landforms*, 24: 255-270.

van Boxel, J. H., Sterk, G. and Arens, S.M. (2004) Sonic anemometers in aeolian sediment transport research. *Geomorphology*, 59: 131-147.

van Dijk, P.M., Arens, S.M. and van Boxel, J.H. (1999) Aeolian processes across transverse dunes. II: Modelling the sediment transport and profile development. *Earth Surface Processes and Landforms*, 24: 319-333.

Walker, I.J. (1999) Secondary airflow and sediment transport in the lee of a reversing dune. *Earth Surface Processes and Landforms*, 24: 437-448.

Walker , I.J. (2005) Physical and logistical considerations of using ultrasonic anemometry in aeolian sediment transport research. *Geomorphology,* 68: 57-76.

Walker, I.J. and Nickling, W.G. (2002) Dynamics of secondary airflow and sediment transport over and in the lee of transverse dunes. *Progress in Physical Geography*, 26: 47-75.

Walker, I.J. and Nickling, W.G. (2003) Simulation and measurement of surface shear stress over isolated and closely spaced transverse dunes in a wind tunnel. *Earth Surface Processes and Landforms*, 28: 1111-1124.

Walmsley, J.L. and Howard, A.D. (1985) Application of a boundary-layer model to flow over an eolian dune. *Journal of Geophysical Research*, 90 (D6): 10631-10640.

Wang, X., Dong, Z., Zhang, J. and Zhao, A. (2002) Relations between morphology, air flow, sand flux and particle size on transverse dunes, Taklimakan Sand Sea, China. *Earth Surface Processes and Landforms*, 27: 515-526.

Warren, A. (1972) Observations on dunes and bi-modal sands in the Ténéré desert. *Sedimentology*, 19, 37-44.

Warren, A. (1979) Aeolian processes, In *Process in Geomorphology,* Embleton, C. and Thornes, J. (eds.). John Wiley & Sons, Chichester: 325-351.

Warren, A. (1988) The dynamics of dune networks in the Wahiba Sands: a progress report. *Journal of Oman Studies Special Report*, No. 3: 169-180.

Warren, A. and Kay, S. (1987) Dune networks. In *Desert Sediments: Ancient and Modern,* Frostick, L.E. and Reid, I. (eds.). Geological Society Special Publication No. 35, Blackwell, Oxford: 205-212.

Warren, A. and Knott, P. (1983) Desert dunes: a short review of needs in desert dune research and a recent study of micro-meteorological dune-initiation mechanisms. In *Eolian sediments and processes, Developments in Sedimentology*, 38, Brookfield, M. E. and Ahlbrandt, T. S. (eds.). Elsevier, Amsterdam: 343-352.

Wasson, R.J. and Hyde, R. (1983) A test of granulometric control of desert dune geometry. *Earth Surface Processes and Landforms*, 8: 301-312.

Watson, A. (1987) Variations in wind velocity and sand transport on the windward flanks of desert sand dunes: comment. *Sedimentology*, 34: 511-516.

Weng, W.S., Hunt, J.C.R., Carruthers, D.J., Warren, A., Wiggs, G.F.S., Livingstone, I. and Castro, I. (1991) Air flow and sand transport over sand-dunes. *Acta Mechanica Supplement*, 2: 1-22.

Werner, B.T. (1995) Eolian dunes: computer simulations and attractor interpretation. *Geology*, 23: 1107-1110.

Werner, B.T. (1999) Complexity in natural landform patterns. *Science*, 284: 102-104.

Werner, B.T. and Kocurek, G. (1997) Bedform Dynamics: Does the tail wag the dog? *Geology*, 25: 771-774.

Werner, B.T. and Kocurek, G. (1999) Bedform spacing from defect dynamics. *Geology*, 27: 727-730.

Wiggs, G.F.S. (1993) Desert dunes dynamics and the evaluation of shear velocity. In *The Dynamics and Environmental Context of Aeolian Sedimentary Systems*, Pye, K. (ed.). Geological Society, Special Publication No. 72, London: 37-48.

Wiggs, G.F.S. (2001) Desert dune processes and dynamics. *Progress in Physical Geography*, 25: 55-81.

Wiggs, G.F.S., Livingstone, I. and Warren, A. (1996) The role of streamline curvature in sand dune dynamics: evidence from field and wind tunnel measurements. *Geomorphology*, 17: 29-46.

Wilczak, J.M., Oncley, S.P. and Stage, S.A. (2001) Sonic anemometer tilt correction algorithms. *Boundary-Layer Meteorology*, 99: 127-150.

Wilson, I.G. (1972) Aeolian bedforms - their development and origins. *Sedimentology*, 19: 173-210.

Wilson, I.G. (1973) Ergs. *Sedimentary Geology*, 10: 77-106.

Wipperman, F.K. and Gross, G. (1986) The wind-induced shaping and migration of an isolated dune: a numerical experiment. *Boundary-Layer Meteorology*, 36: 319-334

Yalin, M.S. (1977) *Mechanics of Sediment Transport*, 2nd Edition. Pergamon Press, Oxford.

Yoon, J.Y. and Patel, V.C. (1996) Numerical model of turbulent flow over sand dune. *Journal of Hydraulic Engineering*, 122: 10-18.

Zeman, O. and Jensen, N.O. (1987) Modifications of turbulence characteristics in flow over hills. *Quarterly Journal of the Royal Meteorological Society*, 113: 55–80.